



SCUOLA
NORMALE
SUPERIORE

Class of Sciences

Ph.D. in Data Science

36° cycle

On Quantile Regression Forests for Modelling Mixed-Frequency and Longitudinal Data

Scientific Disciplinary Area SECS-S/01

Candidate

Mila Andreani

Supervisors

Prof. Francesca Chiaromonte

Prof. Lea Petrella

Prof. Nicola Salvati

Academic Year 2023-2024

Abstract

The aim of this thesis is to extend the applications of the Quantile Regression Forest (QRF) algorithm to handle mixed-frequency and longitudinal data. To this end, standard statistical approaches have been exploited to build two novel algorithms: the Mixed-Frequency Quantile Regression Forest (MIDAS-QRF) and the Finite Mixture Quantile Regression Forest (FM-QRF).

The MIDAS-QRF combines the flexibility of QRF with the Mixed Data Sampling (MIDAS) approach, enabling non-parametric quantile estimation with variables observed at different frequencies. FM-QRF, on the other hand, extends random effects machine learning algorithms to a QR framework, allowing for conditional quantile estimation in a longitudinal data setting. The contributions of this dissertation lie both methodologically and empirically.

Methodologically, the MIDAS-QRF and the FM-QRF represent two novel approaches for handling mixed-frequency and longitudinal data in QR machine learning framework. Empirically, the application of the proposed models in financial risk management and climate-change impact evaluation demonstrates their validity as accurate and flexible models to be applied in complex empirical settings.

Contents

1	Introduction and Overview	2
2	Mixed-Frequency Quantile Regression Forests	5
2.1	Introduction	5
2.2	Quantile Regression Forest: Notation and Preliminary Results	8
2.3	Methodology	10
2.3.1	The MIDAS-QRF Model	10
2.3.2	Variable Importance computation	12
2.3.3	Dynamic MIDAS-QRF	12
2.4	Empirical Application	13
2.4.1	Backtesting Procedures	16
2.4.2	MIDAS-QRF Results	16
2.4.3	Dynamic MIDAS-QRF Results	20
2.4.4	Variable Importance	24
2.5	Conclusions	28
3	Finite mixtures of Quantile Regression Forests and their application to GDP growth-at-risk from climate change	30
3.1	Introduction	30
3.2	Methodology	32
3.2.1	Finite Mixtures of Quantile Regression Forest	32
3.2.2	Parameters Estimation with the EM Algorithm	34
3.2.3	Closed Form Solutions to the EM Algorithm	36
3.3	Simulation Study	37
3.4	Empirical Application	40
3.4.1	Preliminary Analysis	43
3.4.2	Projection Results	46
3.5	Conclusions	53

4	The Impact of the COVID-19 Pandemic on Risk Factors for Children’s Mental Health: Evidence from the UK Household Longitudinal Study	54
4.1	Introduction	54
4.2	The Data	56
4.3	Analysis of the UK Household Longitudinal Study Data	59
4.3.1	Risk Factors Analysis	60
4.3.2	Comparison with the LQMM Results	63
4.4	Conclusions	65
A	Mixed-Frequency Quantile Regression Forests	78
B	Finite mixtures of Quantile Regression Forests and their application to GDP growth-at-risk from climate change	83
C	The Impact of the COVID-19 Pandemic on Risk Factors for Children’s Mental Health	98

List of Figures

2.1	Heating Oil (black line) index out-of-sample predictions at quantile levels $\tau = 0.01, 0.025, 0.05$. The top panel and the bottom panel show the predictions obtained with the dynamic MIDAS-QRF model, respectively.	24
2.2	Variable importance for the static MIDAS-QRF at $\tau = 0.01$ for the Heating Oil index	26
2.3	Variable importance for the static MIDAS-QRF at $\tau = 0.025$ for the Heating Oil index	27
2.4	Variable importance for the static MIDAS-QRF at $\tau = 0.05$ for the Heating Oil index	28
3.1	Average variable importance across quantiles I_j for each covariate. . . .	44
3.2	Permutation-based variable importance $I_{j,\tau}$ for each covariate included in the training set.	45
3.3	Map showing ΔQ_{it}^τ in years $t = 2030, 2050, 2100$ for quantile at probability level $\tau = 0.01$	48
3.4	Map showing ΔQ_{it}^τ in years $t = 2030, 2050, 2100$ for quantile at probability level $\tau = 0.05$	49
3.5	Map showing ΔQ_{it}^τ in years $t = 2030, 2050, 2100$ for quantile at probability level $\tau = 0.50$	50
3.6	Map showing ΔQ_{it}^τ in years $t = 2030, 2050, 2100$ for quantile at probability level $\tau = 0.95$	51
3.7	Map showing ΔQ_{it}^τ in years $t = 2030, 2050, 2100$ for quantile at probability level $\tau = 0.99$	52
4.1	Normal probability plot of the linear mixed model residuals for SDQ total score with with random-effects specified at child level	59
4.2	Bar plot showing the Variable Importance extracted from the FM-QRF for each covariate at quantile level $\tau = 0.1$. The blue bars represent the Variable Importance in the Pre-pandemic period and the red bars are related to the pandemic period. Numbers at the top of the bars indicate the ranking position of each variable in terms of Variable Importance. . .	61

4.3	Bar plot showing the Variable Importance extracted from the FM-QRF for each covariate at quantile level $\tau = 0.5$. The blue bars represent the Variable Importance in the Pre-pandemic period and the red bars are related to the pandemic period. Numbers at the top of the bars indicate the ranking position of each variable in terms of Variable Importance.	61
4.4	Bar plot showing the Variable Importance extracted from the FM-QRF for each covariate at quantile level $\tau = 0.9$. The blue bars represent the Variable Importance in the pre-pandemic period and the red bars are related to the pandemic period. Numbers at the top of the bars indicate the ranking position of each variable in terms of Variable Importance.	62
A.1	WTI index time series. the black line represents the training set and the red line the out-of-sample period.	79
A.2	Brent index time series. the black line represents the training set and the red line the out-of-sample period.	80
A.3	Heating oil index time series. the black line represents the training set and the red line the out-of-sample period.	80
A.4	Brent index (black line) out-of-sample predictions at quantile levels $\tau = 0.01, 0.025, 0.05$. The top panel and the bottom panel show the predictions obtained with the dynamic MIDAS-QRF model, respectively.	81
A.5	WTI index (black line) out-of-sample predictions at quantile levels $\tau = 0.01, 0.025, 0.05$. The top panel and the bottom panel show the predictions obtained with the dynamic MIDAS-QRF model, respectively.	82
C.1	Bar plot showing the number of children interviewed 1, 2, 3 or 4 times during the sample period.	98
C.2	Bar plot showing the Variable Importance extracted from the FM-QRF for each covariate at quantile level $\tau = 0.25$	99
C.3	Bar plot showing the Variable Importance extracted from the FM-QRF for each covariate at quantile level $\tau = 0.75$	99

List of Tables

2.1	Models specifications	15
2.2	Loss and Backtesting results of the MIDAS-QRF for the Brent Index. The shade of grey indicate models for which the p-value of the test in greater than the 1% significance level.	17
2.3	Loss and Backtesting results of the MIDAS-QRF for the WTI Index. The shade of grey indicate models for which the p-value of the test in greater than the 1% significance level.	18
2.4	Loss and Backtesting results of the MIDAS-QRF for the Heating Oil Index. The shade of grey indicate models for which the p-value of the test in greater than the 1% significance level.	19
2.5	Loss and Backtesting results of the Dynamic MIDAS-QRF for the Brent Index. The shade of grey indicate models for which the p-value of the test in greater than the 1% significance level.	21
2.6	Loss and Backtesting results of the Dynamic MIDAS-QRF for the WTI Index. The shade of grey indicate models for which the p-value of the test in greater than the 1% significance level.	22
2.7	Loss and Backtesting results of the Dynamic MIDAS-QRF for the Heating Oil Index. The shade of grey indicate models for which the p-value of the test in greater than the 1% significance level.	23
3.1	Loss values for each scenario computed on the test set of the four fitted models. Bold values indicate the smallest loss.	39
3.2	Summary statistics of the variables included in the sample. The table reports the number of observations (Obs), the minimum (Min), maximum (Max) along with the median, mean and standard deviation (SD). . . .	42
3.3	ANOVA test results for different values of τ . The 'Tn' column reports the test statistic and the 'P-Value' column reports the level of significance of the test at 5% significance level.	43
3.4	Average mean and bootstrap standard error across countries obtained with N=500 iterations.	46
4.1	Summary statistics related to the pre-COVID period of the variables included in the sample after the data cleaning procedure. The Null column reports the number of null values (not applicable or missing items) before the data cleaning procedure.	58

4.2	Summary statistics related to the COVID period of the variables included in the sample after the data cleaning procedure. The Null column reports the number of null values (not applicable or missing items) before the data cleaning procedure.	58
4.3	ANOVA test results for different values of τ . The 'Tn' column reports the test statistic and the 'P-Value' column reports the level of significance of the test at 5% significance level.	59
4.4	Pseudo- R^2 values related to the pre-pandemic period for the LQMM and the FM-QRF models. Values are expressed in percentages.	64
4.5	Pseudo- R^2 values related to the pandemic period for the LQMM and the FM-QRF models. Values are expressed in percentages.	64
4.6	LQMM results coefficients for the pre-pandemic and the pandemic period at five quantile levels $\tau = 0.1, 0.5, 0.9$. The symbol '***' denotes significance at 1% level and '**' significance at 5%.	65
A.1	Summary statistics of the variables included in the sample. The table reports the number of observations (Obs), the minimum (Min), maximum (Max) along with the mean, standard deviation (SD), skewness and excess kurtosis.	78
A.2	Ratio between the number of times quantiles computed at level τ indicated in the rows are higher than those computed at level τ in the columns.	79
B.1	Mean (in bold) and standard error of the quantile estimates at level $\tau = 0.01, 0.5, 0.99$ for the SSP1 scenario.	90
B.2	Mean (in bold) and standard error of the quantile estimates at level $\tau = 0.01, 0.5, 0.99$ for the SSP5 scenario.	97

Chapter 1

Introduction and Overview

Quantile Regression (QR) has been introduced in Koenker and Bassett Jr (1978) as a powerful technique to model the entire conditional distribution of a response variable given a set of covariates. This approach is particularly useful when the standard regression models fail at correctly modeling the relationship between the response and the covariates, or when the gaussianity assumption on the outcome's distribution is untenable. In such scenarios, QR allows to obtain more robust and reliable results by modeling location parameters beyond the conditional mean, and a variety of fields, such as economics, finance, healthcare, and environmental science (Koenker, 2005, Koenker et al., 2017), have reaped the benefits of this approach.

The recent development of non-parametric QR models have further extended the applications of QR, including the machine learning realm. In this context, QR machine learning algorithms represent one of the main advancements in overcoming the limits of the parametric formulation of standard QR models. As a matter of fact, machine learning algorithms do not require any a-priori assumption on the functional form of the relationship between the outcome and the covariates, resulting more flexible and reliable than standard QR in empirical applications involving unknown and highly complex relationships among variables.

Few examples of QR machine learning algorithms are the QR neural network model of White (1992), QR Support Vector Machines (Hwang and Shim, 2005, Xu et al., 2015) and QR Random Forests (Meinshausen, 2006, Athey et al., 2019).

Despite the benefits of these algorithms, their application is constrained to standard experimental designs, as they often falter in non-standard empirical settings, such as those involving mixed-frequency or longitudinal data.

The former case is particularly relevant in time series analysis, in which information is often available at different temporal resolutions. Standard statistical and econometrics models, including QR, usually require the use of variables observed at the same frequency, causing potentially useful predictors to be excluded due to the temporal mismatch. One of the main contributions to address this issue is the Mixed Data Sampling (MIDAS) approach proposed in Ghysels et al. (2007). This model allows to include variables

observed at different frequencies, allowing to expand the research methodology beyond the standard statistical setting.

Given its innovativity, the MIDAS approach has been extended to QR and applied in a variety of fields, such as finance and economics (Kuzin et al., 2011, Andreani et al., 2021, Candila et al., 2023), environmental sciences (Oloko et al., 2022, Jiang and Yu, 2023) and tourism (Bangwayo-Skeete and Skeete, 2015, Wen et al., 2021).

In the longitudinal data setting instead, previous contributions to the QR literature have exploited mixed-effects or random effects models to account for the potential association between dependent observations (Farcomeni, 2012a, Smith et al., 2015, Alfò et al., 2017, Marino et al., 2018, Merlo et al., 2021, 2022c,b). Although these models incorporate an individual-specific random intercept to model unobserved heterogeneity, their parametric formulation may not be suitable in various empirical applications, leading to potentially inaccurate inferences.

Non-parametric approaches have been proposed, but in the machine learning realm, the algorithms that have been extended to handle mixed-frequency data (Xu et al., 2019) and longitudinal data (Xiong et al., 2019, Luts et al., 2012, Hajjem et al., 2014, 2011, Sela and Simonoff, 2012) lack the capability to estimate conditional quantiles, as they have been developed only in a standard regression setting.

Thus, the aim of this dissertation is to bridge this gap in the literature by introducing two novel machine learning algorithms that allow to estimate conditional quantiles in the mixed-frequency and longitudinal data frameworks.

Both proposed models build upon the Quantile Regression Forest (QRF) algorithm, ensuring a high level of accuracy and computational efficiency. The choice of the QRF algorithm stems from its inherent flexibility, allowing for easy comparison with standard econometric models in terms of statistical adequacy, accuracy, interpretability, and computational effort. Empirical results presented in this thesis demonstrate that the proposed extensions outperform commonly used econometric and statistical models in the QR literature.

The main contributions of this dissertation are twofold. Methodologically, it introduces two algorithms: the Mixed-Frequency Quantile Regression Forest (MIDAS-QRF, detailed in Chapter 2) and the Finite Mixture Quantile Regression Forest (FM-QRF, presented in Chapter 3). The MIDAS-QRF is based on a novel methodology that merges the MIDAS approach and the QRF algorithm, enabling non-parametric estimation of quantiles using data observed at different frequencies. The FM-QRF, on the other hand, builds upon random effects machine learning algorithms and it is based on leaving the random effects distribution unspecified and on estimating the fixed part of the model with QRF. Quantile estimates are obtained using an iterative procedure based on the Expectation Maximization-type algorithm with the Asymmetric Laplace distribution as the working likelihood. This methodology extends the work of Geraci and Bottai (2007, 2014), Alfò

et al. (2017) to a non-linear and non-parametric framework and adapts the mixed-modeling approach presented in Hajjem et al. (2014) to a QR framework.

The validity of the proposed models has been tested empirically in the financial and economics settings. As a matter of fact, the recent emerging risks concerning financial crises and climate change have required financial institutions, policymakers, and researchers to develop novel methodological approaches to capture complex relationships and manage such risks.

The two innovative methodological approaches result particularly useful in this settings, where non-Gaussian characteristics and mixed-frequency or longitudinal data are common. The MIDAS-QRF is empirically applied in a financial risk management setting for computing the well-known financial risk measure Value-at-Risk. Empirical findings demonstrate that the MIDAS-QRF delivers statistically adequate forecasts that outperform popular models in terms of accuracy (refer to Section 2.4).

The FM-QRF is applied in a climate-change impact evaluation setting to predict the Growth-at-Risk (GaR) of GDP growth for 210 countries. Climate-related variables are used as covariates, revealing heterogeneous effects of unsustainable climate practices among countries.

In order to test the flexibility of the proposed FM-QRF, the model is applied on an additional longitudinal dataset concerning the effects of the COVID-19 pandemic on children's mental health to extend previous findings based on standard linear models (refer to Section 3.4).

Chapter 2

Mixed-Frequency Quantile Regression Forests

2.1 Introduction

Standard regression models infer the effects of a set of covariates on the conditional expected value of the response variable. However, in real-world scenarios the effects of the covariates may vary across different parts of the outcome variable's conditional distribution. In this case, standard regression models may provide misleading results, and a more complete picture of the response variable's distribution would allow to obtain more robust results, especially if the distribution of the outcome exhibits non-Gaussian characteristics.

To this end, a variety of models has been developed to estimate location parameters beyond the expected value, with Quantile Regression (QR) being one of the most important ones. Introduced in Koenker and Bassett Jr (1978) as a generalization of median regression, QR represents a flexible methodology to model data that violate the gaussianity assumptions of standard regression models. As a result, QR has become widely popular among scholars and practitioners in several fields, such as environmental science (Reich, 2012, Vasseur and Aznarte, 2021, Coronese et al., 2019), healthcare and medicine (Wei et al., 2006, Merlo et al., 2022a, Borgoni et al., 2018), finance and economics (Taylor, 1999, Merlo et al., 2022c, Bernardi et al., 2018, Petrella and Raponi, 2019, Daouia et al., 2018, 2021).

Although being widely applied in several empirical studies, the standard QR model may be affected by two main limitations. The first one arises when dealing with data collected at mixed-frequencies, as in time series modelling. In this domain, it is often necessary to incorporate information with different temporal resolution to uncover meaningful relations among the phenomena of interest. The application of standard statistical and econometrics models, including QR, usually requires the use of variables observed at the same frequency, causing potentially useful predictors to be excluded due to the temporal mismatch. One of the most relevant approaches developed to overcome this issue is the Mixed Data Sampling (MIDAS) model proposed by Ghysels et al. (2007). This approach

includes mixed-frequency variables as covariates in linear models, allowing to obtain more accurate predictions. For this reason, it has been applied to a variety of fields, such as finance and economics (Kuzin et al., 2011, Andreani et al., 2021, Candila et al., 2023), environmental sciences (Oloko et al., 2022, Jiang and Yu, 2023) and tourism (Bangwayo-Skeete and Skeete, 2015, Wen et al., 2021).

Another possible limitation of the standard QR model is its reliance on the a-priori specification of the functional form of the relation between the outcome and the covariates. In many empirical applications, this relationship is often unknown and highly complex, and more robust results could be obtained employing a non-parametric approach. To address this issue, the standard QR approach has been extended to the machine learning realm: starting from White (1992), which applies neural networks to QR, other contributions have incorporated QR in the most common machine learning algorithms, such as Support Vector Machines (Hwang and Shim, 2005, Xu et al., 2015) and Random Forests (Meinshausen, 2006, Athey et al., 2019). However, the majority of these models cannot handle mixed-frequency data. For this reason, recently Xu et al. (2019, 2021a) extended QR neural networks to the MIDAS framework, although they showed the presence of some drawbacks related to the low interpretability, high computational effort and high number of observations needed to train the model.

Thus, the aim of this chapter is to propose a comprehensive methodology to estimate quantiles that addresses the limitations of both standard QR and complex machine learning models. To this end, the MIDAS-QRF is introduced as a novel machine learning algorithm able to embed the MIDAS component into the Quantile Regression Forest algorithm (QRF) proposed by Meinshausen (2006).

Being based on the QRF algorithm, the proposed model offers several advantages with respect to deep learning algorithms. The MIDAS-QRF is easier to train and it also allows to extract the so called "variable importance" of each covariate, giving insight into the relative importance of different covariates in forecasting the response variable. These features make MIDAS-QRF particularly flexible and useful in a variety of domains and applications. Moreover, the MIDAS components introduced in the QRF allow to model non-linear relationships among variables sampled at different frequencies without specifying a-priori any particular functional form and without making any assumption on the dependent variable's distribution. The proposed model also expands the applicability of the well known QRF, since it handles mixed-frequency data often involved in real empirical applications. Last but not least, the proposed MIDAS-QRF model is particularly suitable for empirical applications involving variables with skewed and fat-tailed distributions.

Moreover, the MIDAS-QRF offer advantages also over standard statistical methods, such as multivariate splines on the covariate space. This is due to the MIDAS-QRF (and Random Forest algorithms in general) nature as an ensemble method. By combining the predictions of multiple decision trees, the MIDAS-QRF allows to reduce overfitting and improve accuracy with respect to individual models. Moreover, Contributions to

the literature (Genuer, 2012, Breiman, 1996, 2001, Hastie et al., 2009) show that this approach based on aggregation also helps in reducing the variance of the model, leading to increased stability in forecasts. Moreover, algorithms based on Random Forests are particularly effective in handling high-dimensional data, thanks to the random selection of features at each split, which mitigates the curse of dimensionality and provides insights into feature importance. Additionally, they are flexible, scalable, and can naturally handle missing values (Breiman, 2001).

It is quite common to encounter dependent variables in the financial domain that are not normally distributed, and are further influenced by additional covariates observed at lower frequencies, often exhibiting non-linear relationships.

For this reason, the MIDAS-QRF is employed to estimate the well-known financial risk measure Value-at-Risk (VaR), which is one of key risk metrics employed for capital calculation, decision-making, and risk management within the Basel III banking framework. (Jorion, 1997). From a statistical point of view, VaR represents the conditional quantile of a financial variable's distribution, and a variety of models have been applied to its estimation, such as QR, linear ARCH models (Koenker and Zhao, 1996, Taylor, 1999), GARCH models (Xiao and Koenker, 2009, Lee and Noh, 2013, Zheng et al., 2018), penalized QR (Bayer, 2018), models based on the Asymmetric Laplace distribution (Merlo et al., 2021, Taylor, 2019), as well as extensions to multivariate settings (Petrella and Raponi, 2019, Bernardi et al., 2017, Merlo et al., 2022c). Some of these models have been also extended to account for mixed-frequency data, see for example Engle et al. (2013), Candila et al. (2023) and Mo et al. (2018).

In empirical applications involving time series, it may be useful to estimate quantiles in a dynamic framework to model the time-varying distribution of the variable of interest. In the financial literature, the Conditional Autoregressive Value-at-Risk (CAViaR) model of Engle and Manganelli (2004) has been proposed to accurately model the time-changing distribution of portfolio returns. This approach is based on directly estimating the conditional quantile via a linear autoregressive model, and it has been recently extended to the mixed-frequency framework by Xu et al. (2021b).

In the spirit of the CaViaR, this chapter proposes also an extension of the MIDAS-QRF to a dynamic framework. The resulting Dynamic MIDAS-QRF allows to estimate quantiles in an autoregressive framework by introducing the lagged quantile predictions as additional covariate similarly to the CaViaR model.

Given that financial data are usually observed at different frequencies and are often characterized by the well-known stylized facts (Cont, 2001), they are rarely well-fitted by linear models. In this context, the proposed MIDAS-QRF may be more appropriate than others to obtain accurate quantile estimates.

For this reason, the proposed model is applied in an empirical setting related to the financial field. In particular, this chapter focuses on the emerging topic of the financialization of energy commodities. These products have been widely employed over the two

past decades as hedging and speculative assets, especially during periods of financial and economic downturns. This phenomenon, along with the deregulation of over-the-counter markets, led to a significant increase of the volatility of energy commodities returns. Thus, the study of the risks linked to such commodities is particularly relevant under a risk management framework. The empirical application is focused on three daily energy commodities indexes, the West Texas Intermediate (WTI) Crude Oil, the Brent Crude Oil and the Heating Oil. The aim of the empirical application is to employ the proposed MIDAS-QRF and its dynamic version to predict VaR, defined as the maximum loss that a financial operator can incur over a defined time horizon for a given confidence level. The time series spans from July 2014 to March 2022, including observations collected during the COVID-19 pandemic and at the beginning of Russian-Ukrainian conflict. In order to measure the risks associated with energy commodities, three different low-frequency covariates are considered: the monthly Real Broad Dollar Index, whose effects on oil prices have been investigated in Lin et al. (2016), Akram (2009), the quarterly Natural Gas returns and the quarterly Saudi Arabia Crude Oil Production, whose link to oil prices has been extensively studied by the U.S. Energy Information Administration (EIA) ¹.

The statistical validity of the out-of-sample VaR forecasts is tested by means of back-testing procedures (Christoffersen, 1998, Christoffersen and Pelletier, 2004, Engle and Manganelli, 2004). The empirical results show that the proposed models outperform several well-known statistical and machine learning models often considered in the literature. A variable importance analysis is also reported to show which variables may be considered the most relevant in predicting the VaR. The rest of the chapter is organized as follows: Section 2.2 gives preliminary information on QRF, Section 2.3 describes the proposed methodology, Section 2.4 presents the empirical application of MIDAS-QRF and Section 2.5 concludes.

2.2 Quantile Regression Forest: Notation and Preliminary Results

This section reports the notation and some preliminars on QRF useful for the rest of the chapter.

Let $\mathcal{S} = \{(Y_i, \mathbf{X}_i)\}_{i=1}^N$ be a random sample of dimension N of random variables drawn from the unknown joint distribution of the random variables $(Y, \mathbf{X}) \in \mathbb{R} \times \mathbb{R}^p$ with realisation $\mathbf{s} = \{(y_i, \mathbf{x}_i)\}_{i=1}^N$, where Y is the response variable and \mathbf{X} the vector of p covariates.

The QRF algorithm (Meinshausen, 2006) has been developed as an extension to the Random Forests (RF) algorithm introduced by Breiman (2001). Both models rely on the Classification and Regression Trees (CART) (Breiman et al., 1984) algorithm. Differently

¹https://www.eia.gov/finance/markets/crudeoil/spot_prices.php

from the the Random Forest approach, which estimates the conditional expected value, the QRF estimates the quantile of the conditional distribution of Y .

Specifically, each decision tree in the QRF is trained with the CART algorithm, that consists in recursively partitioning the training sample \mathcal{S} into M disjoint sub-samples denoted with $R_m, m = 1, \dots, M$ according to a splitting rule. In this setting, the splitting rule is based on minimizing the the Sum of Squared Errors (SSE) in each sub-sample of R_m :

$$SSE_{R_m} = \sum_{y_i \in R_m} (\bar{y}_m - y_i)^2, \quad (2.1)$$

where \bar{y}_m is the mean of the observations in R_m ².

At the end of the tree training, each sub-sample that is no further splitted is denoted as "terminal node" and indicated with R_m^* .

The QRF prediction of the conditional quantile $Q_\tau(Y|\mathbf{X} = x)$ is obtained from the estimated conditional distribution $F(y|\mathbf{X} = x)$, defined as follows:

$$\begin{aligned} F(y|\mathbf{X} = x) &:= P(Y \leq y|\mathbf{X} = x) \\ &:= \mathbb{E}[\mathbf{1}_{\{Y \leq y\}}|\mathbf{X} = x] \end{aligned} \quad (2.2)$$

In particular, given a new set of observations, $\hat{F}(y|\mathbf{X} = x)$ is estimated by individuating one terminal node R_m^* in each tree and by averaging the estimations of the B trees:

$$\hat{F}(y|\mathbf{X} = x) = \frac{1}{B} \sum_{b=1}^B \sum_{Y_i \in R_{m,b}^*} \frac{\mathbf{1}_{\{Y_i \leq y\}}}{|R_{m,b}^*|}, \quad (2.3)$$

Subsequently, the quantile at probability level $\tau \in (0, 1)$ is estimated as follows:

$$\hat{Q}_\tau(Y|\mathbf{X} = x) := \inf \{y : \hat{F}(y|\mathbf{X} = x) \leq \tau\} \quad (2.4)$$

The QRF also computes the Variable Importance of each covariate, i.e. the influence of each covariate on the model's performance. The bigger the importance, the greater the positive effect of the variable on the model's accuracy. This feature improves the interpretability of the phenomena of interest and it can be considered as a nice property held by Random Forests with respect, for instance, to Neural Networks.

As mentioned in the introduction, the standard QRF algorithm cannot handle directly mixed-frequency data as many other models, and the aim of this chapter is to fill this gap

²Other splitting rules can be considered. For instance, Athey et al. (2019) proposes to use a quantile loss-base splitting rule. The choice of the splitting rule depends mainly on the empirical application of interest and the final forecast accuracy, as no contribution in the literature offers clear and robust evidence for choosing one approach over another in quantile regression settings. In this thesis, the standard QRF approach of Meinshausen (2006) has been chosen since it is more established in the machine learning literature. However, the proposed model can be easily adapted to consider other QRF models with different splitting rules.

by introducing mixed frequency variables in a QRF framework exploiting the MIDAS approach.

The methodology of the resulting MIDAS-QRF is presented in the next section.

2.3 Methodology

This section describes the MIDAS-QRF methodological approach, developed to extend the QRF algorithm of Meinshausen (2006) via the MIDAS approach of Ghysels et al. (2007) in order to handle mixed-frequency data in quantiles estimation via Random Forests.

2.3.1 The MIDAS-QRF Model

Let $Y_{i,t}$ and $\mathbf{X}_{i,t}$, $i = 1, \dots, N_t$, $t = 1, \dots, T$ be the high-frequency response variable and the set of high-frequency covariates observed at time i of the $t - th$ period of the year. Moreover, $\mathbf{Z}_t = \{Z_t^h\}_{h=1}^H$ is the vector of H low-frequency covariates observed in the $t - th$ period of the year. In this sense, T represents the overall number of low-frequency periods.

For instance, if Z_t is observed monthly, $T = 12$ and the value N_t represents the total number of days in the $t - th$ month. In a financial setting, the variable $Y_{i,t}$ may represent the daily financial returns sampled at day i while the low-frequency variables might be monthly economic variables measuring the general state of the economy, sampled at the $t - th$ month of the year.

The MIDAS approach proposed by Ghysels et al. (2007) allows to include mixed-frequency variables in the QRF model, where the dependent variable is observed at a higher-frequency than the covariates.

The simplest MIDAS linear regression is:

$$Y_{i,t} = \beta_0 + \beta_1 MC_{i-1,t}^1 + \dots + \beta_H MC_{i-1,t}^H + \varepsilon_{i,t} \quad (2.5)$$

where the covariate $MC_{i,t}^h = (\sum_{j=1}^K \phi_k(\boldsymbol{\omega}) Z_{t-j}^h)_{i,t}$ is the MIDAS component, a filter of the last K observations of Z^h up to time $i - 1$ of the t -th period. The number of lags k can be chosen arbitrarily or via grid search. For interpretability purposes, in this chapter the number k is chosen so that to consider meaningful fraction of the year (for instance, for monthly variables it would makes sense to consider three months, that is $k = 3$).

The function $\phi_k(\boldsymbol{\omega})$ is the Beta weighting function (see Candila et al. (2023) and references therein) in which $\boldsymbol{\omega} = (\omega_1, \omega_2)$:

$$\phi_k(\omega_1, \omega_2) = \frac{(k/K)^{\omega_1-1} (1 - k/K)^{\omega_2-1}}{\sum_{j=1}^K (j/K)^{\omega_1-1} (1 - j/K)^{\omega_2-1}}. \quad (2.6)$$

This function allows to impute a greater weight to more recent observations by setting $\omega_1 = 1$ and optimising ω_2 with respect to the model's likelihood or a proper loss function. Other weighting functions are discussed in Ghysels and Qian (2019).

In this chapter, the linear specification of (2.5) is relaxed by considering:

$$Y_{i,t} = f(\mathbf{X}_{i-1,t}, \mathbf{MC}_{i-1,t}) + \varepsilon_{i,t} \quad (2.7)$$

where $f(\cdot)$ is a non-parametric function and $\mathbf{MC}_{i-1,t} = \{MC_{i-1,t}^h\}_{h=1}^H$ is the matrix of MIDAS components related to the set of covariates \mathbf{Z}_t .

Being interested in the VaR of $Y_{i,t}$, the MIDAS-QRF estimates the conditional quantile:

$$\hat{Q}_\tau(Y_{i,t} | \mathbf{X}_{i-1,t}, \mathbf{MC}_{i-1,t}) = f_\tau(\mathbf{X}_{i-1,t}, \mathbf{MC}_{i-1,t}) \quad (2.8)$$

by including the MIDAS covariates in the QRF model. This is achieved by training the QRF with the training set $\mathbf{s}^* = \{(y_{i,t}, \mathbf{x}_{i-1,t}, \mathbf{MC}_{i-1,t})\}_{i=1,t=1}^{N_t,T}$, which includes the observations of the MIDAS component of each low-frequency covariate.

In this non-parametric context, the likelihood of the MIDAS-QRF model cannot be computed, and consequently ω_2 cannot be optimized via maximum likelihood as in the standard MIDAS model. To overcome this issue, the optimal ω_2 could be found via grid search as the one delivering the higher forecast accuracy. A similar approach is also discussed in Candila et al. (2023). However, this procedure can be particularly burdensome if the vector \mathbf{Z}_t is large.

Thus, proposed methodology reduces the computational effort of the MIDAS-QRF training as follows. For each covariate Z_h , a set of $MC_{i-1,t}^h$ is computed by using different values of ω_2 , obtaining a matrix of MIDAS components. Then, the Principal Component Analysis (PCA) is applied on the resulting matrix to reduce its dimensionality, and the first component of the PCA is used in \mathbf{s}^* as MIDAS component related to Z_h . This procedure is performed separately for each low-frequency covariate in the training set.

The main benefit of this approach is that it retains the most important information in Z_h while reducing computational effort and training time for the MIDAS-QRF. Additionally, like the standard QRF, the MIDAS-QRF assesses the relevance of each covariate in predicting the response variable through the Variable Importance measure. Although this measure cannot be interpreted as the coefficients in parametric models, it allows to enhance the interpretability of Random Forests-based models compared to other machine learning algorithms.

A potential limitation of the MIDAS-QRF is that the estimation procedure to obtain MC values can increase variability in MIDAS-QRF estimates, a common issue in MIDAS models. However, being based on Random Forests, the MIDAS-QRF algorithm allows to reduce estimates variability due to its ensemble nature. Additionally, the MIDAS-QRF retains all statistical properties of the standard QRF algorithm since the MIDAS

component is considered as an additional covariate in the training set. For more details on the MIDAS-QRF and QRF statistical properties, refer to Meinshausen (2006), in which the model's consistency is shown along with numerical examples.

2.3.2 Variable Importance computation

Variable Importance is usually computed permuting the observations of the generic p -th covariate and measuring the effect on the model's forecast accuracy. The idea behind this procedure is that if a covariate significantly affects the model's performance, permuting its values would result in a decrease in forecast accuracy. On the contrary, if the covariate is less important, permuting its values should have minimal influence on the model's performance.

More in detail, the Variable Importance is computed in two steps. In the first step, Out-Of-Bag (OOB) observations of the training set are used to compute the Sum of Squared Residuals (SSR) of the QRF, denoted with m :

$$m = \sum_{i=1}^S (y_i^{OOB} - \hat{y}_i)^2 \quad (2.9)$$

where S denotes the total number of OOB observations selected in the procedure (in empirical setting, this number is usually pre-determined by the function used to implement the algorithm) and y_i^{OOB} is the i -th OOB observation of the outcome variable.

Subsequently, the observations of the p -th covariate are permuted, and the SSR is re-calculated. The resulting SSR is denoted with m^* . The importance of the p -th variable at each quantile level τ , denoted with $I_{p,\tau}$, is measured as:

$$I_{p,\tau} = m - m^* \quad (2.10)$$

The bigger the decrease of the SSR after permutation, the greater the variable importance. The ability to extract the Variable Importance measure allows the MIDAS-QRF to retain the grade of interpretability of standard Random Forest-based algorithms.

In this chapter, the Variable Importance of the covariates included in the training set is extracted to gain a deeper insight into the results obtained in Section 2.4.

2.3.3 Dynamic MIDAS-QRF

In order to model the quantile in a dynamic framework, the MIDAS-QRF approach is extended to an autoregressive framework. A dynamic approach to quantile estimation has already been introduced in a parametric setting with the CaViaR model of Engle and Manganelli (2004). The aim of this study is to apply this well-established autoregressive approach to the MIDAS-QRF. Thus, the resulting Dynamic MIDAS-QRF relies on considering lagged values of the quantile predictions as additional covariate used to train the model.

The iterative algorithm of the Dynamic MIDAS-QRF consists in an initialisation phase and a two-step procedure. Denoting with $R = \sum_{t=1}^T N_t$ the total number of observations in \mathbf{s}^* , in the initialization consists in computing a vector of quantile forecasts $\hat{\mathbf{Q}}_0^\tau = \{\hat{Q}_r^\tau\}_{r=1}^{V-1}$ with $V < R$ using any suitable autoregressive model, such as CaViaR.

Then, the two-step procedure consists in:

1. **First step:** a MIDAS-QRF is trained considering the training set $\mathbf{s}^* = \{y_r, \mathbf{x}_{r-1}, \mathbf{MC}_{r-1}, \hat{Q}_{r-1}^\tau\}_{r=1}^V$ and used to compute the quantile prediction \hat{Q}_V^τ .
2. **Second step:** the training set is updated with the additional quantile prediction \hat{Q}_V^τ and the MIDAS-QRF is trained again.

The algorithm iterates between these two steps until the entire dataset

$\mathbf{s}^* = \{y_r, \mathbf{x}_{r-1}, \mathbf{MC}_{r-1}, \hat{Q}_{r-1}^\tau\}_{r=1}^R$ is included in the training set with their respective quantile predictions. Finally, a vector of quantile predictions $\hat{\mathbf{Q}}^\tau = \{\hat{Q}_r^\tau\}_{r=1}^R$ is obtained and can be used also to evaluate the forecast accuracy of the model.

2.4 Empirical Application

Over the past two decades, there has been a growing interest among investors in using energy commodities as hedging and speculative assets, especially during periods of financial and economic downturns. This phenomenon, known as the financialization of energy commodities, along with the deregulation of over-the-counter markets, led to a significant increase of the volatility of energy commodities returns.

Thus, the study of the risks linked to such commodities is particularly relevant under a risk management framework. For this reason, this section shows the empirical application of the static and dynamic versions of the MIDAS-QRF to forecast the well-known financial risk measure VaR of three energy commodities: WTI Crude Oil, Brent Crude Oil and Heating Oil. The performance of the proposed models is measured in terms of statistical adequacy by means of backtesting procedures, and in terms of forecast accuracy, measured using the quantile loss function, i.e. the check function, of Koenker and Bassett Jr (1978) $\rho_\tau(u) = u(\tau - \mathbf{1}_{\{u < 0\}})$. The data summary statistics of the log-returns of each index are reported in Table A.1 along with their graphs in Figures A.1-A.2-A.3.

The MIDAS-QRF and its dynamic specification are employed to estimate one-step-ahead VaR forecasts at three different probability levels ($\tau = 0.01, 0.025, 0.05$) with an expanding-window approach by refitting the models every ten days. The training set considers time series spanning from September 2014 to October 2019. The forecasts are made on an out-of-sample test set composed of 700 observations from November 2019 to April 2022, covering the pre-pandemic, pandemic and post-pandemic period, including the beginning of the Russian-Ukrainian conflict. The richness of information contained in this specific time span allows to train the model in "standard" settings and testing

it in setting in which low volatility periods are alternated by periods of high volatility. This approach allows to test the ability of the model to obtain reliable forecast both in standard settings and in unseen and unexpected situations.

The covariates set includes both low-frequency and daily variables. The low-frequency variables are the monthly Real Broad Dollar Index (DOLL), the quarterly Natural Gas returns (NATGAS) and the quarterly Saudi Arabia Crude Oil Production (SAUDI-PROD). Daily variables are the daily lag 1 and lag 2 of the indexes of interest along with the daily Standard and Poor's 500 Index (SP500). The number of lags was selected to create a dataset of manageable size, enabling a comparison between the proposed MIDAS-QRF model and simpler models that consider only a single covariate. All the daily, monthly and quarterly time series have been by computing their log-returns. The dynamic MIDAS-QRF is trained with the same dataset used for the static version, but the lagged vector of quantile forecasts is introduced as additional covariate, denoted with lag_quant .

Thus, the MIDAS-QRF equation in this empirical application is:

$$\hat{Q}_\tau(Y_{i,t}|X_{i,t}, \mathbf{MC}_{i-1,t})^{MIDAS-QRF} = f_\tau(SP500_{i,t}, MC_{i-1,t}^{DOLL}, MC_{i-1,t}^{NATGAS}, MC_{i-1,t}^{SAUDI}) \quad (2.11)$$

And the dynamic MIDAS-QRF model equation is:

$$\hat{Q}_\tau(Y_{i,t}|\mathbf{X}_{i,t}, \mathbf{MC}_{i-1,t})^{DYN} = f_\tau(lag_quant_{i-1,t}, SP500_{i,t}, MC_{i-1,t}^{DOLL}, MC_{i-1,t}^{NATGAS}, MC_{i-1,t}^{SAUDI}) \quad (2.12)$$

The benchmark models set includes the parametric models GARCH and GARCH-MIDAS (Engle et al., 2013) with Gaussian and Student's-t distributions of the errors, semi-parametric models, that are the four different specifications of the CaViaR model, namely Asymmetric Slope (AS), Symmetric Absolute Value (SAV), Indirect GARCH (IG) and Adaptive (AD), and the standard Quantile Regression Forest of Meinshausen (2006). The functional form of the parametric and semi-parametric models is reported in Table 2.1.

<i>Model</i>	<i>Functional Form</i>	<i>Err. Distr.</i>
GARCH-norm	$Y_{i,t} \mathcal{F}_{i-1,t} = \sqrt{h_{i,t}}\eta_{i,t}$ $h_{i,t} = \omega + \alpha Y_{i-1,t}^2 + \beta h_{i-1,t}$	$\eta_{i,t} \stackrel{i.i.d}{\sim} \mathcal{N}(0, 1)$
GARCH-t	$Y_{i,t} \mathcal{F}_{i-1,t} = \sqrt{h_{i,t}}\eta_{i,t}$ $h_{i,t} = \omega + \alpha Y_{i-1,t}^2 + \beta h_{i-1,t}$	$\eta_{i,t} \stackrel{i.i.d}{\sim} t_\nu$
GM	$\xi_{i,t} = (1 - \alpha - \beta - \gamma/2) + \left(\alpha + \gamma \cdot \mathbb{1}_{(Y_{i-1,t} < 0)} \right) \frac{Y_{i-1,t}^2}{\pi_t} + \beta \xi_{i-1,t}$ $\pi_t = \exp \left\{ m + \zeta \sum_{k=1}^K \delta_k(\omega) Z_{t-k} \right\}$	
CAVIAR-SAV	$Q_{i,t}^\tau = \beta_0 + \beta_1 Q_{i-1,t}^\tau + \beta_2 Y_{i-1,t} $	
CAVIAR-AD	$Q_{i,t}^\tau(\boldsymbol{\beta}) = Q_{i-1,t}^\tau(\beta_1) + \beta_1 \{ [1 + \exp(G[Y_{i-1,t} - Q_{i-1,t}^\tau(\beta_1)])]^{-1} - \tau \}$	
CAVIAR-AS	$Q_{i,t}^\tau = \beta_0 + \beta_1 Q_{i-1,t}^\tau + (\beta_2 \mathbb{1}_{(Y_{i-1,t} > 0)} + \beta_3 \mathbb{1}_{(Y_{i-1,t} < 0)}) Y_{i-1,t} $	
CAVIAR-IG	$Q_{i,t}^\tau = -\sqrt{\beta_0 + \beta_1 (Q_{i-1,t}^\tau)^2 + \beta_2 Y_{i-1,t}^2}$	

Functional forms of the parametric models, that is GARCH, with Gaussian and Student's t distributions for the errors (GARCH-norm, GARCH-std, respectively) and GARCH-MIDAS (GM) models with the four different low-frequency variables. The semi-parametric models are the Aymmetric Absolute Value (SAV), Adaptive (AD), Asymmetric Slope (AS)and Indirect GARCH (IG) specifications of the CaViaR model. We denote with $\mathcal{F}_{i-1,t}$ the information available up to time $i - 1, t$.

Table 2.1: Models specifications

The computational time to fit the MIDAS-QRF and its dynamic specification is equal, on average, to 471 seconds on an ordinary multi-CPU server Intel Xeon with 24 cores.

2.4.1 Backtesting Procedures

Backtesting procedures represent statistical tests employed in VaR analysis to assess the accuracy and reliability of the the models used to forecast VaR.

The main backtesting procedures commonly used in the VaR literature and used in this thesis are:

- **Unconditional Coverage Test** (Kupiec, 1995): tests whether the actual frequency of VaR violations (instances where actual losses exceed the predicted VaR) matches the expected violation frequency. For accurate models, the proportion of VaR violations should align with the VaR confidence level (e.g., for a 5% VaR, breaches should occur about 5% of the time).
- **Conditional Coverage Test** (Christoffersen, 1998): combines the Unconditional Coverage Test with an independence test to evaluate whether the VaR violations are randomly distributed over time and are, thus, independent. As a matter of fact, the presence of clustered violations might indicate a not reliable and robust model.
- **Dynamic Quantile Test** (Manganelli, 2004): tests whether the VaR violations are serially uncorrelated conditional on previous quantile estimates.

2.4.2 MIDAS-QRF Results

The results in terms of quantile loss and backtesting procedures for the MIDAS-QRF model are presented in Tables 2.2-2.3-2.4. The columns UC_pval, CC_pval and DQ_pval indicate the p-value results of the Unconditional Coverage, Conditional Coverage and Dynamic Quantile tests, respectively. The AE column reports the Actual over Expected exceedance ratio. The column %Loss indicates the ratio between the loss of the static version of the MIDAS-QRF model with respect to the other benchmark models:

$$\% Loss = \frac{Loss_{MIDAS-QRF}}{Loss_{Benchmark}}$$

The results of the backtesting procedures show that, differently from the benchmark models, the MIDAS-QRF consistently delivers adequate forecasts at all quantile levels for each index. For instance, for the Brent index the MIDAS-QRF is the only model passing all the backtesting procedures at quantile level 0.01. In terms of forecast accuracy, the MIDAS-QRF outperforms every benchmark model for all index, with a consistent increase in accuracy at the lower quantile levels of the Brent and WTI index.

BRENT						
$\tau = 0.01$						
	<i>Loss</i>	<i>UC_pval</i>	<i>CC_pval</i>	<i>DQ_pval</i>	<i>AE</i>	<i>%Loss</i>
MIDAS-QRF	16.927	0.013	0.025	0.302	2.167	
GARCH-norm	32.498	0.000	0.000	0.001	6.000	52%
GARCH-std	21.138	0.000	0.000	0.000	3.333	80%
CAViAR-SAV	22.302	0.005	0.012	0.863	2.333	76%
CAViAR-AD	30.301	0.001	0.001	0.495	2.667	56%
CAViAR-AS	17.763	0.000	0.000	0.476	3.000	95%
CAViAR-IG	17.672	0.005	0.012	0.743	2.333	96%
STD-RF	26.989	0.000	0.000	0.000	4.333	53%
GM-DOLL	21.986	0.000	0.000	0.063	3.500	77%
GM-NATGAS	23.698	0.000	0.000	0.000	5.500	72%
GM-SAUDIPROD	23.040	0.000	0.000	0.001	4.167	74%
$\tau = 0.025$						
	<i>Loss</i>	<i>UC_pval</i>	<i>CC_pval</i>	<i>DQ_pval</i>	<i>AE</i>	<i>%Loss</i>
MIDAS-QRF	27.956	0.052	0.150	0.661	1.533	
GARCH-norm	43.322	0.000	0.000	0.448	2.867	65%
GARCH-t	35.528	0.000	0.001	0.004	2.067	79%
CAViAR-SAV	31.118	0.213	0.426	0.999	1.333	90%
CAViAR-AD	41.668	0.087	0.028	0.621	1.467	67%
CAViAR-AS	30.157	0.001	0.002	0.981	1.933	93%
CAViAR-IG	29.786	0.213	0.426	1.000	1.333	94%
QRF	36.670	0.000	0.000	0.000	2.333	76%
GM-DOLL	33.193	0.001	0.001	0.567	2.000	84%
GM-NATGAS	33.926	0.000	0.000	0.007	3.133	82%
GM-SAUDIPROD	33.301	0.000	0.000	0.251	2.333	84%
$\tau = 0.05$						
	<i>Loss</i>	<i>UC_pval</i>	<i>CC_pval</i>	<i>DQ_pval</i>	<i>AE</i>	<i>%Loss</i>
MIDAS-QRF	41.602	1.000	0.517	0.990	1.000	
GARCH-norm	56.708	0.000	0.000	1.000	1.733	73%
GARCH-t	50.389	0.022	0.061	0.543	1.433	82%
CAViAR-SAV	44.244	1.000	0.920	1.000	1.000	94%
CAViAR-AD	54.762	0.361	0.006	0.331	1.167	76%
CAViAR-AS	42.719	0.074	0.186	0.930	1.333	97%
CAViAR-IG	44.391	0.580	0.850	1.000	1.100	94%
QRF	49.901	0.005	0.020	0.224	1.533	83%
GM-DOLL	47.451	0.074	0.196	0.999	1.333	88%
GM-NATGAS	47.105	0.000	0.000	0.212	2.167	88%
GM-SAUDIPROD	46.437	0.001	0.003	0.914	1.633	89%

Table 2.2: Loss and Backtesting results of the MIDAS-QRF for the Brent Index. The shade of grey indicate models for which the p-value of the test is greater than the 1% significance level.

WTI		$\tau = 0.01$					
	<i>Loss</i>	<i>UC_pval</i>	<i>CC_pval</i>	<i>DQ_pval</i>	<i>AE</i>	<i>%Loss</i>	
MIDAS-QRF	16.539	0.066	0.078	0.908	1.83		
GARCH-norm	34.805	0.000	0.000	0.682	3.00	47%	
GARCH-t	24.362	0.001	0.002	0.035	2.67	68%	
CAViaR-SAV	24.996	0.013	0.025	0.403	2.17	66%	
CAViaR-AD	33.682	0.005	0.000	0.177	2.33	49%	
CAViaR-AS	24.817	0.000	0.000	0.347	3.00	67%	
CAViaR-IG	25.017	0.066	0.078	0.921	1.83	66%	
QRF	31.076	0.000	0.000	0.003	3.83	53%	
GM-DOLL	17.640	0.005	0.002	0.056	2.33	93%	
GM-NATGAS	17.773	0.013	0.025	0.034	2.17	93%	
GM-SAUDIPROD	18.845	0.000	0.000	0.000	3.33	88%	
		$\tau = 0.025$					
	<i>Loss</i>	<i>UC_pval</i>	<i>CC_pval</i>	<i>DQ_pval</i>	<i>AE</i>	<i>%Loss</i>	
MIDAS-QRF	28.277	0.609	0.201	1.000	1.13		
GARCH-norm	48.663	0.030	0.095	0.874	1.60	58%	
GARCH-t	37.256	0.002	0.010	0.068	1.87	76%	
CAViaR-SAV	31.218	0.087	0.032	0.680	1.47	90%	
CAViaR-AD	45.144	0.139	0.000	0.673	1.40	62%	
CAViaR-AS	29.696	0.052	0.026	0.987	1.53	95%	
CAViaR-IG	30.968	0.087	0.032	1.000	1.47	91%	
QRF	41.786	0.005	0.002	0.807	1.80	67%	
GM-DOLL	29.507	0.087	0.032	0.859	1.47	95%	
GM-NATGAS	29.092	0.017	0.039	0.286	1.67	97%	
GM-SAUDIPROD	30.501	0.000	0.000	0.047	2.27	92%	
		$\tau = 0.05$					
	<i>Loss</i>	<i>UC_pval</i>	<i>CC_pval</i>	<i>DQ_pval</i>	<i>AE</i>	<i>%Loss</i>	
MIDAS-QRF	43.150	0.050	0.113	0.997	1.37		
GARCH-norm	66.613	0.149	0.202	0.703	1.27	62%	
GARCH-t	53.153	0.002	0.004	0.132	1.60	81%	
CAViaR-SAV	46.644	0.361	0.510	0.997	1.17	92%	
CAViaR-AD	62.262	0.205	0.000	0.564	1.23	69%	
CAViaR-AS	49.768	0.022	0.040	0.985	1.43	87%	
CAViaR-IG	46.762	0.149	0.212	1.000	1.27	92%	
QRF	56.984	0.149	0.202	0.996	1.27	76%	
GM-DOLL	45.487	0.580	0.093	0.996	1.10	95%	
GM-NATGAS	44.453	0.022	0.020	0.520	1.43	97%	
GM-SAUDIPROD	45.606	0.005	0.015	0.459	1.53	95%	

Table 2.3: Loss and Backtesting results of the MIDAS-QRF for the WTI Index. The shade of grey indicate models for which the p-value of the test is greater than the 1% significance level.

HEATING OIL						
	$\tau = 0.01$					
	<i>Loss</i>	<i>UC_pval</i>	<i>CC_pval</i>	<i>DQ_pval</i>	<i>AE</i>	<i>%Loss</i>
MIDAS-QRF	12.120	0.134	0.116	0.11	1.67	
GARCH-norm	12.948	0.030	0.047	0.266	2.00	93%
GARCH-t	12.519	0.252	0.152	0.298	1.50	97%
CAViaR-SAV	12.646	0.134	0.010	0.302	1.67	96%
CAViaR-AD	20.670	0.001	0.000	0.000	2.67	59%
CAViaR-AS	13.217	0.134	0.116	0.294	1.67	92%
CAViaR-IG	51.123	0.252	0.452	0.356	1.50	24%
QRF	14.545	0.001	0.002	0.009	2.67	83%
GM-DOLL	12.946	0.005	0.002	0.063	2.33	94%
GM-NATGAS	12.992	0.134	0.010	0.292	1.67	93%
GM-SAUDIPROD	14.354	0.000	0.000	0.000	3.83	84%
	$\tau = 0.025$					
	<i>Loss</i>	<i>UC_pval</i>	<i>CC_pval</i>	<i>DQ_pval</i>	<i>AE</i>	<i>%Loss</i>
MIDAS-QRF	22.461	0.052	0.085	0.247	1.53	
GARCH-norm	22.756	0.213	0.039	0.974	1.33	99%
GARCH-t	22.808	0.213	0.039	0.974	1.33	98%
CAViaR-SAV	22.638	0.796	0.180	0.967	1.07	99%
CAViaR-AD	31.125	0.001	0.000	0.000	1.93	73%
CAViaR-AS	23.138	0.213	0.426	0.978	1.33	97%
CAViaR-IG	23.137	0.009	0.010	0.966	1.73	97%
QRF	26.242	0.000	0.000	0.000	2.20	86%
GM-DOLL	22.730	0.05	0.09	0.65	1.53	99%
GM-NATGAS	22.610	0.14	0.15	0.78	1.40	99%
GM-SAUDIPROD	24.230	0.000	0.000	0.14	2.20	93%
	$\tau = 0.05$					
	<i>Loss</i>	<i>UC_pval</i>	<i>CC_pval</i>	<i>DQ_pval</i>	<i>AE</i>	<i>%Loss</i>
MIDAS-QRF	35.515	0.034	0.024	0.014	1.40	
GARCH-norm	35.763	0.852	0.566	0.995	1.03	99%
GARCH-t	35.893	0.580	0.276	0.997	1.10	98%
CAViaR-SAV	35.399	0.275	0.467	0.997	1.20	100%
CAViaR-AD	42.767	0.034	0.000	0.000	1.40	83%
CAViaR-AS	35.540	0.205	0.108	0.998	1.23	99%
CAViaR-IG	37.269	0.009	0.031	0.985	1.50	95%
QRF	39.255	0.005	0.015	0.022	1.53	90%
GM-DOLL	35.315	0.463	0.763	0.999	1.13	99%
GM-NATGAS	35.095	0.361	0.281	0.999	1.17	100%
GM-SAUDIPROD	36.531	0.022	0.040	0.980	1.43	97%

Table 2.4: Loss and Backtesting results of the MIDAS-QRF for the Heating Oil Index. The shade of grey indicate models for which the p-value of the test is greater than the 1% significance level.

2.4.3 Dynamic MIDAS-QRF Results

The forecast accuracy and the results of the backtesting procedures of the dynamic MIDAS-QRF model are presented in Tables 2.5-2.6-2.7.

These results highlight that, similarly to the MIDAS-QRF, the Dynamic MIDAS-QRF passes all of the backtesting procedures at all quantile levels for each index. In terms of forecast accuracy, the dynamic specification of the MIDAS-QRF outperforms all benchmark models at all quantile level of every index, and the most relevant increase in forecast accuracy is achieved for the WTI and Brent index. Moreover, the comparison in terms of forecast accuracy with the static MIDAS-QRF highlights that the autoregressive structure of the dynamic MIDAS-QRF allows to gain a higher degree of accuracy especially at the lower quantile level 0.01 of each index. This result suggests that introducing a dynamic element into the MIDAS-QRF allows to model tail risk more accurately, especially when the distribution of the variable changes over time.

BRENT						
	$\tau = 0.01$					
	<i>Loss</i>	<i>UC_pval</i>	<i>CC_pval</i>	<i>DQ_pval</i>	<i>AE</i>	<i>%Loss</i>
DYN MIDAS-QRF	15.922	0.013	0.025	0.231	2.167	
MIDAS-QRF	16.927	0.013	0.025	0.302	2.167	94%
GARCH-norm	32.498	0.000	0.000	0.001	6.000	49%
GARCH-std	21.138	0.000	0.000	0.000	3.333	75%
CAViAR-SAV	22.302	0.005	0.012	0.863	2.333	71%
CAViAR-AD	30.301	0.001	0.001	0.495	2.667	53%
CAViAR-AS	17.763	0.000	0.000	0.476	3.000	90%
CAViAR-IG	17.672	0.005	0.012	0.743	2.333	90%
STD-RF	26.989	0.000	0.000	0.000	4.333	59%
GM-DOLL	21.986	0.000	0.000	0.063	3.500	72%
GM-NATGAS	23.698	0.000	0.000	0.000	5.500	67%
GM-SAUDIPROD	23.040	0.000	0.000	0.001	4.167	69%
	$\tau = 0.025$					
	<i>Loss</i>	<i>UC_pval</i>	<i>CC_pval</i>	<i>DQ_pval</i>	<i>AE</i>	<i>%Loss</i>
DYN MIDAS-QRF	27.288	1.000	0.682	0.997	1.000	
MIDAS-QRF	27.956	0.052	0.150	0.661	1.533	98%
GARCH-norm	43.322	0.000	0.000	0.448	2.867	63%
GARCH-t	35.528	0.000	0.001	0.004	2.067	77%
CAViAR-SAV	31.118	0.213	0.426	0.999	1.333	88%
CAViAR-AD	41.668	0.087	0.028	0.621	1.467	65%
CAViAR-AS	30.157	0.001	0.002	0.981	1.933	90%
CAViAR-IG	29.786	0.213	0.426	1.000	1.333	92%
QRF	36.670	0.000	0.000	0.000	2.333	74%
GM-DOLL	33.193	0.001	0.001	0.567	2.000	82%
GM-NATGAS	33.926	0.000	0.000	0.007	3.133	80%
GM-SAUDIPROD	33.301	0.000	0.000	0.251	2.333	82%
	$\tau = 0.05$					
	<i>Loss</i>	<i>UC_pval</i>	<i>CC_pval</i>	<i>DQ_pval</i>	<i>AE</i>	<i>%Loss</i>
DYN MIDAS-QRF	41.967	0.711	0.593	0.999	1.067	
QRF	41.602	1.000	0.517	0.990	1.000	101%
GARCH-norm	56.708	0.000	0.000	1.000	1.733	74%
GARCH-t	50.389	0.022	0.061	0.543	1.433	83%
CAViAR-SAV	44.244	1.000	0.920	1.000	1.000	95%
CAViAR-AD	54.762	0.361	0.006	0.331	1.167	77%
CAViAR-AS	42.719	0.074	0.186	0.930	1.333	98%
CAViAR-IG	44.391	0.580	0.850	1.000	1.100	95%
QRF	49.901	0.005	0.020	0.224	1.533	84%
GM-DOLL	47.451	0.074	0.196	0.999	1.333	88%
GM-NATGAS	47.105	0.000	0.000	0.212	2.167	89%
GM-SAUDIPROD	46.437	0.001	0.003	0.914	1.633	90%

Table 2.5: Loss and Backtesting results of the Dynamic MIDAS-QRF for the Brent Index. The shade of grey indicate models for which the p-value of the test is greater than the 1% significance level.

WTI		$\tau = 0.01$				
	<i>Loss</i>	<i>UC_pval</i>	<i>CC_pval</i>	<i>DQ_pval</i>	<i>AE</i>	<i>%Loss</i>
DYN MIDAS-QRF	14.848	0.689	0.166	1.000	1.17	
MIDAS-QRF	16.539	0.066	0.078	0.908	1.83	90%
GARCH-norm	34.805	0.000	0.000	0.682	3.00	43%
GARCH-t	24.362	0.001	0.002	0.035	2.67	61%
CAViaR-SAV	24.996	0.013	0.025	0.403	2.17	59%
CAViaR-AD	33.682	0.005	0.000	0.177	2.33	44%
CAViaR-AS	24.817	0.000	0.000	0.347	3.00	60%
CAViaR-IG	25.017	0.066	0.078	0.921	1.83	59%
QRF	31.076	0.000	0.000	0.003	3.83	48%
GM-DOLL	17.640	0.005	0.002	0.056	2.33	84%
GM-NATGAS	17.773	0.013	0.025	0.034	2.17	84%
GM-SAUDIPROD	18.845	0.000	0.000	0.000	3.33	79%
		$\tau = 0.025$				
	<i>Loss</i>	<i>UC_pval</i>	<i>CC_pval</i>	<i>DQ_pval</i>	<i>AE</i>	<i>%Loss</i>
DYN MIDAS-QRF	28.160	0.609	0.201	1.000	1.13	
MIDAS-QRF	28.277	0.609	0.201	1.000	1.13	100%
GARCH-norm	48.663	0.030	0.095	0.874	1.60	58%
GARCH-t	37.256	0.002	0.010	0.068	1.87	76%
CAViaR-SAV	31.218	0.087	0.032	0.680	1.47	90%
CAViaR-AD	45.144	0.139	0.000	0.673	1.40	62%
CAViaR-AS	29.696	0.052	0.026	0.987	1.53	95%
CAViaR-IG	30.968	0.087	0.032	1.000	1.47	91%
QRF	41.786	0.005	0.002	0.807	1.80	67%
GM-DOLL	29.507	0.087	0.032	0.859	1.47	95%
GM-NATGAS	29.092	0.017	0.039	0.286	1.67	97%
GM-SAUDIPROD	30.501	0.000	0.000	0.047	2.27	92%
		$\tau = 0.05$				
	<i>Loss</i>	<i>UC_pval</i>	<i>CC_pval</i>	<i>DQ_pval</i>	<i>AE</i>	<i>%Loss</i>
DYN MIDAS-QRF	43.800	0.568	0.672	0.991	0.90	
MIDAS-QRF	43.150	0.050	0.113	0.997	1.37	102%
GARCH-norm	66.613	0.149	0.202	0.703	1.27	66%
GARCH-t	53.153	0.002	0.004	0.132	1.60	82%
CAViaR-SAV	46.644	0.361	0.510	0.997	1.17	94%
CAViaR-AD	62.262	0.205	0.000	0.564	1.23	70%
CAViaR-AS	49.768	0.022	0.040	0.985	1.43	88%
CAViaR-IG	46.762	0.149	0.212	1.000	1.27	94%
QRF	56.984	0.149	0.202	0.996	1.27	77%
GM-DOLL	45.487	0.580	0.093	0.996	1.10	96%
GM-NATGAS	44.453	0.022	0.020	0.520	1.43	99%
GM-SAUDIPROD	45.606	0.005	0.015	0.459	1.53	96%

Table 2.6: Loss and Backtesting results of the Dynamic MIDAS-QRF for the WTI Index. The shade of grey indicate models for which the p-value of the test is greater than the 1% significance level.

HEATING OIL						
$\tau = 0.01$						
	<i>Loss</i>	<i>UC_pval</i>	<i>CC_pval</i>	<i>DQ_pval</i>	<i>AE</i>	<i>%Loss</i>
DYN MIDAS-QRF	11.827	0.252	0.153	0.178	1.50	
MIDAS-QRF	12.120	0.134	0.116	0.11	1.67	98%
GARCH-norm	12.948	0.030	0.047	0.266	2.00	91%
GARCH-t	12.519	0.252	0.152	0.298	1.50	94%
CAViaR-SAV	12.646	0.134	0.010	0.302	1.67	94%
CAViaR-AD	20.670	0.001	0.000	0.000	2.67	57%
CAViaR-AS	13.217	0.134	0.116	0.294	1.67	89%
CAViaR-IG	51.123	0.252	0.452	0.356	1.50	23%
QRF	14.545	0.001	0.002	0.009	2.67	81%
GM-DOLL	12.946	0.005	0.002	0.063	2.33	91%
GM-NATGAS	12.992	0.134	0.010	0.292	1.67	91%
GM-SAUDIPROD	14.354	0.000	0.000	0.000	3.83	82%
$\tau = 0.025$						
	<i>Loss</i>	<i>UC_pval</i>	<i>CC_pval</i>	<i>DQ_pval</i>	<i>AE</i>	<i>%Loss</i>
DYN MIDAS-QRF	20.975	0.213	0.177	0.777	1.33	
MIDAS-QRF	22.461	0.052	0.085	0.247	1.53	93%
GARCH-norm	22.756	0.213	0.039	0.974	1.33	92%
GARCH-t	22.808	0.213	0.039	0.974	1.33	92%
CAViaR-SAV	22.638	0.796	0.180	0.967	1.07	93%
CAViaR-AD	31.125	0.001	0.000	0.000	1.93	67%
CAViaR-AS	23.138	0.213	0.426	0.978	1.33	91%
CAViaR-IG	23.137	0.009	0.010	0.966	1.73	91%
QRF	26.242	0.000	0.000	0.000	2.20	80%
GM-DOLL	22.73	0.05	0.09	0.65	1.53	92%
GM-NATGAS	22.61	0.14	0.15	0.78	1.40	93%
GM-SAUDIPROD	24.230	0.000	0.000	0.14	2.20	87%
$\tau = 0.05$						
	<i>Loss</i>	<i>UC_pval</i>	<i>CC_pval</i>	<i>DQ_pval</i>	<i>AE</i>	<i>%Loss</i>
DYN MIDAS-QRF	34.416	0.106	0.090	0.046	1.30	
MIDAS-QRF	35.515	0.034	0.024	0.014	1.40	97%
GARCH-norm	35.763	0.852	0.566	0.995	1.03	96%
GARCH-t	35.893	0.580	0.276	0.997	1.10	96%
CAViaR-SAV	35.399	0.275	0.467	0.997	1.20	97%
CAViaR-AD	42.767	0.034	0.000	0.000	1.40	80%
CAViaR-AS	35.540	0.205	0.108	0.998	1.23	97%
CAViaR-IG	37.269	0.009	0.031	0.985	1.50	92%
QRF	39.255	0.005	0.015	0.022	1.53	88%
GM-DOLL	35.315	0.463	0.763	0.999	1.13	97%
GM-NATGAS	35.095	0.361	0.281	0.999	1.17	98%
GM-SAUDIPROD	36.531	0.022	0.040	0.980	1.43	94%

Table 2.7: Loss and Backtesting results of the Dynamic MIDAS-QRF for the Heating Oil Index. The shade of grey indicate models for which the p-value of the test is greater than the 1% significance level.

Figure 2.1 displays the predictions at the three quantile levels of the Heating Oil indexes obtained with both versions of the MIDAS-QRF model. Predictions of the remaining two indexes are represented in Figures A.4-A.5. It is worth noticing that, for all three indexes, both the MIDAS-QRF and its dynamic specification effectively manage to obtain accurate forecasts both in situations similar to the one in the training set, as well as during the unexpected high volatility periods related to the pandemic and the Russian-Ukrainian conflict.

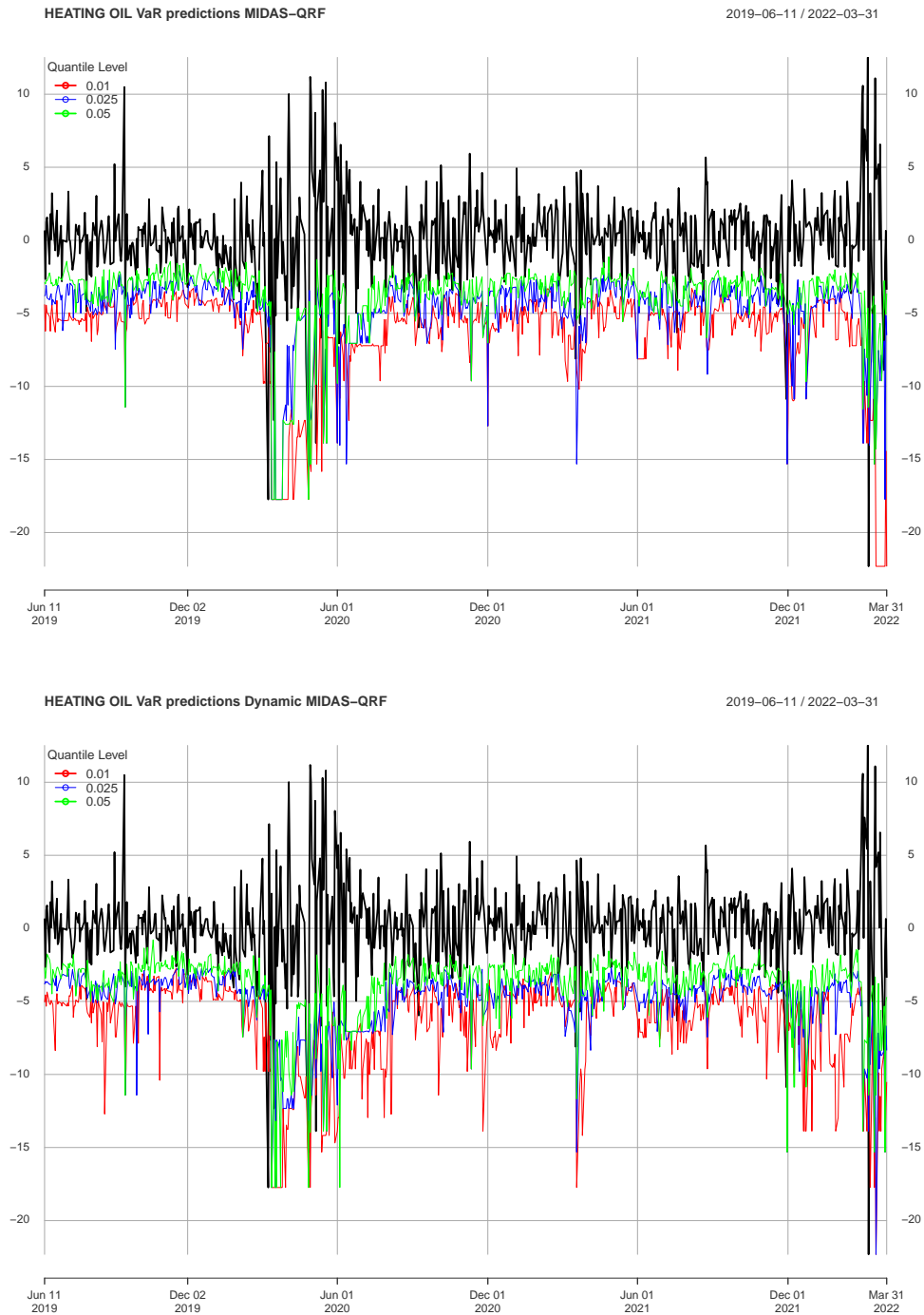


Figure 2.1: Heating Oil (black line) index out-of-sample predictions at quantile levels $\tau = 0.01, 0.025, 0.05$. The top panel and the bottom panel show the predictions obtained with the dynamic MIDAS-QRF model, respectively.

2.4.4 Variable Importance

The variable importance of the static and dynamic MIDAS-QRF is computed to evaluate the relevance of macroeconomic variables and the *lag_quant* variable in training the

MIDAS-QRF and the dynamic MIDAS-QRF. Figures 2.2-2.3-2.4 depict the bar graphs showing the variable importance of the proposed models at all three quantile levels for the Heating Oil index.

The variable importance analysis reveals the significant role of macroeconomic variables in both the static and dynamic MIDAS-QRF models. For instance, in the MIDAS-QRF the variable DOLL is among the top three important variables across all quantile levels. The importance of the other two low-frequency variables changes across quantile levels, but it is always positive. Concerning the dynamic MIDAS-QRF instead, the most important variable at all quantile level is *lag_quant*, highlighting the relevant role of the dynamic component in training the proposed model. Similarly to the static MIDAS-QRF, the most important low-frequency variable is DOLL, whereas the importance of the other two low-frequency variables remains positive at all quantile levels.

As well as for the Heating Oil index, also for the other two indexes, all the macroeconomic variables and the *lag_quant* variable play a significant role in training the two versions of the proposed model. In particular, for the Brent index all three macroeconomic variables are among the most important variables both in the static and dynamic MIDAS-QRF, especially the DOLL one.

In conclusion, these results highlight the relevant role of macroeconomic variables in capturing market risk at low quantile levels and in delivering accurate forecasts. The results also show that the forecast accuracy of the MIDAS-QRF can be further improved by adding a dynamic component. In this case, empirical results show that also the dynamic MIDAS-QRF outperforms benchmark models and passes all the backtesting procedures.

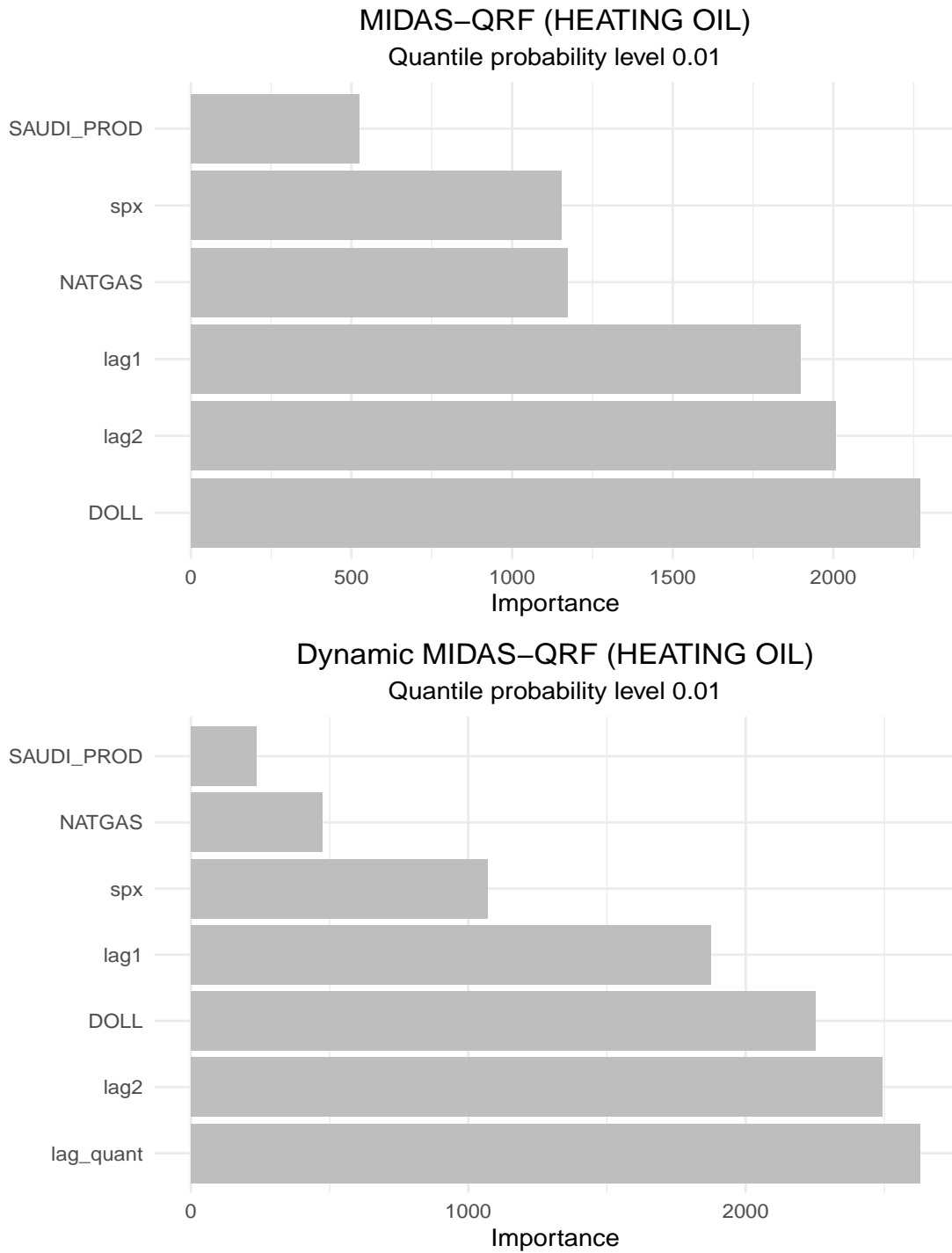


Figure 2.2: Variable importance for the static MIDAS-QRF at $\tau = 0.01$ for the Heating Oil index

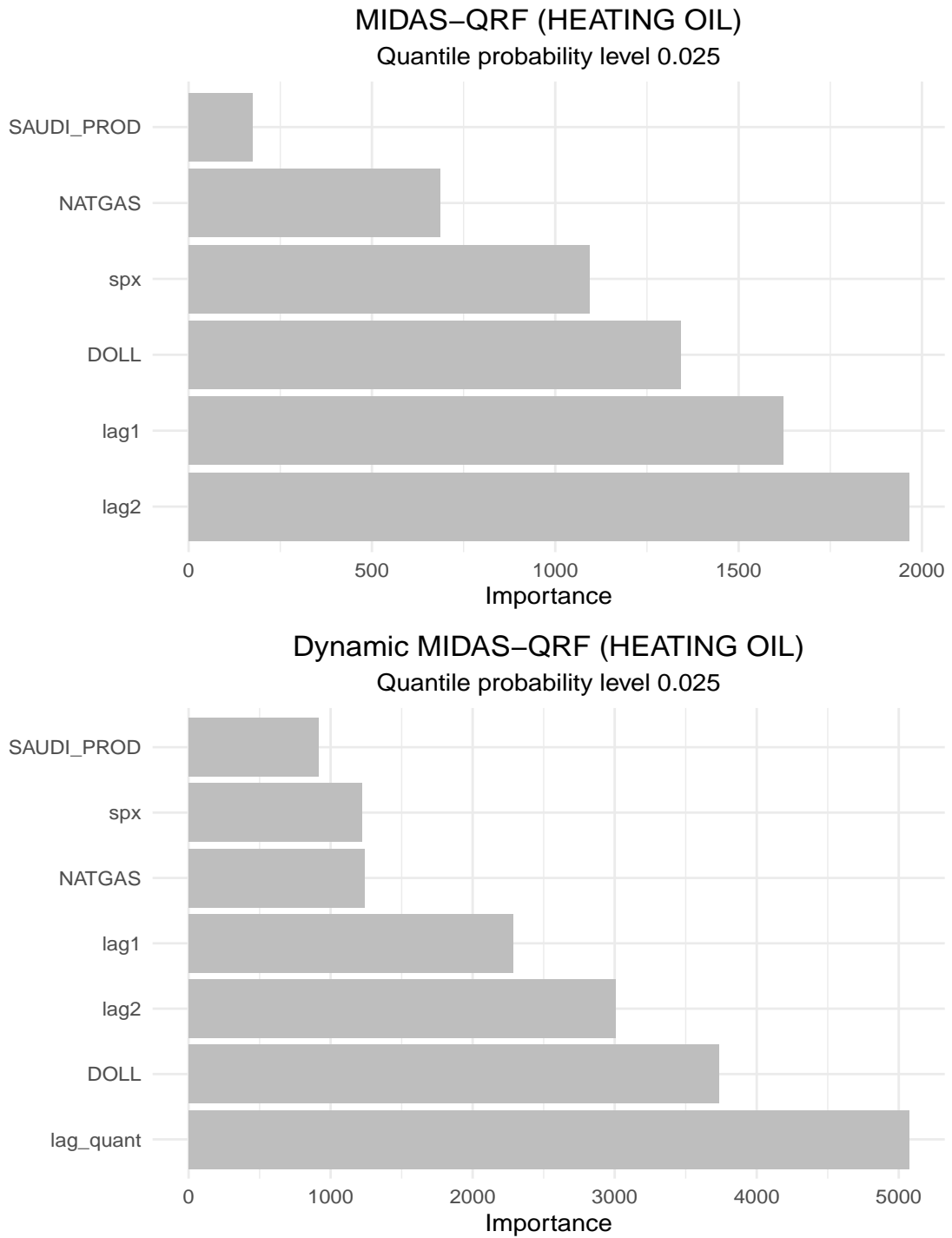


Figure 2.3: Variable importance for the static MIDAS-QRF at $\tau = 0.025$ for the Heating Oil index

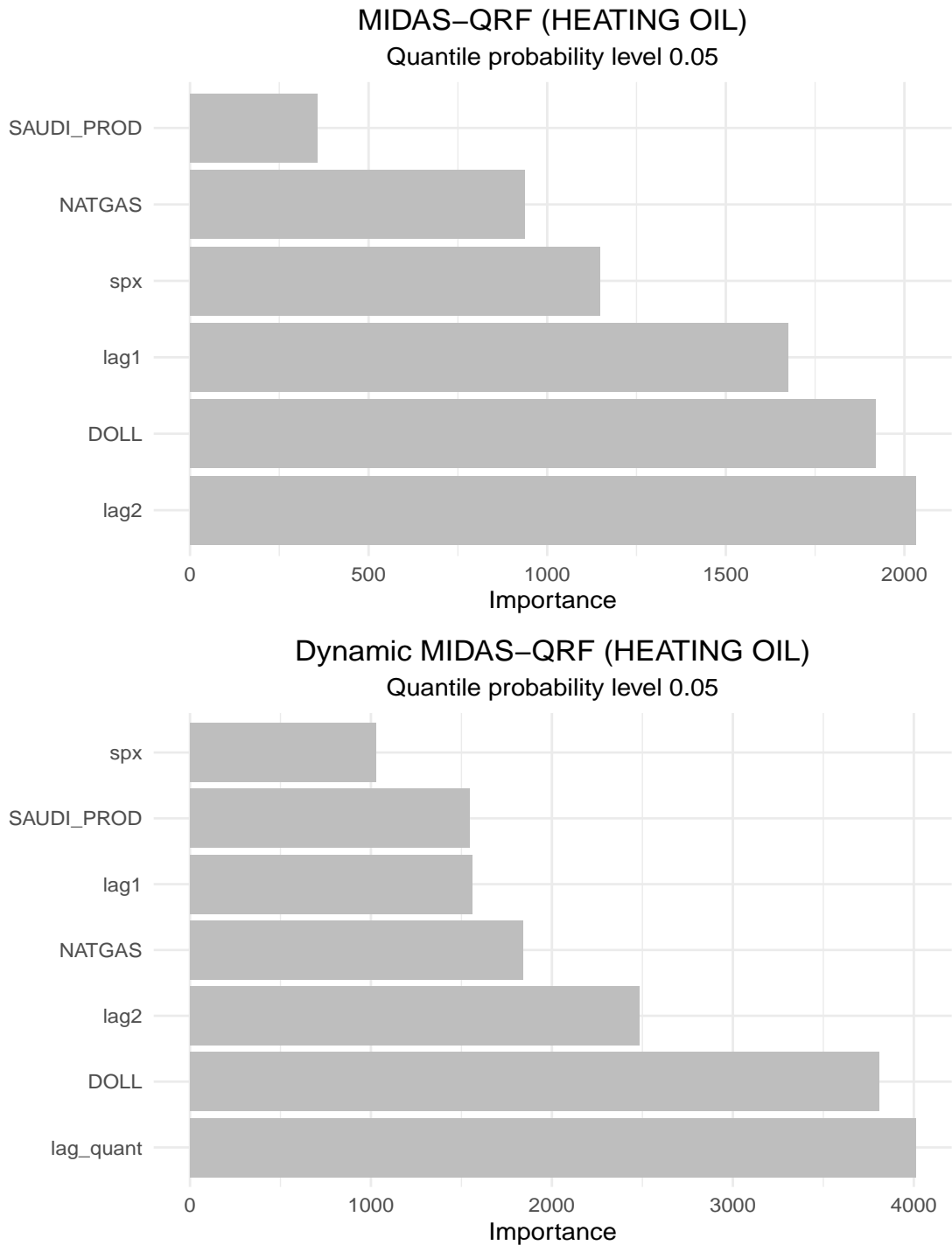


Figure 2.4: Variable importance for the static MIDAS-QRF at $\tau = 0.05$ for the Heating Oil index

2.5 Conclusions

This chapter introduces a new model called MIDAS-QRF to compute conditional quantiles in a machine learning framework to jointly account for complexity, non-

linearity and mixed-frequencies in data. The proposed model relies on the MIDAS methodology of Ghysels et al. (2007) to exploit information coming from low-frequency variables in order to compute quantiles through the QRF algorithm of Meinshausen (2006), which allows to infer the entire conditional distribution of the response variable through the Random Forest algorithm (Breiman, 2001).

The benefits of this approach are twofold: first, it allows to model non-linear relations among variables without making any parametric assumption and to study the behaviour of the phenomena on the tails. In this sense, the MIDAS-QRF results particularly useful in settings characterised by complex relationships among variables, such as the financial and economics one. Second, it extends the QRF algorithm by considering mixed-frequency data by introducing a feature that has never been considered in in Random Forests algorithms. Moreover, the employment of the PCA on the low-frequency variables to compute the MIDAS components offers a novel perspective on estimating the ω_2 parameter of the MIDAS model while shrinking the computational burden of the MIDAS-QRF training.

The proposed model is applied to a real financial dataset to forecast the VaR of three commodities index. The empirical findings highlight the relevant role of macroeconomic variables in capturing market risk at low quantile levels to deliver accurate forecasts. The results also show that the forecast accuracy of a MIDAS-QRF model can be further improved by adding a dynamic component to model the dynamic distribution of financial variables. In this case, also the dynamic MIDAS-QRF outperforms benchmark models and passes all the backtesting procedures.

Chapter 3

Finite mixtures of Quantile Regression Forests and their application to GDP growth-at-risk from climate change

3.1 Introduction

Regression models target the expected value of the conditional distribution of the outcome given a set of covariates. When the distribution of the outcome is asymmetric, modelling other location parameters, e.g. percentiles of the conditional distribution, may offer a more complete picture of the outcome of the distribution compared with models describing only its centre.

The idea of modelling location parameters has a long history in statistics. The seminal paper of Koenker and Bassett Jr (1978) is regarded as the first detailed development of Quantile Regression (QR), which represents a generalization of median regression. QR approach is particularly useful when modeling data characterised by skewness, heavy tails, outliers, truncation, censoring and heteroschedasticity. The flexibility of this model allows for a wide range of applications in fields such as economics, finance, healthcare, environmental science, and marketing; for a detailed review of the most used QR techniques, see Koenker (2005) and Koenker et al. (2017).

Recently, extensions of QR modelling have been proposed in high dimensional framework and in a non-parametric context including the QR Neural Networks (White, 1992), the QR Support Vector Machines (Hwang and Shim, 2005, Xu et al., 2015) the QR kernel based algorithms (Christmann and Steinwart, 2008) the QR Forests (QRF) (Meinshausen, 2006) and the Generalized QR Forests (Athey et al., 2019).

Empirical applications often entail dependent observations in the form of hierarchically structured data: this is the case of spatial, multilevel or longitudinal sample designs. In these contexts, when regression models are considered, the potential association between

dependent observations should be taken into account in order to provide valid and efficient inferences. This is often achieved by using random of mixed effects model where subject-specific random effects are considered in the linear predictors.

Throughout the statistical and econometrics literature only recently random effects models have been used to capture the dependence from a QR perspective for clustered, multilevel, spatial and repeated measurements. Applications in fields such as medicine, environmental science, finance and economics have been particularly studied: for a detailed review of these techniques see for example Farcomeni (2012a), Smith et al. (2015), Alfò et al. (2017), Marino et al. (2018), Merlo et al. (2021), Hendricks and Koenker (1992), Pandey and Nguyen (1999), Reich et al. (2011), Bassett and Chen (2002), Kozumi and Kobayashi (2011), Bernardi et al. (2015, 2018), Merlo et al. (2022c,b).

In these models, individual-specific random effects (coefficients) result useful to describe the influence of omitted covariates on parameter estimates of the observed ones. In this context, the random effects (coefficients) are often thought of as representing (individual-specific) unobserved heterogeneity, while observed covariates describe the observed counterpart (the fixed part of the models). However, in some applications a parametric assumption on the fixed part of the model may not be appropriate, leading to inaccurate conclusions regarding the phenomenon of interest. For this reason, QR machine learning models, incorporating random effects, may be more suitable to model complex and non-linear relationships among the response variable and the covariates in case of hierarchically structured data.

Only recently random effects machine learning algorithms have been introduced to model dependence in a standard regression framework; see, for example, Mixed-Effects Neural Networks (Xiong et al., 2019), Mixed-Effects Support Vector Machines (Luts et al., 2012) and Mixed-Effects Random Forests (Hajjem et al., 2014, 2011, Sela and Simonoff, 2012)). These models are inadequate when the main interest of the research is the conditional quantiles of the distribution of the outcome.

This chapter aims at filling this gap by introducing a new model called Finite Mixtures of Quantile Regression Forests (FM-QRF). The aim of the proposed methodology is to build a data-driven model to estimate quantiles of longitudinal data in a non-parametric framework. To this end, the QR finite mixtures approach of (Merlo et al., 2022a, Tian et al., 2014, 2016, Alfò et al., 2017) is extended to the machine learning realm. The FM-QRF is based on well known random effects machine learning algorithms, but leaves the random effects distribution unspecified and estimates the fixed part of the model with a QRF.

The quantile estimates are obtained with an iterative procedure based on the Expectation Maximization-type algorithm (EM) using the Asymmetric Laplace distribution (AL) as working likelihood. The suggested methodology may be considered as an extension to a non-linear and non-parametric framework the work of Geraci and Bottai (2007, 2014), Alfò et al. (2017) as well as an extension to a QR framework of the mixed-modeling approach presented in Hajjem et al. (2014).

The FM-QRF performance is tested with a large scale simulation study and its behaviour is compared with a set of competitor models. The FM-QRF is empirically applied to a longitudinal dataset to assess the effects of climate-change on the distribution of future growth of GDP of 210 worldwide countries. One of the first contributions in investigating the effects of climate change on GDP growth is by Kiley (2021), based on the concept of Growth-at-risk (GaR) introduced in Yao and Wang (2001). GaR is represented by the lower quantiles of the GDP growth and measures the expected maximum economic downturn given a probability level over a certain time-period.

The aim of this chapter is to extend the findings of Kiley (2021) by employing the FM-QRF to unveil non-linear complex relationship among GDP growth and climate-related variables in a mixed-effects framework. In particular, the long-term estimate of the future GaR is obtained by considering covariates related to temperature and precipitations. Consistent with prior literature, the findings shown in this chapter indicate that unsustainable climate practices will have adverse impacts on most of the countries, with significant heterogeneous effects among them. It is also found that temperature and precipitations differently affect upper and lower quantiles of the GDP growth conditional distribution, and that, in contrast to previous findings based on linear approaches, precipitations also play a relevant role in affecting its tails, especially in the upper quantiles.

The rest of the chapter is organized as follows. Section 3.2 describes the methodology of the FM-QRF. Section 3.3 shows the results of the simulation study. Section 3.4 shows the results of the case study on climate-change related data and Section 3.5 contains concluding remarks and outlines possible future research agenda.

3.2 Methodology

This chapter introduces the FM-QRF and provides a detailed explanation of the EM algorithm used to train the proposed model.

3.2.1 Finite Mixtures of Quantile Regression Forest

Let $Y_{it}, i = 1, \dots, N, t = 1, \dots, T_i$ be the response variable for the i -th statistical unit observed at time t . Let y_{it} be the realisation of the outcome variable and denote with $\mathbf{x}_{it} \in \mathbb{R}^p$ the vector of observed explanatory variables with components $x_{it,j}, j = 1, \dots, p$ and $x_{it,1} \equiv 1$. For a given quantile level $\tau \in (0, 1)$, in a longitudinal and clustered data setting, denote $\mathbf{b}_\tau = \{b_{1,\tau}, \dots, b_{N,\tau}\}$ the vector of unit- and quantile-specific random coefficients. The response Y_{it} is assumed to follow an Asymmetric Laplace density (ALD - Yu and Moyeed, 2001):

$$f_{y|b}(y_{it}|b_{i,\tau}; \tau) = \frac{\tau(1-\tau)}{\sigma_\tau} \exp \left\{ -\rho_\tau \left(\frac{y_{it} - \mu_{it,\tau}}{\sigma_\tau} \right) \right\}, \quad (3.1)$$

where $\tau, \sigma_\tau > 0$ and $\mu_{it,\tau}$ represent, respectively, the skewness, the scale, and the location parameter of the distribution while the latter one is also the quantile of the conditional

distribution. The function $\rho_\tau(u) = u(\tau - \mathbf{1}_{\{u < 0\}})$ represents the quantile loss function of Koenker and Bassett Jr (1978). As it is well known in the literature the ALD is used as a working model able to recast estimation of parameters for the linear QR model in a Maximum Likelihood framework.

In the QR framework, the location parameter $\mu_{it,\tau}$ is often modeled as:

$$\mu_{it,\tau} = \mathbf{x}'_{it}\boldsymbol{\beta}_\tau + b_{i,\tau} \quad \tau \in (0, 1), \quad (3.2)$$

where the random effect $b_{i,\tau}$ is time-constant and varies across statistical units according to a distribution $f_b(\cdot)$ with support \mathcal{B} where $E[b_{i,\tau}] = 0$ is used for parameter identifiability. Rather than specifying such a distribution parametrically as in, e.g., Geraci and Bottai (2007), here it is left unspecified and estimated directly from the observed data via a Non-Parametric Maximum Likelihood approach (NPML - Laird, 1978). Moreover, the model (3.2) is extended to a machine learning framework using a non-parametric unknown function $g_\tau(\mathbf{x}_{it})$ instead of the traditional linear one $\mathbf{x}'_{it}\boldsymbol{\beta}_\tau$.

More in detail, the distribution $f_b(\cdot)$ is approximated by a discrete distribution on $K < N$ locations $\alpha_{k,\tau}$ so that:

$$\alpha_{k,\tau} \sim \sum_{k=1}^K \pi_{k,\tau} \delta_{\alpha_{k,\tau}}, \quad (3.3)$$

where the probability $\pi_{k,\tau}$ is defined as $\pi_{k,\tau} = \mathbb{P}(b_{i,\tau} = \alpha_{k,\tau})$ with $i = 1, \dots, N$ and $k = 1, \dots, K$ and $\delta_{\alpha_{k,\tau}}$ is a one-point distribution putting a unit mass at $\alpha_{k,\tau}$. Under this approach, for $b_{i,\tau} = \alpha_{k,\tau}$, the location parameter of the ALD in equation (3.2) becomes

$$\mu_{itk,\tau} = g_\tau(\mathbf{x}_{it}) + \alpha_{k,\tau} \quad \tau \in (0, 1), \quad (3.4)$$

where $g_\tau : \mathbb{R}^p \rightarrow \mathbb{R}$.

The model likelihood becomes:

$$L(\Phi_\tau) = \prod_{i=1}^N \sum_{k=1}^K \left\{ \prod_{t=1}^{T_i} f_{y|b}(y_{it}|b_{i,\tau} = \alpha_{k,\tau}; \tau) \right\} \pi_{k,\tau}, \quad (3.5)$$

where $\Phi_\tau = \{\sigma_\tau, g_\tau(\mathbf{x}_{it}), \alpha_{1,\tau}, \dots, \alpha_{K,\tau}, \pi_{1,\tau}, \dots, \pi_{K,\tau}\}$ is the vector of unknown parameters.

It is worth highlighting that the proposed FM-QRF can be also considered as an extension of: (i) the QRF (Meinshausen, 2006) because a random part is added to the non-parametric unknown function of QRF; (ii) the QR for longitudinal data based on latent Markov subject-specific parameters (Farcomeni, 2012b) because the linear fixed-part is replaced by the function $g_\tau(\mathbf{x}_{it})$.

Differently from previous contributions (see Geraci and Bottai, 2007, 2014, Farcomeni, 2012a), the FM-QRF relies on the NPML, which is based on a finite-mixture representa-

tion of the random part of model (3.2). This approach does not require to make any a-priori assumption on the distribution of the random effects, making the FM-QRF a valid data-driven approach resistant to misspecification (Alfò et al., 2017, Farcomeni, 2012a).

The simultaneous estimation of $g_\tau(\mathbf{x}_{it})$ and $b_{k,\tau}$ in a QR setting poses several challenges, and the next section reports the EM algorithm developed to estimate both $g_\tau(\mathbf{x}_{it})$ and the $\alpha_{k,\tau}$ of the proposed FM-QRF.

3.2.2 Parameters Estimation with the EM Algorithm

Following previous contributions (Tian et al., 2014, Merlo et al., 2022a, Alfò et al., 2017), the estimates $\hat{g}_\tau(\mathbf{x}_{it})$ and $\hat{b}_{k,\tau}$ of (3.4) are computed iteratively: in the first step the $g_\tau(\mathbf{x}_{it})$ function is estimated using the algorithm developed for the QRF approach (Meinshausen, 2006), then, in the second step, given $\hat{g}_\tau(\mathbf{x}_{it})$, the random-effects $b_{k,\tau}$ s are obtained by maximising (3.6) with the EM algorithm.

The complete data log-likelihood function employed in the EM algorithm is obtained starting from the finite mixture representation in (3.5), in which each observation i can be considered as drawn from one of the K locations. Let w_{ik} be the indicator variable equal to 1 if the i -th unit belongs to the k -th component of the finite mixture, and 0 otherwise. The EM algorithm treats as missing data the component membership w_{ik} . Thus the log-likelihood for the complete data is:

$$\ell_c(\Phi_\tau) = \sum_{i=1}^N \sum_{k=1}^K w_{ik,\tau} \left\{ \sum_{t=1}^{T_i} \log(f_{y|b}(y_{it}|b_{i,\tau} = \alpha_{k,\tau}; \tau)) + \log(\pi_{k,\tau}) \right\}. \quad (3.6)$$

The algorithm for the estimation of the parameters in model (3.4) is as it follows. Firstly, the values of $\hat{\alpha}_{k,\tau}^{(0)}$, $\hat{\sigma}_\tau^{(0)}$, $\hat{\pi}_{k,\tau}^{(0)}$, $\hat{g}_\tau(\mathbf{x}_{it})^{(0)}$ are initialised. The value of $\hat{g}_\tau(\mathbf{x}_{it})^{(0)}$ at level τ is estimated by means of the algorithm used for QRF, fitted with the training set $\mathcal{T}^{(0)} = \{(y_{it}, \mathbf{x}_{it})\}_{\substack{i=1, \dots, N \\ j=1, \dots, T_i}}$ ignoring the clustered structure of the data.

Subsequently, given $\hat{g}_\tau(\mathbf{x}_{it})^{(0)}$, in the **E-step** the estimates $\hat{w}_{ik,\tau}^{(r+1)}$, $\hat{\pi}_{k,\tau}^{(r+1)}$, $\hat{g}_\tau(\mathbf{x}_{it})^{(r+1)}$ are computed. The estimate values $\hat{w}_{ik,\tau}^{(r+1)}$ and $\hat{\pi}_{k,\tau}^{(r+1)}$ are obtained with the following expressions:

$$\hat{w}_{ik,\tau}^{(r+1)} = \mathbb{E}[w_{ik,\tau} | \mu_{itk}, \hat{\Phi}_\tau^{(r)}] = \frac{\prod_{t=1}^{T_i} f_{y|b}(y_{it}|b_{i,\tau} = \alpha_{k,\tau}; \tau)^{(r)} \hat{\pi}_{k,\tau}^{(r)}}{\sum_{l=1}^K \prod_{t=1}^{T_i} f_{y|b}(y_{it}|b_{i,\tau} = \alpha_{l,\tau}; \tau)^{(r)} \hat{\pi}_{l,\tau}^{(r)}}, \quad (3.7)$$

$$\hat{\pi}_{k,\tau}^{(r+1)} = \frac{1}{N} \sum_{i=1}^N \hat{w}_{ik,\tau}^{(r+1)}, \quad (3.8)$$

where $f_{y|b}(y_{it}|b_{i,\tau} = \alpha_{k,\tau}; \tau)^{(r)}$ is the value of the ALD (3.1) at step r related to the t -th measurement of the i -th statistical unit when considering the k -th component of the finite mixture.

Then, given $\hat{w}_{ik,\tau}^{(r+1)}$ and $\hat{\pi}_{k,\tau}$, $\hat{g}_\tau(\mathbf{x}_{it})^{(r+1)}$ is updated as it follows. First, the quantity $y_{it}^{*(r+1)} = y_{it} - \hat{\alpha}_{k,\tau}^{(r)}$ is computed, which represents the unknown function of the model at step $r + 1$. The resulting training set $\mathcal{T}^{(r+1)} = \left\{ \left(y_{it}^{*(r+1)}, \mathbf{x}_{it} \right) \right\}_{\substack{i=1,\dots,N \\ j=1,\dots,T_i}}$ is used to fit a QRF to estimate $\hat{g}_\tau(\mathbf{x}_{it})^{(r+1)}$ at level τ accounting for the weight $\hat{w}_{ik,\tau}^{(r+1)}$ of each observation.

Then, in the **M-step** the estimation of $\hat{\sigma}_\tau$ and $\hat{\alpha}_{k,\tau}$ are obtained by maximising the expectation $\mathbb{E}[\ell_c(\Phi_\tau) | \mu_{itk}, \hat{\Phi}_\tau^{(r)}]$ with respect to $\hat{\sigma}_\tau$ and $\hat{\alpha}_{k,\tau}$ by numerical optimisation techniques. In particular, in this chapter the Nelder-Mead algorithm (Nelder and Mead, 1965) has been implemented. Subsequently, $\hat{\alpha}_{i,\tau}^{(r)}$ are estimated by means of (3.3).

The E- and M-steps are alternated iteratively until convergence, that is reached when difference between the likelihood of two consecutive steps is smaller than a certain threshold. A schematic description of the algorithm is presented below.

Algorithm 1: Mixed-Effects Quantile Regression Forest

Data: For a fixed quantile level τ , $\mathcal{T} = \{(y_{it}, \mathbf{x}_{it})\}_{\substack{i=1,\dots,N \\ j=1,\dots,T_i}}$

$$\alpha_{k,\tau} = \sum_{k=1}^K \pi_{k,\tau} \delta_{b_{k,\tau}}.$$

Result: Quantile estimate $\hat{Q}_\tau^s(y_{it} | \mathbf{x}_{it}) = \hat{g}_\tau(\mathbf{x}_{it}) + \hat{\alpha}_{k,\tau}$

- 1 $r \leftarrow 0$;
- 2 $\hat{\alpha}_{k,\tau}^{(r)} \leftarrow 0$;
- 3 $\hat{\sigma}_\tau^{(r)} \leftarrow \sum_{s=1}^S \frac{1}{N} \sum_{i=1}^N \frac{1}{T_i} \sum_{t=1}^{T_i} \rho(u_{it})$ where $u_{i,t} = y_{i,t} - \hat{Q}_\tau^s(y_{it} | \mathbf{x}_{it})$;
 $\hat{\pi}_{k,\tau}^{(r)} \leftarrow K$ weights of a Gaussian quadrature;
- 4 $\hat{g}_\tau(\mathbf{x}_{it})^{(r)} \leftarrow$ estimate of the unknown function at level τ obtained by fitting the QRF with \mathcal{T} ;
- 5 **E-step:** Update estimates $\hat{w}_{ik,\tau}^{(r+1)}$ and $\hat{g}_\tau(\mathbf{x}_{it})^{(r+1)}$:
 - Update $w_{ik,\tau}^{(r+1)}$ with equation (3.7)
 - Update $\hat{g}_\tau(\mathbf{x}_{it})^{(r+1)}$ using a QRF fitted with $\mathcal{T}^{(r+1)} = \left\{ \left(y_{it}^{*(r+1)}, \mathbf{x}_{it} \right) \right\}_{\substack{i=1,\dots,N \\ j=1,\dots,T_i}}$ where $y_{it}^{*(r+1)} = y_{it} - \hat{\alpha}_{k,\tau}^{(r)}$ and accounting for the weight $\hat{w}_{ik,\tau}^{(r+1)}$ of each observation.

M-step: Update estimates $\hat{\alpha}_{k,\tau}^{(r+1)}$ and $\hat{\sigma}_\tau^{(r+1)}$ by maximising (3.6)

Keep iterating between **E-step** and **M-step** until convergence.

One of the main drawbacks of the traditional EM algorithm is that the M-step may be particularly burdensome in empirical applications involving a large set of covariates, in particular in terms of computational effort. Hence, in order to overcome this issue,

the closed-form solutions approach used in Merlo et al. (2022a) and Tian et al. (2014) and reported in the next section is applied.

3.2.3 Closed Form Solutions to the EM Algorithm

As shown in Merlo et al. (2022a) and Tian et al. (2014), closed form solutions to the EM algorithm are obtained considering the location-scale mixture representation of Y_{it} presented in Kozumi and Kobayashi (2011):

$$Y_{it} = \theta V_{it} + \tau \sqrt{V_{it}} Z_{it} \quad (3.9)$$

where V_{it} is an exponential random variable with realization v_{it} and Z_{it} a standard Normal random variable.

In this setting, $f(v_{it,\tau}|y_{it}, \mu_{itk,\tau}, \sigma_\tau)$ is a Generalized Inverse Gaussian (GIG) distribution (Tian et al., 2014, 2016):

$$f(v_{it,\tau}|y_{it}, \mu_{itk,\tau}, \sigma_\tau) \sim \text{GIG}\left(\frac{1}{2}, \frac{(y_{it} - \mu_{itk,\tau})^2}{\rho^2 \sigma_\tau}, \frac{2\rho^2 + \theta^2}{\rho^2 \sigma_\tau}\right). \quad (3.10)$$

where $\theta = \frac{1-2\tau}{\tau(1-\tau)}$ and $\rho^2 = \frac{2}{\tau(1-\tau)}$. Starting from (3.9) and (3.10), the complete data log-likelihood function of the EM algorithm is based on:

$$f(y_{it}, v_{it,\tau}|\mu_{itk}, \sigma_\tau) = \frac{1}{\sigma_\tau \rho \sqrt{2\pi \sigma_\tau v_{it,\tau}}} \exp\left(-\frac{(y_{it} - \mu_{itk,\tau} - \theta v_{it,\tau})^2}{2\rho^2 \sigma_\tau v_{it,\tau}} - \frac{v_{it,\tau}}{\sigma_\tau}\right). \quad (3.11)$$

From (3.11), the complete data log-likelihood function is proportional to:

$$\begin{aligned} \ell_c(\alpha_{1,\tau}, \dots, \alpha_{K,\tau}) &\propto \frac{1}{2} \sum_{i=1}^N \sum_{k=1}^K \sum_{t=1}^{T_i} w_{ik,\tau} v_{it,\tau}^{-1} (y_{it} - g_\tau(\mathbf{x}_{it}) - \alpha_{k,\tau})^2 \\ &\quad - \theta \sum_{i=1}^N \sum_{k=1}^K \sum_{t=1}^{T_i} w_{ik,\tau} (y_{it} - g_\tau(\mathbf{x}_{it}) - \alpha_{k,\tau}). \end{aligned} \quad (3.12)$$

Estimates $\hat{\alpha}_{k,\tau}$ are obtained by alternating between the E-step and the M-step.

In the **E-step** the expectation of (3.12) conditional to the observed data is computed and it is proportional to:

$$\begin{aligned} \mathbb{E}[\ell_c(\alpha_{1,\tau}, \dots, \alpha_{K,\tau}) \mid \mu_{it}, \hat{\Phi}_\tau^{(r)}] &\propto \\ \frac{1}{2} \sum_{i=1}^N \sum_{k=1}^K \sum_{t=1}^{T_i} \hat{w}_{ik}^{(r+1)} \hat{v}_{it,\tau}^{(r+1)} &(y_{it} - \hat{g}_\tau(\mathbf{x}_{it}) - \alpha_{k,\tau})^2 \\ - \theta \sum_{i=1}^N \sum_{k=1}^K \sum_{t=1}^{T_i} \hat{w}_{ik,\tau}^{(r+1)} &(y_{it} - \hat{g}_\tau(\mathbf{x}_{it}) - \alpha_{k,\tau}), \end{aligned} \quad (3.13)$$

where $\hat{w}_{ik,\tau}^{(r+1)}$ is obtained as in (3.7) and the unknown function part $g_\tau(\mathbf{x}_{it})$ is estimated using the QRF algorithm.

The estimates of the latent variable $\hat{v}_{it,\tau}^{(r+1)} = \mathbb{E}[V_{it,\tau}^{-1} \mid \mu_{itk}, \hat{\Phi}_\tau^{(r)}]$ are obtained by exploiting the moment properties of the GIG distribution in (3.10):

$$\hat{v}_{it,\tau}^{(r+1)} = \mathbb{E}[V_{it,\tau}^{-1} \mid \mu_{itk}, \hat{\Phi}_\tau^{(r)}] = \frac{\sqrt{\theta^2 + 2\rho^2}}{|y_{it} - \hat{g}_\tau(\mathbf{x}_{it})^{(r)} - \hat{\alpha}_{k,\tau}^{(r)}|}. \quad (3.14)$$

In the **M-step**, (3.2.3) is maximised with respect to $\alpha_{1,\tau}, \dots, \alpha_{K,\tau}$ and the following update expression for $\hat{\alpha}_{k,\tau}^{(r+1)}$ is obtained:

$$\hat{\alpha}_{k,\tau}^{(r+1)} = \sum_{i=1}^N \sum_{t=1}^{T_i} \frac{\hat{w}_{ik,\tau}^{(r+1)} \hat{v}_{it,\tau}^{(r+1)}}{\hat{w}_{ik,\tau}^{(r+1)} (\hat{v}_{it,\tau}^{(r+1)} (y_{it} - \hat{g}_\tau(\mathbf{x}_{it})^{(r)}) - \theta)}. \quad (3.15)$$

3.3 Simulation Study

This section reports the results of a simulation study carried out to assess the performance of the FM-QRF. The proposed model is tested in a non-linear setting characterised by non-negligible clustering-effects. The FM-QRF is used to predict quantiles at levels $\tau \in \{0.1, 0.5, 0.9\}$.

The data are simulated under the following non-linear data generating process (DGP) (Hajjem et al., 2014):

$$y_{it} = g(\mathbf{x}_{it}) + b_i + \varepsilon_{it}$$

$$g(\mathbf{x}_{it}) = 2x_{it,1} + x_{it,2}^2 + 4 \cdot \mathbf{1}_{\{x_{it,3} > 0\}} + 2x_{it,3} \log |x_{it,1}|$$

The covariates are generated as $x_{it,1}, x_{it,2}, x_{it,3} \sim \mathcal{N}(0, 1)$. The random-effects parameters and the error terms are generated independently according to four DGPs with small and large proportion of random-effects variance (PREV, computed as in Hajjem et al. (2014)). DGPs with a large PREV are characterised by the presence of a larger proportion of total variance explained by the random effects, implying that the clustered structure of the data is more pronounced:

1. **(NN-S)** $b_i \sim N(0, 1)$, $\varepsilon_{it} \sim N(0, 1)$ with small PREV
2. **(NN-L)** $b_i \sim N(0, 1)$, $\varepsilon_{it} \sim N(0, 1)$ with large PREV
3. **(TT-S)** $b_i \sim t(3)$, $\varepsilon_{it} \sim t(3)$ with small PREV
4. **(TT-L)** $b_i \sim t(3)$, $\varepsilon_{it} \sim t(3)$ with large PREV

Under scenarios NN-S and NN-L the assumptions of the linear quantile mixed model (LQMM) of Gaussian random parameters hold, whereas for scenarios TT-S and TT-L

these hypotheses are violated. In particular, a DGP with heavier tails represented by a Student's t distribution with three degrees of freedom is assumed.

As in Hajjem et al. (2011), for each scenario are considered a training set of 500 observation for $N = 100$ statistical units and $T_i = 5$ measurements each, and an unbalanced test set with $T_i \in \{9, 27, 45, 63, 81\}$ for a total of 4500 observations. Each scenario has been replicated $S = 100$ times.

The average performance of the ME-QRF across the 100 replications is assessed on the test set in terms of the following three loss functions:

- Average Mean Absolute Error (MAE) and average Mean Squared Error (MSE) with respect to the theoretical quantile of the DGP, computed as in Min and Kim (2004):

$$MAE_\tau = \frac{1}{S} \sum_{s=1}^S \frac{1}{N} \sum_{i=1}^N \frac{1}{T_i} \sum_{t=1}^{T_i} |Q_\tau^s(y_{it}|\mathbf{x}_{it}) - \hat{Q}_\tau^s(y_{it}|\mathbf{x}_{it})| \quad (3.16)$$

$$MSE_\tau = \frac{1}{S} \sum_{s=1}^S \frac{1}{N} \sum_{i=1}^N \frac{1}{T_i} \sum_{t=1}^{T_i} (Q_\tau^s(y_{it}|\mathbf{x}_{it}) - \hat{Q}_\tau^s(y_{it}|\mathbf{x}_{it}))^2 \quad (3.17)$$

where $Q_\tau^s(y_{it}|\mathbf{x}_{it})$ and $\hat{Q}_\tau^s(y_{it}|\mathbf{x}_{it}) = \mu_{it,\tau}$ are the theoretical and estimated conditional quantiles at level τ of the s -th simulated dataset, respectively.

- Average Ramp loss (RAMP) as proposed in Takeuchi et al. (2006). This loss is used to measure the quantile property of estimator $\hat{Q}_\tau^s(y_{it}|\mathbf{x}_{it})$ in dividing the data so that τ percent of observations fall below $\hat{Q}_\tau^s(y_{it}|\mathbf{x}_{it})$ and $1 - \tau$ are above:

$$RAMP_\tau = \frac{1}{S} \sum_{s=1}^S \frac{1}{N} \sum_{i=1}^N \frac{1}{T_i} \sum_{t=1}^{T_i} \mathbf{1}_{\{u_{it} < 0\}} \quad (3.18)$$

where $u_{it} = y_{it} - \hat{Q}_\tau^s(y_{it}|\mathbf{x}_{it})$. The model satisfies the quantile property for ramp loss values close to τ .

The performance in term of losses of the FM-QRF is compared with three benchmark models: LQMM, Quantile Regression Forest (QRF) and the Quantile Mixed Model (QMM) of Merlo et al. (2022a) adapted to a no two-part model. The latter model exploits the same methodological approach of the FM-QRF in a linear setting. The number of mixture components has been set to $K = 11$ with a grid search approach for all models, and the hyper-parameters of the FM-QRF (that is, number of trees, minimum number of observations in terminal nodes, number of features to consider for splitting nodes) have been optimized by Bayesian Optimization using the `ParallelBayesOptQRF` package

implemented in R ¹. The QRF has been trained by using the same hyper-parameters settings of the FM-QRF.

Results are reported in Table 3.1.

	NN-S			NN-L		
	MAE	MSE	RAMP	MAE	MSE	RAMP
$\tau = 0.1$						
FM-QRF	1.54	4.93	0.1	1.83	5.87	0.1
LQMM	2.45	10.20	0.1	1.86	5.89	0.1
QRF	1.50	4.49	0.1	2.64	10.98	0.1
QMM	4.38	35.34	0.2	4.67	40.62	0.2
$\tau = 0.5$						
FM-QRF	1.56	4.41	0.5	1.65	4.62	0.5
LQMM	2.09	8.11	0.5	1.72	5.27	0.5
QRF	1.46	3.72	0.5	2.11	7.15	0.5
QMM	2.33	10.36	0.5	2.80	14.61	0.5
$\tau = 0.9$						
FM-QRF	1.49	4.46	0.9	1.67	4.86	0.9
LQMM	2.15	7.90	0.9	1.57	4.34	0.9
QRF	1.32	3.57	0.9	2.20	7.93	0.9
QMM	6.39	79.14	0.7	5.16	61.12	0.8

	TT-S			TT-L		
	MAE	MSE	RAMP	MAE	MSE	RAMP
$\tau = 0.1$						
FM-QRF	2.11	9.03	0.1	1.80	6.66	0.1
LQMM	2.57	11.09	0.1	1.94	6.42	0.1
QRF	2.22	11.09	0.1	2.02	7.88	0.1
QMM	4.94	49.44	0.2	4.11	33.16	0.2
$\tau = 0.5$						
FM-QRF	1.62	5.31	0.5	1.43	4.32	0.5
LQMM	2.02	7.45	0.5	1.57	4.48	0.5
QRF	1.55	4.93	0.5	1.44	4.51	0.5
QMM	2.51	12.16	0.5	2.01	7.82	0.5
$\tau = 0.9$						
FM-QRF	2.11	8.64	0.9	1.87	7.10	0.9
LQMM	2.71	11.53	0.9	2.06	6.81	0.9
QRF	2.22	9.23	0.9	2.06	8.02	0.9
QMM	7.91	218.196	0.8	5.13	50.79	0.8

Table 3.1: Loss values for each scenario computed on the test set of the four fitted models. Bold values indicate the smallest loss.

In the first scenario, in which data meet the Gaussianity assumptions of the LQMM model, the FM-QRF performance mainly depends on the relevance of the clustering effect in the simulated data.

When the clustering effect is small, the best performing model is the QRF algorithm. This is due to the fact that, in this setting, the QRF is more well specified than the LQMM, which is a linear model, and the FM-QRF model, which is designed for non-linear setting in which the clustering effect is large. As a matter of fact, when the clustering

¹<https://github.com/mila-andreani/ParallelBayesOptQRF>

effect is more relevant, the best performing model is the FM-QRF for almost all quantile levels.

In the second scenario, the simulated data violate the gaussianity assumptions of the LQMM. In this case, the FM-QRF outperforms the benchmark models both when the clustering effect is small and large for almost all quantile levels.

The only exception is represented by the performance of the FM-QRF in terms of MSE in the large clustering effect setting when $\tau = 0.01, 0.9$. In this case, a larger training set could lead to an improved performance of the FM-QRF in terms of MSE in predicting extreme quantile values.

In conclusion, the main finding in this simulation study is that the performance of the FM-QRF improves as the clustering effect increases, and when data violate the gaussianity assumptions of the LQMM model.

3.4 Empirical Application

The study of the effects of climate change is a widely discussed topic in several fields, and a variety of studies have highlighted the relevant and multifaceted role of the growing frequency and intensity of natural disasters in determining economic output of countries (Mele et al., 2021, Tol, 2018, Palagi et al., 2022, Peng et al., 2011, Deschênes and Greenstone, 2007, Dell et al., 2014, 2012, Weitzman, 2014, Barro, 2015, Fankhauser and Tol, 2005).

Extreme weather events, including floods, droughts, and escalating temperatures, exert direct influence on the economic output of countries, especially those heavily relying on the agricultural sector. This impact primarily stems from infrastructural damages and fluctuations in crop yields and livestock productivity, resulting in significant economic losses (Nelson et al., 2014, Aydinalp and Cresser, 2008, Orlov et al., 2021). Other studies have shown that climate change affects economic output of countries also indirectly, by altering migratory flows (Cattaneo and Peri, 2016, Marotzke et al., 2020), demography (Barreca et al., 2015), criminality (Burke et al., 2018b) productivity and labor supply (Somanathan et al., 2021, Heal and Park, 2016, Graff Zivin and Neidell, 2014), energy production and consumption (Burke et al., 2015, 2018a). These results highlight the relevance of considering climate change related risks in macroeconomic policy analyses, although evaluating the economic impact of climate change is a quite difficult task. A variety of statistical and econometric models has been proposed in literature (Kolstad and Moore, 2020, Carleton and Hsiang, 2016, Mendelsohn et al., 2006, Coronese et al., 2018, 2019, Hsiang, 2016); in particular, several studies have exploited standard regression approaches to analyse the relation between climate-related variables and economic aggregates, such as GDP and GDP growth; see for example Hsiang (2016), Dell et al. (2012), Kahn et al. (2021), Burke et al. (2015, 2018a).

Nevertheless, the effects of climate change may extend beyond the typical GDP distri-

bution, potentially heightening the vulnerability to economic downturns, as evidenced by the lower tails of GDP growth distribution, and amplifying systemic risks through the intersection of climate change impacts and human systems (e.g. international food markets, international security and countries' economic arrangements King et al., 2017).

In order to uncover vulnerabilities and potential systemic risks overlooked by standard regression approaches, the focus of more recent analyses shifted from measures of central tendency of the GDP growth distribution (Kahn et al., 2021, Dell et al., 2012, Burke et al., 2015, 2018a, Kalkuhl and Wenz, 2020), towards its upper and lower tails (Kiley, 2021, Yao and Wang, 2001, Coronese et al., 2018, 2019). Indeed, analysing the relation between climate change and the tails of GDP growth provides useful information to enhance policy effectiveness, especially when the policy maker aims at preventing and mitigating the impact of extreme events, such as economic downturns or recessions, caused by climate change. Moreover, information on the tails of GDP growth can be used as a measure of economic resilience, offering insights into how well an economy can endure and recover from extreme events.

One of the most used risk measures concerning the tails of the GDP growth distribution is the GDP Growth-at-Risk (GaR) (Yao and Wang, 2001, Adrian et al., 2022, 2019), representing the expected maximum economic downturn given a probability level over a certain time-period. GaR may be estimated in a QR framework as the conditional quantile of the GDP growth distribution at 1% or 5% quantile level.

In the recent work of Kahn et al. (2021), a linear QR parametric approach is used to predict the effects of different climate-change scenarios on future GaR of a basket of countries. The results highlight that unsustainable climate practices will have a negative effect on the GaR on the majority of countries included in the sample, increasing their risk of experiencing an extreme economic downturn.

Given the relevance of the approach of Kahn et al. (2021), the aim of this chapter is to extend their findings to a non-linear QR setting by applying the proposed FM-QRF to an unbalanced panel of 3045 country-year observations from 1995 to 2015 for 210 countries. The outcome variable is the first difference of the natural logarithm of the yearly GDP per capita. The yearly covariates set includes the current value of: Temperature (*TMP*), Precipitation (*PRE*), Magnitude of precipitations greater than 20mm (*r20mm*), maximum number of Consecutive Wet Days (*cwd*), maximum number of Consecutive Dry Days (*cdd*) and Maximum temperature of the year (*txx*). All variables have been differentiated. Also four lags of each covariate have been included in the covariates set for a total of 30 predictors.

The GDP data have been retrieved from the World Bank², and the covariates observations represent the historical values of the projected variables considered in the CMIP6 dataset³. The final dataset and the R code used to create the dataset is available

²<https://data.worldbank.org>

³<https://climateknowledgeportal.worldbank.org>

	Obs	Min	Max	Median	Mean	SD
<i>GDP</i>	2782	-0.70	0.63	0.04	0.04	0.05
<i>TMP</i>	2782	-0.64	0.81	0.02	0.03	0.12
<i>PRE</i>	2782	-496.06	484.47	-0.08	-0.23	64.17
<i>r20mm</i>	2782	-10.00	7.01	0.00	0.01	1.16
<i>cwd</i>	2782	-22.94	18.00	0.00	0.00	2.88
<i>cdd</i>	2782	-40.21	51.47	0.01	0.04	5.51
<i>txx</i>	2782	-2.64	2.13	0.03	0.04	0.35

Table 3.2: Summary statistics of the variables included in the sample. The table reports the number of observations (Obs), the minimum (Min), maximum (Max) along with the median, mean and standard deviation (SD).

on Github ⁴. The summary statistics of the variables included in the sample are reported in Table 3.2.

The empirical analysis presented here is developed in two parts. In the first subsection (3.4.1), the validity of a non-linear QR approach over a standard linear one is evaluated by means of an analysis of variance (ANOVA) test (Sthle et al., 1989), and the Variable Importance of each covariate is analysed to measure its relevance in predicting GDP growth quantiles.

The second subsection (3.4.2) focuses on the application of the FM-QRF model to forecast quantiles of the GDP growth at five different probability levels $\tau = 0.01, 0.05, 0.5, 0.95, 0.99$ at three horizons $t = 2030, 2050, 2100$. The conditional lower quantile levels 0.01 and 0.05 measure the downside risk of GDP growth (GaR). This risk measure represents the maximum probable loss in GDP growth caused by climate change. The upper two conditional quantiles levels 0.95 and 0.99 represent the upside risk of GDP growth, measuring the maximum probable growth of GDP conditional on the covariates set.

The conditional quantiles forecasts at different τ are computed using the projected values of the covariates from the CMIP6 dataset (O'Neill et al., 2016, Li et al., 2021). In particular, the effects of climate change are measured by comparing two alternative climate scenarios formulated in the CMIP6 experiments. Such scenarios are denoted as Shared Socio-economic Pathways (SSPs) (Riahi et al., 2017), and each SSP outlines the progression of climate variables conditional on the future trajectory of socio-economic factors and climate policies implemented by individual countries up to the year 2100. Five different SSP are available, and in this chapter two different SSPs are considered: SSP1 (Van Vuuren et al., 2017) and SSP5 (Kriegler et al., 2017), which are two opposite scenarios of climate change. In SSP5 a future energy-intensive economy based on fossil fuels is hypothesised, whereas in SSP1 climate sustainable practices will prevail. Thus, the SSP5 represents the worst-case scenario in terms of climate change, and SSP1 represents the best-case one.

The aim of this analysis is to evaluate whether the fossil fuel-based economy of the SSP5

⁴<https://github.com/mila-andreani/climate-change-dataset>

scenario will negatively affect the future GDP growth distribution at different quantile levels. The results provide evidence that unsustainable climate policies (SSP5 scenario) will increase the GaR of the majority of the countries included in the considered sample. Moreover, differently from results obtained in the related literature Dell et al. (2012), and as recently demonstrated in Damania et al. (2020), this analysis shows that changes in precipitations-related variables due to climate change also represent a relevant risk factor undermining future economic growth.

3.4.1 Preliminary Analysis

This section reports the results of the preliminary analysis on the dataset of interest. Within the machine learning framework of this chapter, first the validity of a non-linear QR approach over a standard linear one is evaluated with an analysis of variance (ANOVA) test (Sthle et al., 1989) to compare a spline QR model (Marsh and Cormier, 2001, Koenker et al., 1994, Wang, 1998) and standard QR at five quantile levels $\tau = 0.01, 0.05, 0.5, 0.95, 0.99$.

The spline QR model is an extension of the standard QR model based on piecewise-defined polynomial functions. Differently from the linear QR modeling framework, the splines model adapts to non-linear relationships with a series of knot points, where each different polynomial segment originates. This feature makes this model particularly suitable to model complex and non-linear relationships among the variables of interest.

In this section, both the QR spline model and the linear one consider the same covariates of the FM-QRF. In particular, the QR spline model is represented by a piecewise cubic polynomial with 2 knots for each covariate. The results of the ANOVA test, in Table 4.3, reveal that a non-linear approach, such as the one in FM-QRF, results more valid than the linear one.

τ	0.1	0.25	0.5	0.75	0.9
Tn	1.513	3.585	10.686	27.329	2.2
$P\text{-Value}$	0.001**	0***	0***	0***	0***

Table 3.3: ANOVA test results for different values of τ . The 'Tn' column reports the test statistic and the 'P-Value' column reports the level of significance of the test at 5% significance level.

In the second part of the preliminary analysis the relevance of each covariate in predicting the quantiles of the GDP growth distribution is assessed by extracting the Variable Importance measure from the FM-QRF.

The analysis is performed by fitting a FM-QRF for each τ and by computing the Variable Importance measure (Breiman et al., 1984) for each p -th covariate as follows. First, the sum of squared residuals (SSR), denoted with $m_{p,\tau}$, is computed by using Out-Of-Bag observations of the covariate. Then, the observations are permuted and the SSR is re-calculated. The SSR after the permutation is denoted with $m_{p,\tau}^*$. The

Variable Importance of the p -th covariate for the τ quantile, denoted with $I_{p,\tau}$, is finally computed as:

$$I_{p,\tau} = m_{p,\tau} - m_{p,\tau}^*. \quad (3.19)$$

The higher the reduction in the SSR following the permutation, the higher the importance of the variable. The results of variable importance are shown in figures 3.1- 3.2. Figure 3.1 shows the average I_p across quantiles, whereas figures 3.2 show the $I_{p,\tau}$ at each quantile level for each variable.

Figure 3.1 shows that, at an aggregate level, the most important set of variables used to predict quantiles are the lags of the Temperature variable. The second set of variables is represented by the consecutive number of Dry Spells. This pattern is similar to the one observed at a disaggregate level, represented in Figure 3.2 at different quantile probability levels.

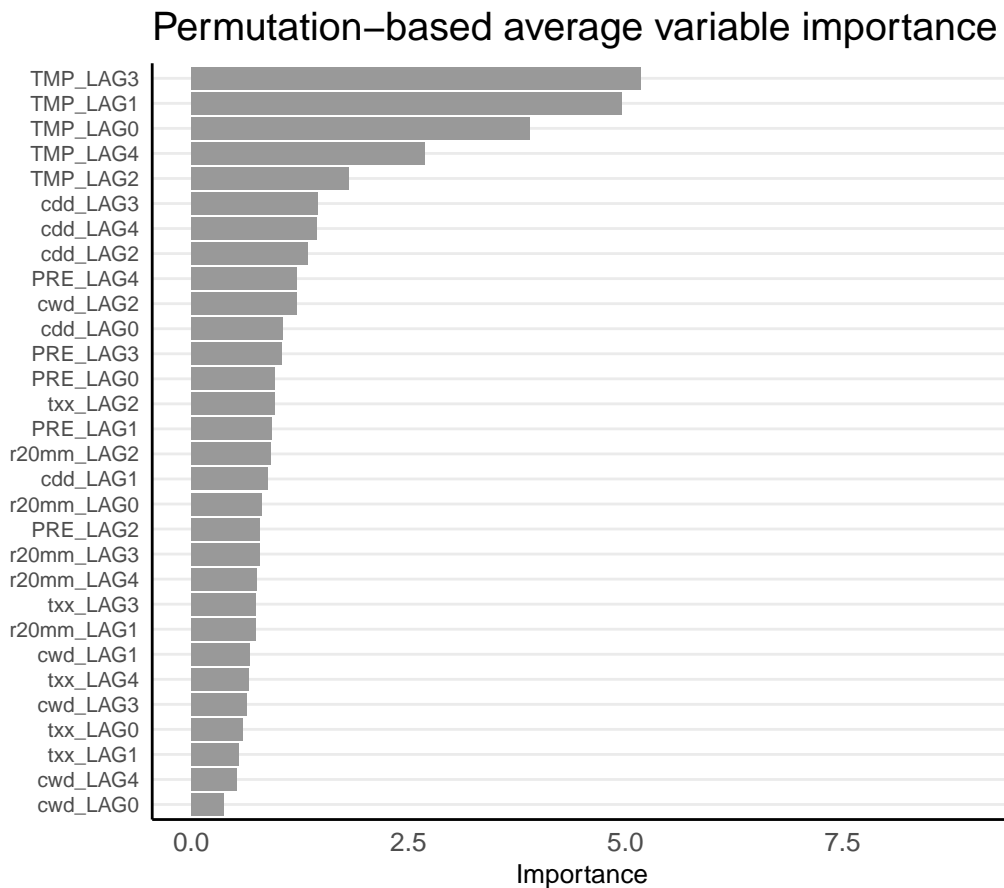


Figure 3.1: Average variable importance across quantiles I_j for each covariate.

Permutation-based Variable Importance

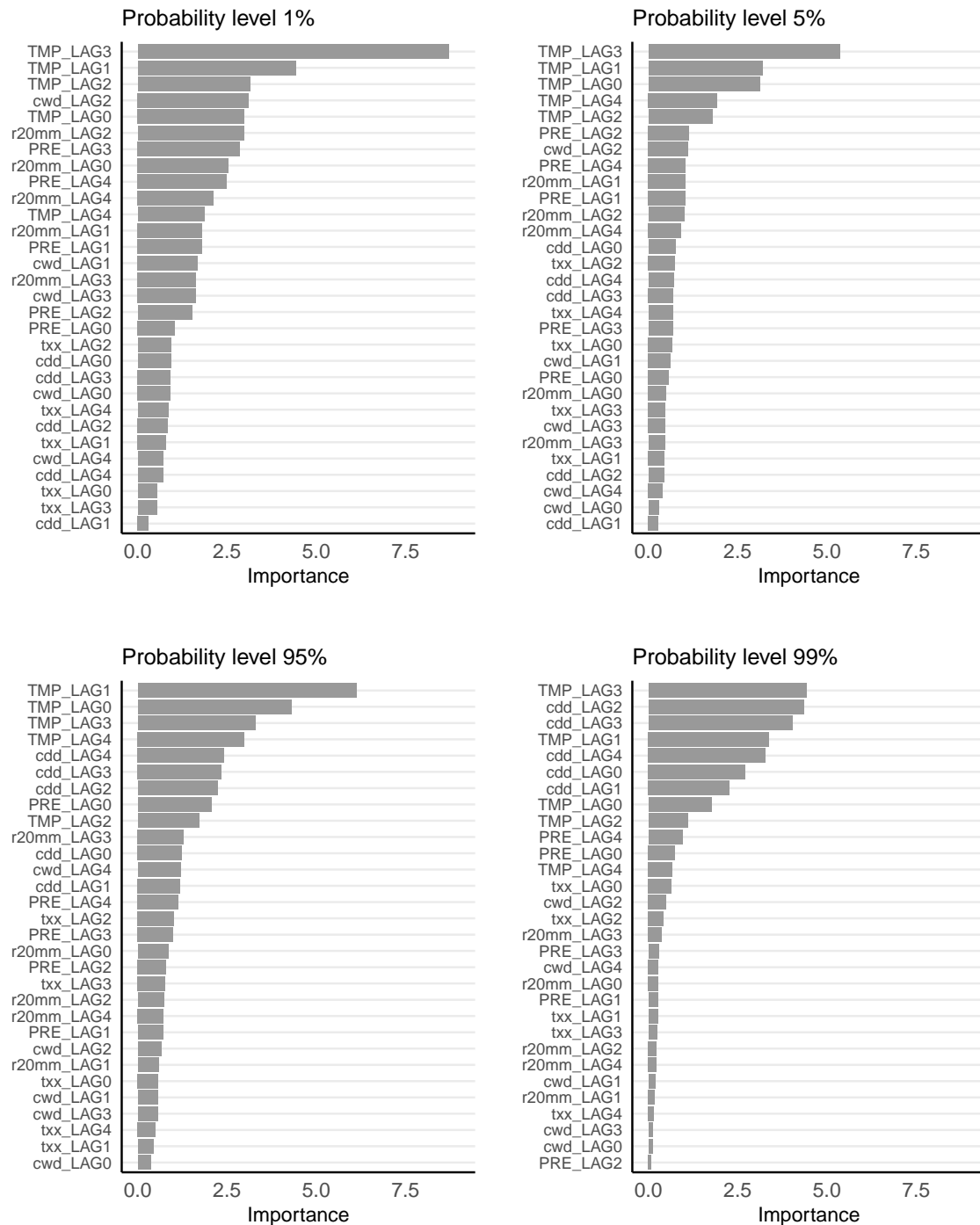


Figure 3.2: Permutation-based variable importance $I_{j,\tau}$ for each covariate included in the training set.

These results highlight that both temperature and precipitations affect the GDP growth distribution of each country to a different extent. Although being in contrast with previous contributions (Dell et al., 2012), the obtained results are confirmed by more

	0.01						0.5						0.99					
year	2030	2030	2050	2050	2100	2100	2030	2030	2050	2050	2100	2100	2030	2030	2050	2050	2100	2100
SSP1	-7.68	0.51	-7.76	0.55	-7.87	0.61	3.67	0.25	3.74	0.25	3.65	0.24	12.1	0.37	12.09	0.38	12.1	0.37
SSP5	-7.55	0.48	-7.7	0.52	-7.61	0.54	3.75	0.24	3.75	0.25	3.75	0.24	12.09	0.37	12.13	0.37	12.12	0.37

Table 3.4: Average mean and bootstrap standard error across countries obtained with N=500 iterations.

recent findings (Damania et al., 2020), which show that precipitations-related variables play a more relevant role with respect to temperature at the upper quantiles of the GDP growth distribution, representing a relevant factor influencing upside risk of economic productivity growth.

3.4.2 Projection Results

This section reports the quantile estimates along with their standard errors projected in 2030, 2050, 2100 under the SSP1 and SSP5 scenarios. The FM-QRF has been fitted using $K = 9$ locations, identified via grid search and the computational time to fit the model is equal, on average, to 620.45 seconds on an ordinary multi-CPU server Intel Xeon with 24 cores.

The mean and the bootstrap standard error of each estimate are obtained with $N = 500$ replications. Table 3.4 report the average mean and standard error across countries for the SSP1 and SSP5 scenarios, respectively. Country specific estimates are reported in Tables B.1 and B.2.

The results obtained under the two scenarios are compared by considering the difference between the values of quantiles estimated in the worst-case scenario in terms of climate policies (SSP5) and the values of quantiles estimated according to the best-case one (SSP1):

$$\Delta Q_{it}^{\tau} = Q_{it}^{\tau, SSP5} - Q_{it}^{\tau, SSP1}, \quad (3.20)$$

where Q_{it}^{τ} represents the estimated values of the quantile of the i -th country at probability level τ projected in year t . Given that the main difference between the SSP1 and SSP5 is related to two opposite climate change mitigation policies scenarios, the magnitude of ΔQ_{it}^{τ} can be attributed only to climate change and its effect on climate variables.

Negative values of ΔQ_{it}^{τ} indicate that $Q_{it}^{\tau, SSP5} < Q_{it}^{\tau, SSP1}$. This means that under the SSP5 scenario, the GDP growth at both low and high quantile levels will be smaller due to inadequate climate-related policies.

The country-specific results of this analysis are mapped in figures 3.3-3.7 at three different time horizons ($t = 2030, 2050, 2100$). The main finding obtained by interpreting the values of ΔQ_{it}^{τ} is that the effects of the unsustainable climate practices hypothesised in the SSP5 scenario are negative at an aggregate level, but their magnitude substantially vary across time and among countries.

For each quantile level, in 2030 – 2050 the value of ΔQ_{it}^{τ} is estimated to be negative for

almost two thirds of the countries. This points out that the climate change hypothesised in the worst case scenario will increase the downside risk of the majority of the countries in the considered sample, while also representing a limiting factor to the potential country-specific GDP growth.

For instance, figure 3.6 shows the maps at 2030, 2050 and 2100 for quantile at level $\tau = 0.05$. In this case, in 2030 the $\Delta Q_{i,2030}$ assumes values ranging from a minimum of -16% to a maximum of 7%. This indicates that for some countries $Q_{i,2030}^{0.05,SSP5} < Q_{i,2030}^{0.05,SSP1}$, that is, some countries will see their 5% quantile (that represents a negative value of the GDP growth) decreasing more in the “worst-case” climate change scenario with respect to the “best-case” one. Another finding is that the effects of unsustainable climate practices change over time whether the country is considered to be ‘high-income’ with a moderate climate, or ‘low-income’ with more extreme climate conditions.

By comparing the panels reported in Figures 3.3- 3.7, the following results can be deducted. The impact of temperatures and precipitations from 2030 to 2050 on the United States, considered as a high-income and climate-temperate country, are modestly positive at all quantile levels. These findings indicate that high-income countries with economies reliant on energy-intensive sectors could see advantages in scenarios with limited climate policies, indicating a higher capability of high-income countries to adapt more effectively to adverse climate-change scenarios.

For low-income and hot countries instead, such as countries in the African continent and India, the effects of climate-change from 2030 to 2050 are negative at all quantile levels, especially at the medium term (2050). The same holds for Russia, which is a high-income but cold country. In this case, Russia will suffer from adverse climate-change scenarios both in terms of upside and downside risk. The results on the heterogeneity of climate change effects over time on rich/poor and hot/cold countries are confirmed by previous findings (Kiley, 2021).

In general, even though between 2030 and 2050 the majority of the countries will suffer from climate change in terms of GDP growth, in 2100 this heterogeneity will be slightly less pronounced, bringing the number of countries suffering from climate change to two thirds of the sample to 50%. This might result from the optimistic socio-demographic growth scenario hypothesised in SSP5, based on the hypothesis of large public interventions in favor of the communities against climate change. The effects of these interventions could have a positive effect in the long run on the poorest countries which, as shown in the literature, are those which will suffer most from the effects of climate change, precisely due to their socio-economic conditions.

The socio-economic development of these countries would thus ensure that the effects of climate change, even though still existing, will be mitigated by the presence of a growing number of mitigation policies and public intervention.

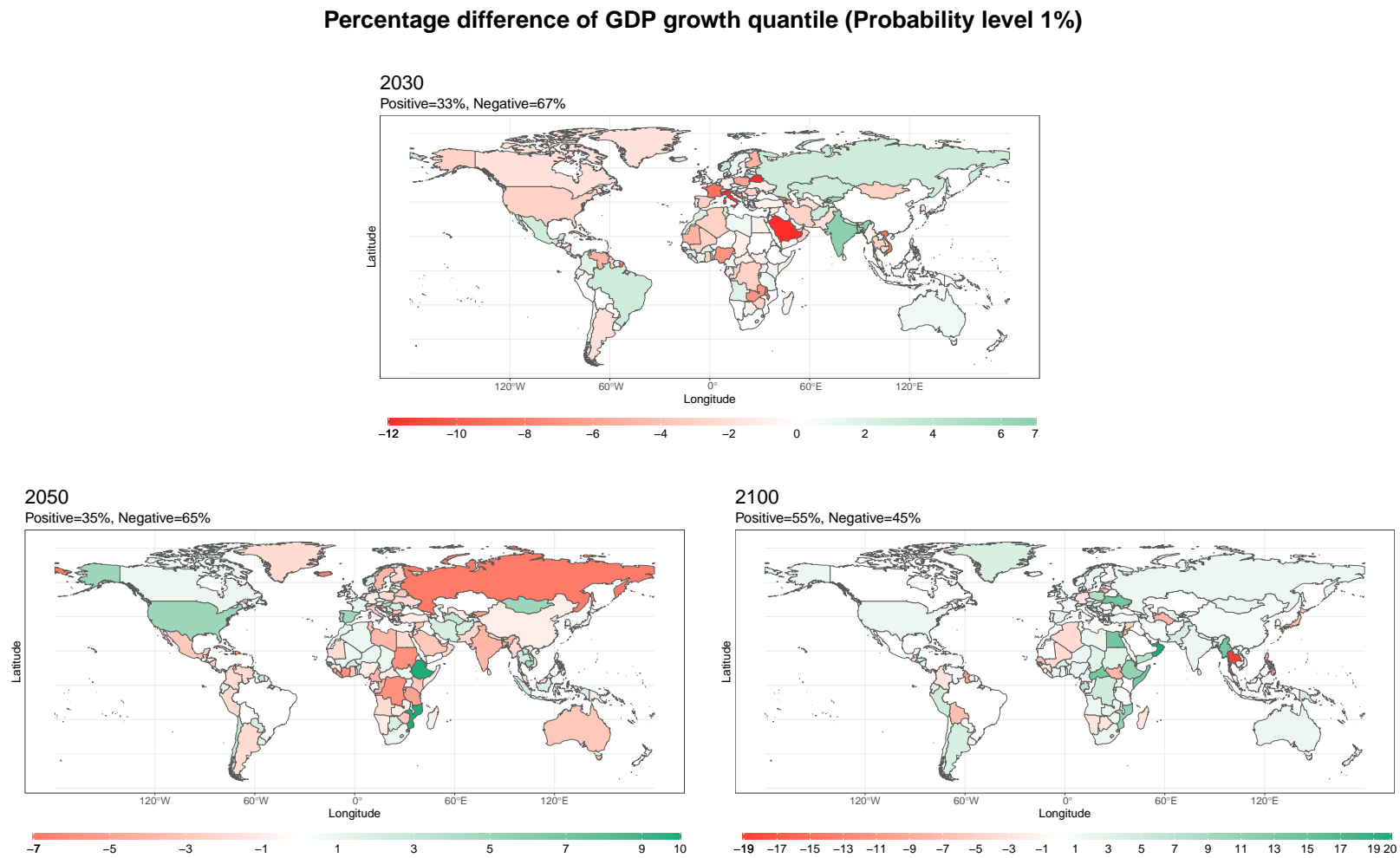


Figure 3.3: Map showing ΔQ_{it}^{τ} in years $t = 2030, 2050, 2100$ for quantile at probability level $\tau = 0.01$.

Percentage difference of GDP growth quantile (Probability level 5%)

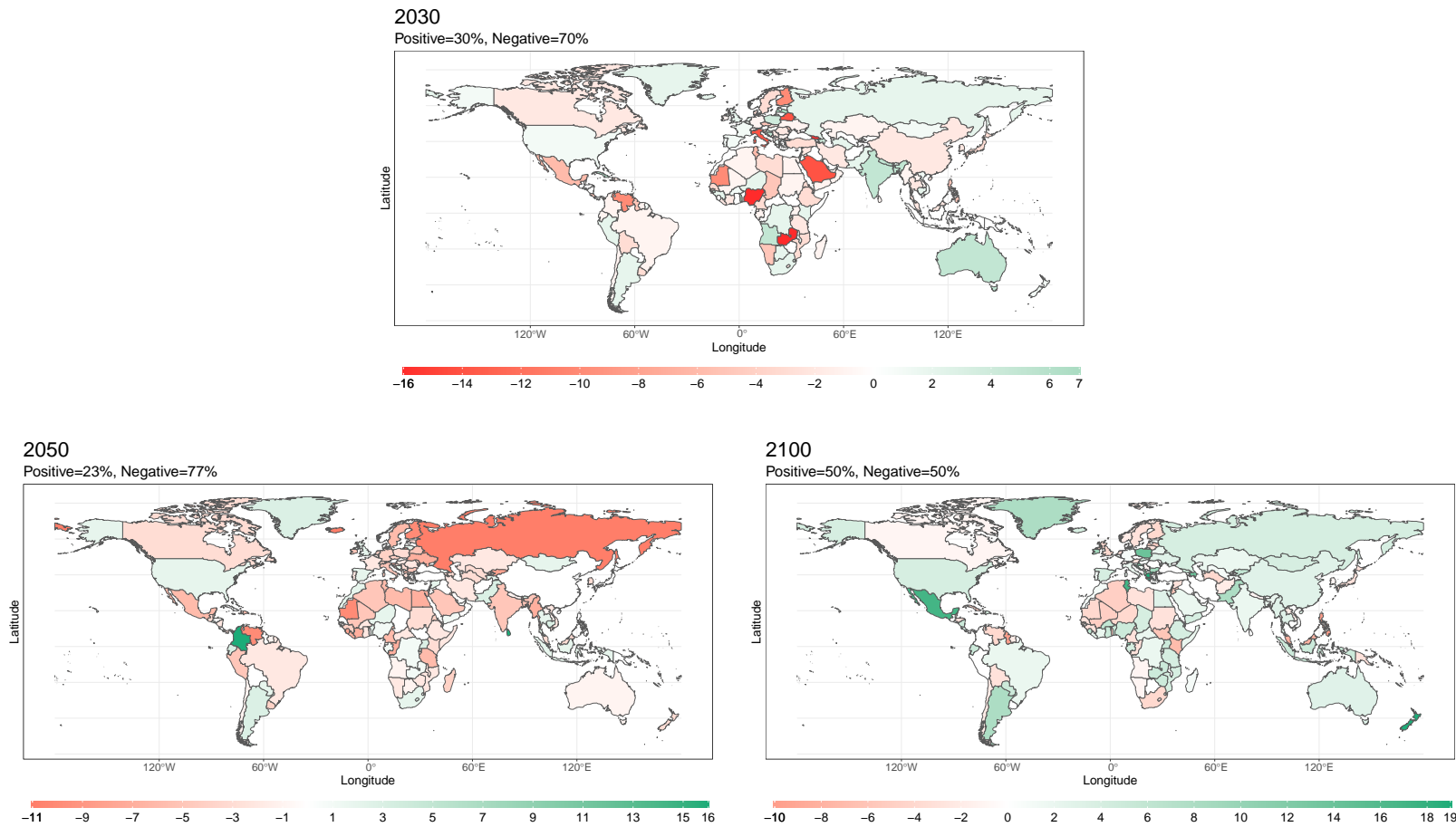


Figure 3.4: Map showing ΔQ_{it}^τ in years $t = 2030, 2050, 2100$ for quantile at probability level $\tau = 0.05$.

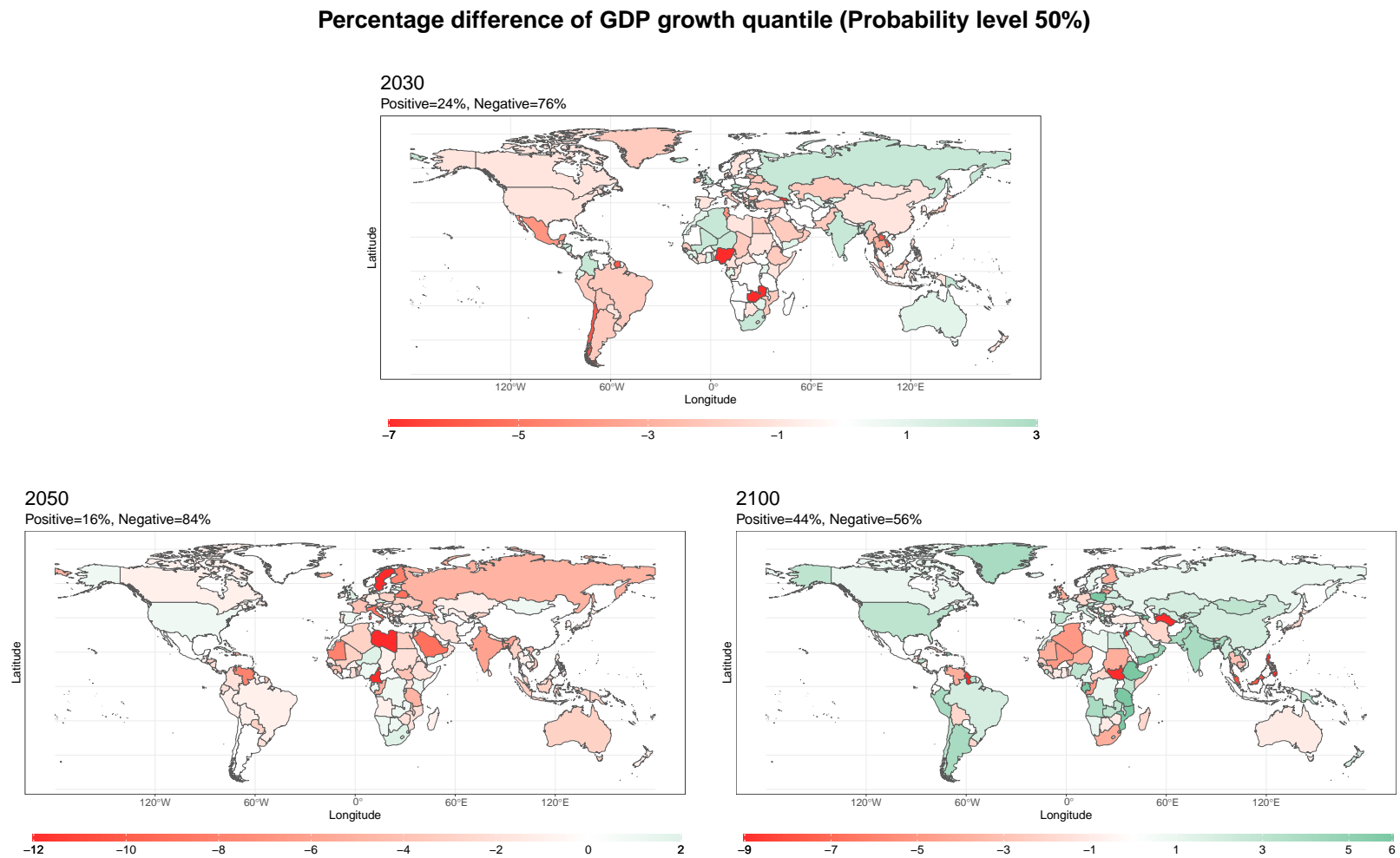


Figure 3.5: Map showing ΔQ_{it}^{τ} in years $t = 2030, 2050, 2100$ for quantile at probability level $\tau = 0.50$.

Percentage difference of GDP growth quantile (Probability level 95%)

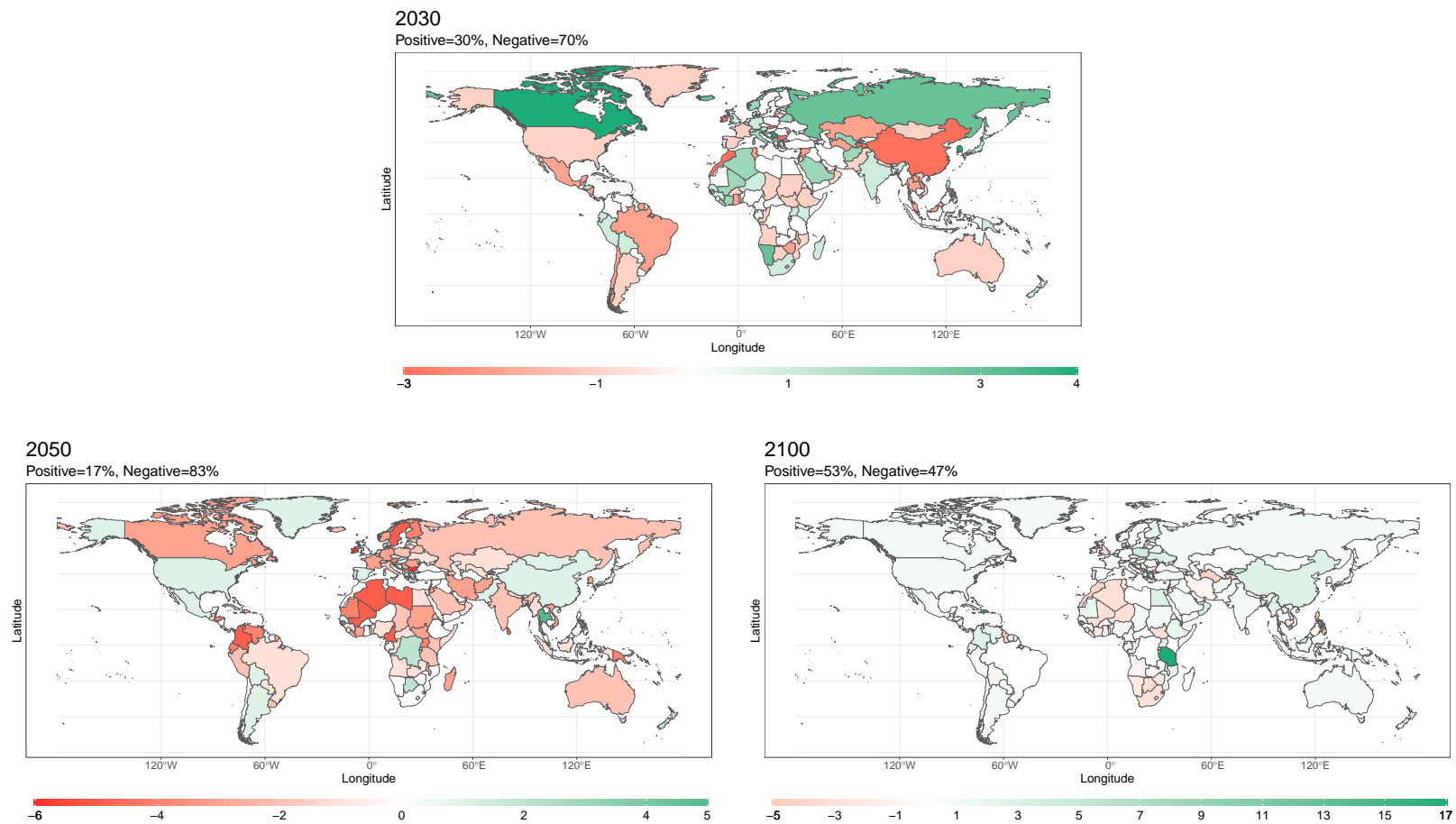


Figure 3.6: Map showing ΔQ_{it}^τ in years $t = 2030, 2050, 2100$ for quantile at probability level $\tau = 0.95$.

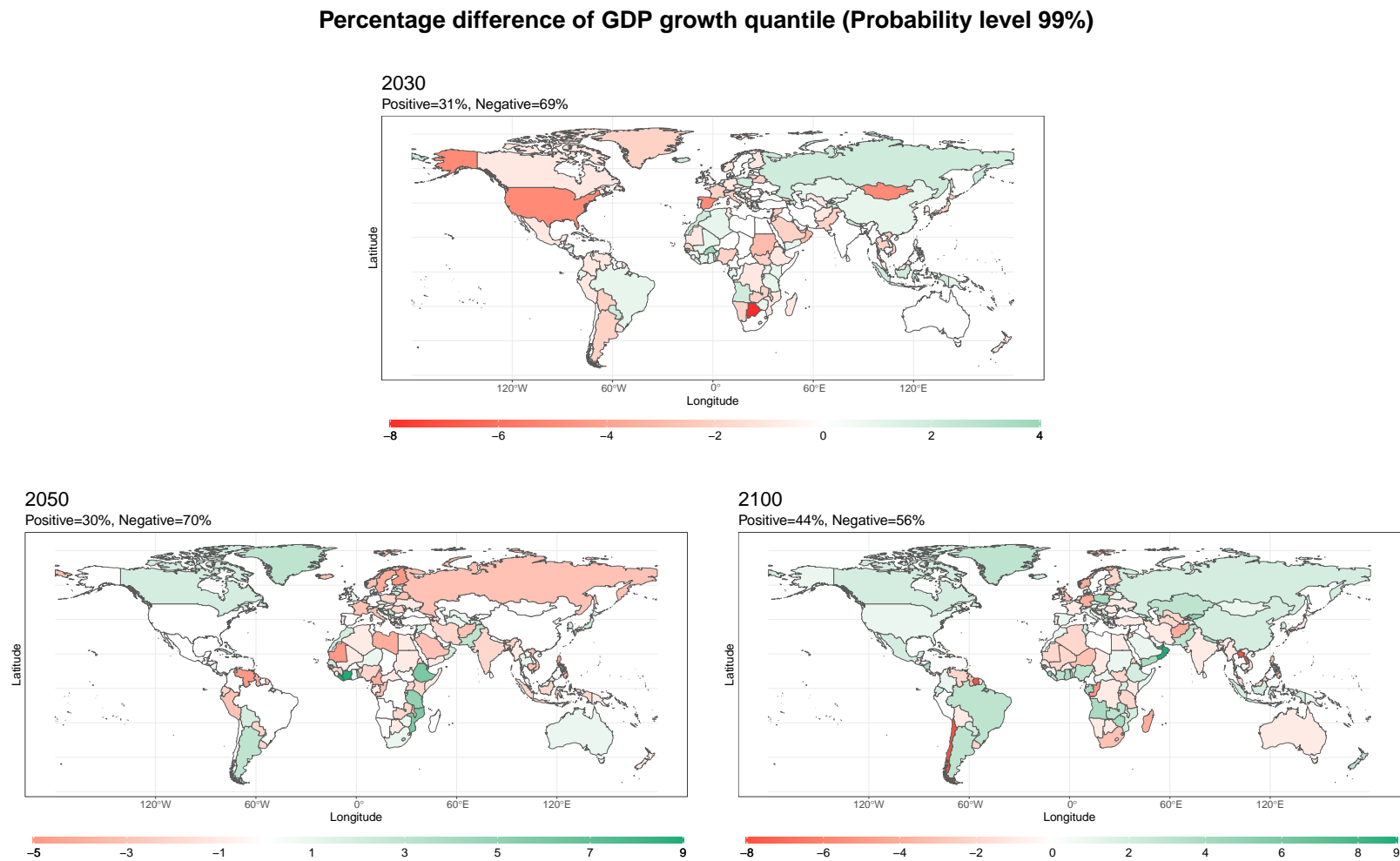


Figure 3.7: Map showing ΔQ_{it}^{τ} in years $t = 2030, 2050, 2100$ for quantile at probability level $\tau = 0.99$.

3.5 Conclusions

This chapter introduces the FM-QRF, a novel model to estimate quantiles of longitudinal data in a non-linear mixed-effects framework by means of QRF and the NPML approach.

A large scale simulation study shows that the FM-QRF outperforms other benchmark models in a non-linear setting. The model is applied empirically to study the long-term effects of climate change on GDP growth-at-risk, unveiling the relevant effects of future changes in temperature and precipitations on the tails of the GDP growth distribution.

The non-linear approach presented in this chapter offers several advantages when assessing the economic effects of climate change compared to a standard linear approach, as the FM-QRF allows to model the complex non-linear relationships between climate-related variables and GDP growth without any a-priori distributional assumption on the form these relationships, on the outcome variable and the random effects parameters. The empirical results presented in this chapter point out that these features make the FM-QRF well-suited for evaluating the future economic effects of climate change, allowing to deliver more accurate forecasts with respect to standard linear approaches.

Possible future developments of the FM-QRF model concern the inclusion of mixed-frequency covariates in order to consider variables observed at a higher frequency with respect to the outcome, that may include important information for understanding the phenomenon under consideration. The analysis of the results of the FM-QRF could be further enriched by including the study of the presence of heterogeneity among statistical units in terms of individual intercepts. Moreover, future model extension could concern the inclusion of time-varying random parameters by exploiting a Markovian structure as proposed in Marino et al. (2018), Merlo et al. (2022b,c).

Chapter 4

The Impact of the COVID-19 Pandemic on Risk Factors for Children's Mental Health: Evidence from the UK Household Longitudinal Study

4.1 Introduction

The recent COVID-19 pandemic sensibly impacted communities, healthcare systems and society, affecting the physical and mental health of people of all ages. Among these broader effects, social isolation and increased household stress particularly affected children, and part of the extensive literature on the pandemic has focused on investigating the effects of such disruptions on children's mental health (Ma et al., 2021, Adegboye et al., 2021, Kauhanen et al., 2023).

In this context, a variety of studies have used longitudinal data concerning the "SDQ score", a widely used measure in pediatric psychological research computed with answers to the Strengths and Difficulties Questionnaire (SDQ) (Panagi et al., 2024, Miall et al., 2023, Merlo et al., 2022c, Ravens-Sieberer et al., 2021, Bignardi et al., 2021, Waite et al., 2021). This metric has been introduced in Goodman (1997) to evaluate children's emotional, social and behavioural characteristics. High SDQ scores indicate a higher prevalence of psychological issues related to conduct or peer-related issues, hyperactivity, and emotional symptoms, including anxiety and depression.

Under a methodological point of view, given the longitudinal structure of these data, part of the above-mentioned studies have implemented standard linear random-effects or mixed-effects models, which allow to estimate the expected value of the conditional distribution of the response variable in a linear modeling framework. However, in many empirical applications, the relationship between the outcome and the covariates is

non-linear, and the outcome's distribution often violates the gaussianity assumptions of random-effects models. This is the case of the SDQ distribution, which is typically asymmetric. Moreover, results of previous contributions point out that the effect of risk factors such as socio-economic disadvantage and maternal depression changes across the SDQ conditional distribution, with a more significant impact on the right tail, which is related to abnormal levels of behavioural issues (Davis et al., 2010, Flouri and Tzavidis, 2008, Flouri et al., 2010, Merlo et al., 2022c, Tzavidis et al., 2016).

These findings highlight that a more complete picture of the SDQ conditional distribution is necessary to gain a deeper understanding of the phenomenon of interest. In this context, contributions such as Tzavidis et al. (2016) and Merlo et al. (2022c) implemented QR mixed-effects models to obtain more robust and accurate results. These approaches allow to infer the entire conditional distribution of the outcome by modeling location parameters beyond the conditional expected value, such as quantiles, in a longitudinal data setting.

To overcome the drawbacks of parametric formulations of these models, QR has been also extended to the non-parametric setting by developing QR machine learning algorithms, such as QR Neural Networks (White, 1992), QR Support Vector Machines (Hwang and Shim, 2005, Xu et al., 2015), QR kernel based algorithms (Christmann and Steinwart, 2008), QR Forests (QRF) (Meinshausen, 2006) and Generalized QR Forests (Athey et al., 2019). However, these models cannot handle longitudinal data in a mixed-effects framework, and for this reason the analysis carried out in this chapter employs the FM-QRF algorithm of Chapter 3.

The FM-QRF extends the traditional QR model to a non-linear setting and it also enhances the QRF algorithm by introducing an additional parameter represented by the random effects part of mixed-effects model, which allows to model unobserved heterogeneity across statistical units. These unique features make the FM-QRF well-suited for modeling phenomena characterized by complex non-linear relationships among the variables of interest, especially in empirical studies involving repeated measurements and longitudinal data, such as SDQ score data.

Thanks to this approach, this study contributes to the strand of literature on children's mental health by uncovering relationships between children's mental health and risk factors during the pandemic that have not have been captured by the standard linear models applied in previous contributions (Walton and Flouri, 2010, Goodnight et al., 2012, Bradley and Corwyn, 2002).

To this end, the data used in this study concern the SDQ scores of children that participated in at the UK Household Longitudinal Study (UKHLS), the largest household panel survey carried out in the United Kingdom since 2009. Data related to this study have been widely used in the literature concerning the effects of the pandemic on mental health (Miall et al., 2023, Bayrakdar and Guveli, 2023, Metherell et al., 2022, Daly and Robinson, 2022, Thorn and Vincent-Lancrin, 2022, Reimers, 2022, Mendolia et al.,

2022), and the aim of this study is to use the SDQ score as outcome variable and a set of variables selected according to previous studies findings as set of covariates.

To compare the set of risk factors before and after the pandemic, the FM-QRF is trained with two datasets: the first contains observations from the pre-pandemic period (2016-2019), and the other from the pandemic period (2020-2021). Then, quantiles at five different probability levels are estimated for each period and the Variable Importance measure is extracted to select the most significant risk factors for children's mental health in the two periods of interest.

The results from the pre-pandemic and pandemic periods are compared to identify patterns and shifts in the most important risk factors. Additionally, these findings are compared with the set of statistically significant variables obtained using the LQMM model.

The empirical findings obtained with the FM-QRF indicate that the key risk factors vary based on the quantile level, justifying the adoption of a QR approach over a standard regression method, and that they differ between the pre-pandemic and pandemic periods. Results also show that relying solely on the LQMM model provides only a partial understanding of the phenomena under investigation, highlighting the relevance of a non-linear approach. In this sense, the FM-QRF proves to be a valuable choice to gain a deeper understanding of the complex relationship between the COVID-19 pandemic and children's mental well-being.

The rest of the chapter is organized as follows. Section 4.2 presents the data used in this empirical study, Section 4.3 reports the results obtained with the FM-QRF and the comparison with the LQMM model and Section 4.4 concludes.

4.2 The Data

The data used in this study concern the SDQ score as outcome variable and a set of covariates selected according to previous results findings.

In particular, the SDQ score data have been retrieved by the UKHLS, the largest household panel survey carried out in the United Kingdom since 2009 involving 40,000 households. The aim of the UKHLS is to capture a broad range of information concerning economic circumstances, employment, education, health, and mental well-being before and after the pandemic. The longitudinal structure of this dataset provides a unique set of information to understand the long-term impact of a variety of factors on households.

The UKHLS collects also data of individual responses from both adults, youngsters and children. In the latter case, data concerning the assessment of children mental health are collected through the SDQ. The focus of the analysis presented in this chapter is the "total difficulties score" (*chsdtotd*) which ranges from 0 to 40 and represents the sum of 25 scores related to five domains comprising emotional symptoms, peer problems, conduct problems, hyperactivity and prosocial behaviour. The response for each item is

evaluated on a 3-points scale, where 0 represents a "not true" answer, 1 is given if the respondent partially agrees with the question statement, and 2 for a "true" answer. High scores indicate a higher prevalence of psychological issues related to conduct or peer-related issues, hyperactivity, inattention, and emotional symptoms, including anxiety and depression.

The covariates have been selected based on previous studies on children's mental health risk factors, such as family poverty, ethnicity, and living area. In particular, the set of covariates is composed of variables whose effects might have changed between before and during the pandemic: social benefit income (*fhhmnsben*), income from investments (*fhhmninu*), household size (*hhsiz*) and number of bedrooms in the house (*hsbeds*), number of employed people in the household (*nemp*) and employed people in the household that are not being paid (*nue*), living area (urban or rural) (*urban*), being up to date with bills payments (*xphsdba*) and internet access (*pcnet*). The belonging to an ethnic minority (*emboost*) is considered as an additional time-invariant variable.

The aim of this chapter is to compare how the main risk factors for children's mental health changed before and during the pandemic period. Thus, the dataset comprises observations from 2016 to 2019 for the pre-pandemic period and from 2020 to 2021 for the pandemic period. As stated above, the outcome variable is the SDQ total score, and after eliminating statistical units with missing data, the final sample including both the pre-pandemic and pandemic periods is composed of 2401 children for a total of $n = 3101$ observations. A total of 1729 and 1028 children are included in the pre-pandemic and pandemic sample, respectively. The barplot showing the number of children interviewed 1, 2, 3 or 4 times during sample period is represented in Figure C.1.

The summary statistics reported in Tables 4.1 and 4.2, related to the pre-COVID and COVID periods respectively, highlight the asymmetry of the SDQ unconditional distribution, whose mean and median sensibly differ especially in the pre-COVID period.

The features of the SDQ conditional distribution given the above-mentioned set of covariates are also investigated by fitting a model for the SDQ score with random-effects at child level. The Q-Q plot shown in Figure 4.1 highlights a severe departure of the model's residuals from the Gaussian distribution, which is one of the key assumption of the linear random-effects model. Thus, it would be useful to estimate more robust measures of central tendency and conditional quantiles to better estimate the relation between the SDQ score and the covariates.

	Obs	Min	Max	Median	Mean	St.Dev	Null
<i>chsdqtd</i>	2006		37.00	8.00	8.51	5.94	8856
<i>urban</i>	2006		2.00	1.00	1.23	0.42	14
<i>hhsz</i>	2006		13.00	4.00	4.32	1.18	8833
<i>hsbeds</i>	2006		8.00	3.00	3.29	0.87	8835
<i>fhhmnsben</i>	2006		6096.14	235.67	605.84	758.22	0
<i>fhhmninv</i>	2006		19416.67	0.00	173.01	845.31	8
<i>nemp</i>	2006		7.00	2.00	1.63	0.71	0
<i>pcnet</i>	2006		2.00	1.00	1.01	0.10	6
<i>nue</i>	2006		6.00	0.00	0.45	0.72	0
<i>xphsdba</i>	2006		3.00	1.00	1.08	0.28	22
<i>emboost</i>	2006		1.00	0.00	0.10	0.30	0

Table 4.1: Summary statistics related to the pre-COVID period of the variables included in the sample after the data cleaning procedure. The Null column reports the number of null values (not applicable or missing items) before the data cleaning procedure.

	Obs	Min	Max	Median	Mean	St.Dev	Null
<i>chsdqtd</i>	1095	0	32.00	7	8.68	6.01	9155
<i>urban</i>	1095	1	2.00	1	1.23	0.42	74
<i>hhsz</i>	1095	2	12.00	4	4.36	1.21	9137
<i>hsbeds</i>	1095	0	8.00	3	3.33	0.92	9141
<i>fhhmnsben</i>	1095	0	4901.66	208	568.05	760.12	0
<i>fhhmninv</i>	1095	0	9683.33	0	211.61	819.50	7
<i>nemp</i>	1095	0	7.00	2	1.62	0.72	0
<i>pcnet</i>	1095	1	2.00	1	1.01	0.07	12
<i>nue</i>	1095	0	6.00	0	0.50	0.83	0
<i>xphsdba</i>	1095	1	3.00	1	1.11	0.33	24
<i>emboost</i>	1095	0	1.00	0	0.10	0.30	0

Table 4.2: Summary statistics related to the COVID period of the variables included in the sample after the data cleaning procedure. The Null column reports the number of null values (not applicable or missing items) before the data cleaning procedure.

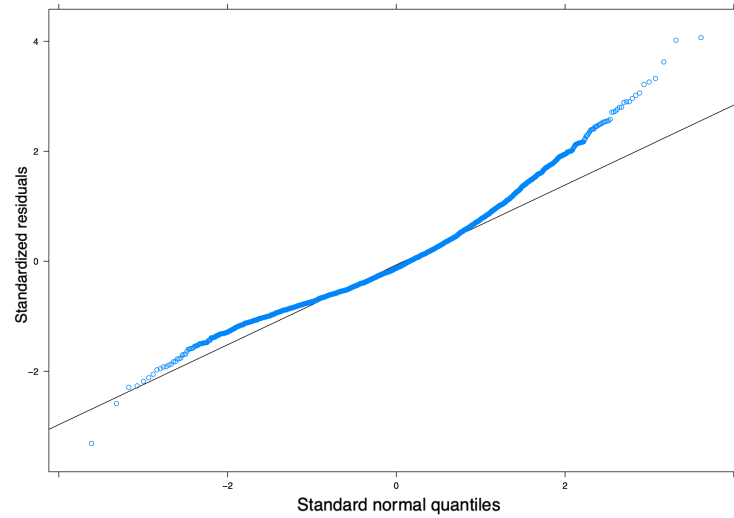


Figure 4.1: Normal probability plot of the linear mixed model residuals for SDQ total score with with random-effects specified at child level

The validity of a non-linear QR approach over a standard linear one is assessed with an analysis of variance (ANOVA) test (Sthle et al., 1989) to compare a spline QR model and standard QR at five quantile levels $\tau = 0.1, 0.25, 0.5, 0.75, 0.9$. The spline QR model is an additive model represented by piecewise-defined polynomial functions. This approach allows to model non-linear relationships by means of knot points, at which each different polynomial segment originates. In particular, in this chapter the the QR spline model is represented by a piecewise cubic polynomial with 3 knots for each covariate.

The results obtained from the ANOVA test in Table 4.3 reveal that, with the dataset of interest, a non-linear approach results more valid than the linear one. This finding supports the adoption of a non-linear QR approach, such as the FM-QRF, as a preferred choice over standard linear QR model, especially in scenarios where the underlying data exhibits non-linear relationships.

τ	0.1	0.25	0.5	0.75	0.9
T_n	3.471	5.478	19.392	6.536	8.895
P -Value	0***	0***	0***	0***	0***

Table 4.3: ANOVA test results for different values of τ . The 'Tn' column reports the test statistic and the 'P-Value' column reports the level of significance of the test at 5% significance level.

4.3 Analysis of the UK Household Longitudinal Study Data

This section reports the results of the analysis of the SDQ total score dataset for the selected UKHLS sample of children. Given previous literature results, the analysis concerns the risk factors for children's emotional and behavioural problems related to family poverty, ethnicity, overcrowding in the household and internet access.

In particular, the analysis considers covariates related to such risk factors whose effects might have changed between before and during the pandemic: social benefit income, household size and number of bedrooms in the house, number of employed people in the household and employed people in the household that are not being paid, living area (urban or rural), being up to date with bills payments and internet access. The belonging to an ethnic minority is included as time-invariant variable.

The FM-QRF described in Chapter 3 is used to model quantiles at five different levels $\tau = 0.1, 0.25, 0.5, 0.75, 0.9$:

$$\hat{Q}_{it,\tau} = \widehat{g_\tau(\mathbf{x}_{it})} + \hat{\alpha}_{k,\tau} \quad \tau \in (0, 1), \quad (4.1)$$

where $g_\tau : \mathbb{R}^p \rightarrow \mathbb{R}$. In this case, $\hat{Q}_{it,\tau}$ is the estimated quantile for the $i - th$ individual at level τ and time t , $g_\tau(\mathbf{x}_{it})$ is the fixed-effects part of the model estimated with a QRF approach and $\alpha_{k,\tau}$ is the random effects part estimated with the finite mixture approach described in Section 3.2.

In this empirical application, the number of mixture components K has been set to 10 via grid search.

For the sake of clarity, this chapter reports only results for $\tau = 0.1, 0.5, 0.9$. Results for the remaining quantile levels, which are similar to the ones reported in this section, are available upon request.

4.3.1 Risk Factors Analysis

The risk factor analysis is run by extracting the Variable Importance measure from the FM-QRF in order to evaluate which covariate has a more relevant role in predicting the SDQ total score quantiles. Figures 4.2-4.4 report the bar graphs in which each bar represents the variable importance of each covariate at quantile levels $\tau = 0.1, 0.5, 0.9$ before and during the COVID-19 pandemic. The variables have been ordered in each graph according to the average variable importance in both periods. This allows to understand both the ranking of the variables in each separate period and the overall ranking at quantile level. The variable importance values for the quantile levels $\tau = 0.25, 0.75$ are shown in Figures C.2-C.3.

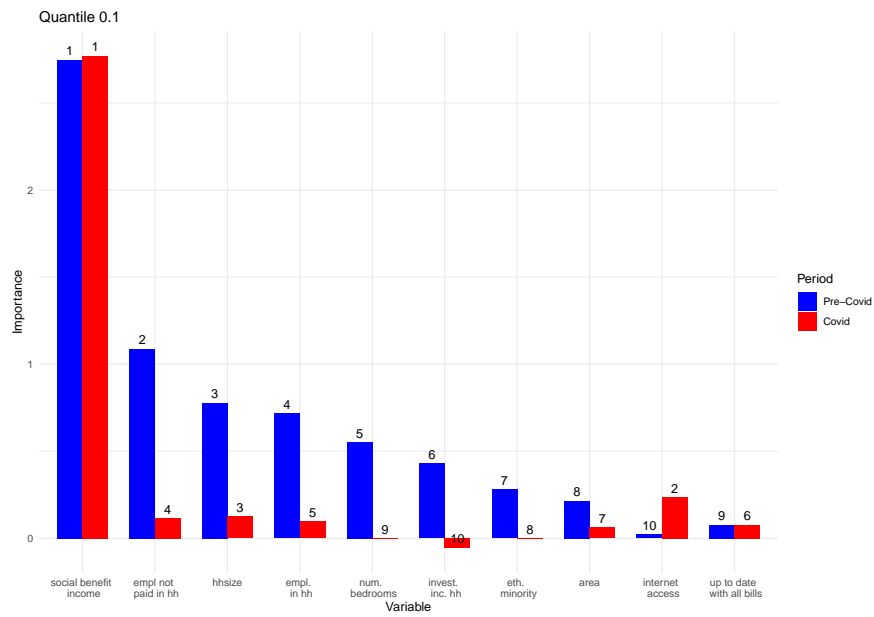


Figure 4.2: Bar plot showing the Variable Importance extracted from the FM-QRF for each covariate at quantile level $\tau = 0.1$. The blue bars represent the Variable Importance in the Pre-pandemic period and the red bars are related to the pandemic period. Numbers at the top of the bars indicate the ranking position of each variable in terms of Variable Importance.

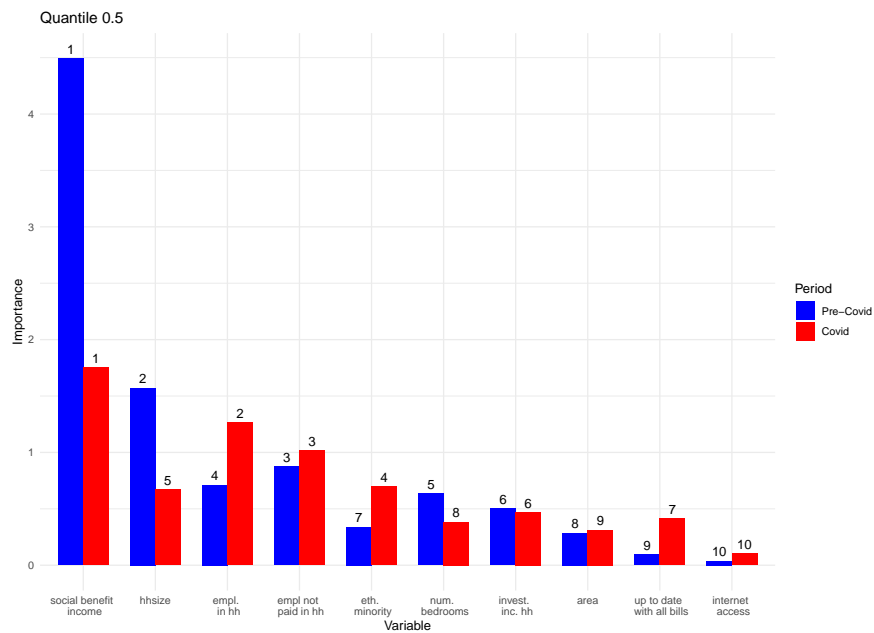


Figure 4.3: Bar plot showing the Variable Importance extracted from the FM-QRF for each covariate at quantile level $\tau = 0.5$. The blue bars represent the Variable Importance in the Pre-pandemic period and the red bars are related to the pandemic period. Numbers at the top of the bars indicate the ranking position of each variable in terms of Variable Importance.

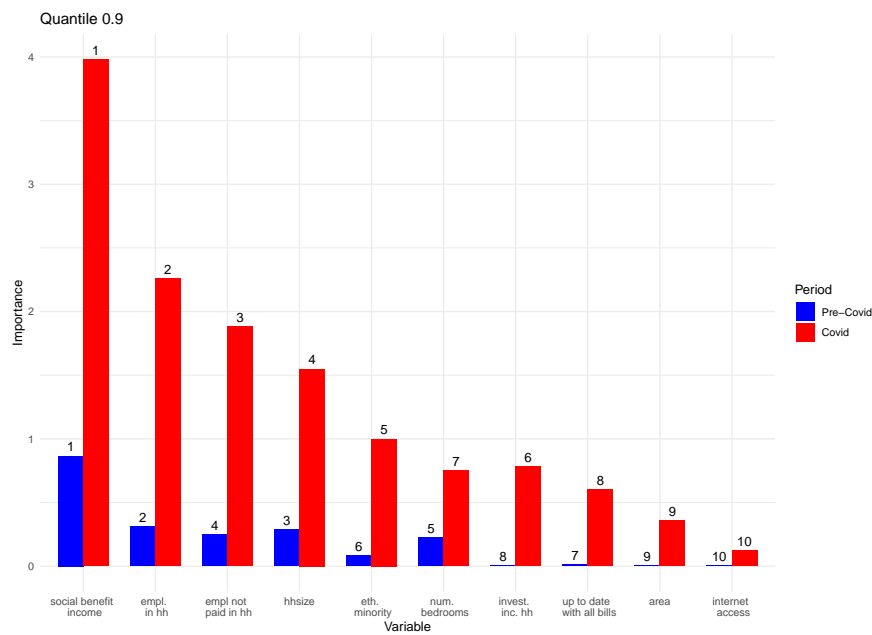


Figure 4.4: Bar plot showing the Variable Importance extracted from the FM-QRF for each covariate at quantile level $\tau = 0.9$. The blue bars represent the Variable Importance in the pre-pandemic period and the red bars are related to the pandemic period. Numbers at the top of the bars indicate the ranking position of each variable in terms of Variable Importance.

At level $\tau = 0.01$, the three most important variables in the pre-pandemic period are social benefit income, number of employed people not paid in the household, both proxies for family poverty, and household size. During the COVID pandemic, social benefit income remains the most important variable, whereas the second most important one shifts from being the number of employed people not paid in the household to internet access, which is among the less important variables before the pandemic. This result highlights how during the pandemic the importance of internet access significantly increased for children with low levels of behavioural issues.

At the median level $\tau = 0.5$, before the pandemic the most important variable is social benefit income, the second important variable is household size and the third one is number of employed people not paid in the household. After the pandemic, the variable importance order changes only at the second place, which is covered by the number of employed people in the household.

At the higher quantile level $\tau = 0.9$, the first three most important variables before the pandemic are social benefit income, number of employed people in the household and household size. During the pandemic, the third most important variable is the number of employed people not being paid. Even if the order is quite similar before and during the pandemic, the main difference between these two periods is that the relevance of the three most important variables is sensibly higher during the pandemic. Being these three variables proxies for the level of family poverty, this result indicates that this factor

became more important after the pandemic for children with a high grade of behavioural issues.

In conclusion, in both periods, the most important variable for children with both high and low levels of behavioural issues is social benefit income. The result of this analysis highlights that during the pandemic the importance of internet access significantly increased during the pandemic in maintaining low levels of behavioural issues, whereas the relevance of family poverty increased for children with high levels of behavioural issues. Moreover, it is also worth noticing that the variable importance changes across quantile levels, corroborating the use of the QR approach proposed in this chapter.

4.3.2 Comparison with the LQMM Results

This section reports the results obtained by fitting the LQMM model of Equation (3.2) with random intercept at the five quantile levels $\tau = 0.1, 0.25, 0.5, 0.75, 0.9$. The aim of this analysis is to investigate whether the non-parametric approach of the FM-QRF might represent an additional valuable approach to investigate the risk factors determining children behavioural issues.

To this end, the sets of significant variables obtained with the LQMM models fitted for each quantile level are compared with the set of most important variables obtained from the FM-QRF using the Variable Importance measure.

The LQMM results coefficients for the pre-pandemic and pandemic period are reported in Table 4.6.

At quantile level $\tau = 0.1$, in the pre-pandemic period the set of significant variables comprises variables proxies of the overcrowding in the household (number of beds and household size), the number of employed people in the household and ethnic minority. During the pandemic, the set of significant variables gets larger and includes also social benefit income and investment income. Similarly to results shown in previous contributions, the significant variables with the higher coefficient during the pandemic period are the employment variable and the ethnic minority dummy variable.

At quantile level $\tau = 0.5$, the set of significant variables remains almost the same in the pre-pandemic and pandemic periods. In the pre-pandemic period the significant variables are household size, number of beds, social benefit income, employed people in the household and ethnic minority. The main difference with the pandemic period is that during the COVID-19 pandemic the set of significant variables includes the investment income and does not include social benefit income and number of beds.

At quantile level $\tau = 0.9$, in the pre-pandemic period the significant variables are social benefit income, number of employed people and ethnic minority. During the pandemic, the set of significant variables includes also household size and number of employed people not paid.

Pre-Pandemic					
τ	0.10	0.25	0.50	0.75	0.90
LQMM	2.85	3.58	4.70	6.64	8.41
FM-QRF	6.56	21.96	13.29	41.88	66.47

Table 4.4: Pseudo- R^2 values related to the pre-pandemic period for the LQMM and the FM-QRF models. Values are expressed in percentages.

Pandemic					
τ	0.10	0.25	0.50	0.75	0.90
LQMM	0.46	1.96	2.08	4.74	10.58
FM-QRF	0.86	16.64	8.57	71.82	35.07

Table 4.5: Pseudo- R^2 values related to the pandemic period for the LQMM and the FM-QRF models. Values are expressed in percentages.

Additionally, the pseudo- R^2 measure is computed for both models to evaluate their goodness of fit. This measure has been proposed in Koenker and Machado (1999) and implemented in the quantile regression literature (see, for instance, Bianchi et al. (2018), Borgoni et al. (2024)) as a valid alternative to the standard R^2 . In particular, the pseudo- R^2 is computed as:

$$R_{\rho}^2(\tau) = 1 - \frac{\sum_{i=1}^n \rho_{\tau}(e_{it})}{\sum_{i=1}^n \rho_{\tau}(\tilde{e}_{it})} \quad (4.2)$$

where $\rho_{\tau}(\cdot)$ is the quantile loss function of Koenker and Bassett Jr (1978), e_{it} are the standardized residuals of the full model trained with the whole set of covariates and \tilde{e}_{it} are the standardized residuals under the null model, which considers only the intercept (the coefficients of the covariates are set to 0). The results concerning the goodness of fit of the LQMM and FM-QRF model in the pre-COVID and COVID periods are reported separately in Tables 4.4 and 4.5.

The values of the pseudo- R^2 highlight that the FM-QRF has a greater goodness of fit with respect to the LQMM at all quantile levels both in the pre-COVID and COVID periods. Moreover, as already noted in for other kind of models, the pseudo- R^2 increases with the quantile level of interest for both the FM-QRF and the LQMM.

From these results a variety of conclusions can be drawn. First, similarly to the FM-QRF analysis results, the significant variables set and the related coefficient values change across quantile levels. This result further justify the relevance of a QR approach. However, the ethnic minority variable and number of employed people in the household are significant at all quantile levels in the pandemic period and their coefficient values are similar across quantiles.

Second, the set of significant variables obtained with the LQMM approach does not always coincide with the set of most important variables obtained with the FM-QRF.

For instance, at quantile level $\tau = 0.1$, the internet access variable is the second most important variable in the FM-QRF analysis, whereas in the LQMM analysis it is not significant neither in the pre-pandemic period nor during the pandemic.

These results highlight how a non-parametric approach might be useful to uncover meaningful non-linear relationships among variables that are being overlooked with a linear approach.

		Pre-Pandemic				Pandemic				
		Variable	Estimate	Std. Error	P-Value	Variable	Estimate	Std. Error	P-Value	
0.1	Intercept	11.153	(1.681)	0.000	***	Intercept	5.447	(4.517)	0.234	
	area	-0.036	(0.173)	0.838		area	0.055	(0.136)	0.690	
	hhszise	-0.887	(0.155)	0.000	***	hhszise	-0.966	(0.25)	0.000	***
	n_beds	-0.759	(0.145)	0.000	***	n_beds	-0.437	(0.209)	0.042	**
	soc_ben_inc	-0.001	(0.001)	0.106		soc_ben_inc	-0.002	(0.001)	0.021	**
	invest_inc	-0.001	(0.001)	0.254		invest_inc	-0.002	(0.001)	0.002	***
	empl_not_paid	-0.241	(0.272)	0.380		empl_not_paid	0.530	(0.484)	0.278	
	internet_access	-0.387	(1.204)	0.750		internet_access	4.197	(4.503)	0.356	
	empl	0.726	(0.284)	0.014	**	empl	1.337	(0.413)	0.002	***
	eth_min	-1.696	(0.288)	0.000	***	eth_min	-1.663	(0.683)	0.019	**
0.5	Intercept	11.236	(1.778)	0.000	***	Intercept	5.517	(5.37)	0.309	
	area	0.065	(0.183)	0.723		area	0.138	(0.126)	0.279	
	hhszise	-0.575	(0.154)	0.000	***	hhszise	-0.699	(0.247)	0.007	***
	n_beds	-0.495	(0.146)	0.001	***	n_beds	-0.204	(0.237)	0.392	
	soc_ben_inc	0.001	(0.000)	0.000	***	soc_ben_inc	0.001	(0.000)	0.145	
	invest_inc	0.000	(0.000)	0.135		invest_inc	0.000	(0.000)	0.026	**
	empl_not_paid	-0.088	(0.249)	0.724		empl_not_paid	0.656	(0.418)	0.122	
	internet_access	-0.303	(1.483)	0.839		internet_access	4.267	(5.078)	0.405	
	empl	0.735	(0.325)	0.028	**	empl	1.346	(0.386)	0.001	***
	eth_min	-1.693	(0.4)	0.000	***	eth_min	-1.662	(0.591)	0.007	***
0.9	Intercept	11.285	(1.531)	0.000	***	Intercept	5.542	(5.511)	0.320	
	area	0.129	(0.22)	0.560		area	0.168	(0.15)	0.268	
	hhszise	-0.385	(0.217)	0.083		hhszise	-0.601	(0.21)	0.006	***
	n_beds	-0.335	(0.196)	0.093		n_beds	-0.122	(0.203)	0.550	
	soc_ben_inc	0.007	(0.001)	0.000	***	soc_ben_inc	0.008	(0.001)	0.000	***
	invest_inc	0.001	(0.001)	0.417		invest_inc	0.001	(0.001)	0.151	
	empl_not_paid	0.006	(0.283)	0.983		empl_not_paid	0.704	(0.345)	0.047	**
	internet_access	-0.253	(1.433)	0.860		internet_access	4.292	(5.184)	0.412	
	empl	0.740	(0.325)	0.027	**	empl	1.350	(0.385)	0.001	***
	eth_min	-1.690	(0.365)	0.000	***	eth_min	-1.660	(0.662)	0.015	**

Table 4.6: LQMM results coefficients for the pre-pandemic and the pandemic period at five quantile levels $\tau = 0.1, 0.5, 0.9$. The symbol '***' denotes significance at 1% level and '**' significance at 5%.

4.4 Conclusions

The COVID-19 pandemic has significantly affected different aspects of society, including children's mental health. This chapter investigates the risk factors driving children's mental health before and during the pandemic using data from the UK Household

Longitudinal Study. The analysis employs the novel machine learning algorithm FM-QRF of Chapter 3 to model the complex relationship between pandemic-related factors and children's mental health, measured with the well-known SDQ score.

The empirical findings reveal that the drivers of children's mental health differ between those with low and high SDQ scores, and that these drivers also vary before and during the pandemic. Moreover, by studying the SDQ conditional distribution at different quantile levels, this study provides a deeper understanding of the impact of the pandemic on children's mental health outcomes with respect to standard linear approaches.

Key findings indicate that social benefit income variable remains a crucial factor across different quantile levels in both pre-pandemic and pandemic periods. Additionally, the importance of internet access significantly increased during the pandemic, especially for children with lower levels of behavioral issues. The study also highlights the higher relevance of family poverty during the pandemic for children with higher levels of behavioral issues.

The comparison with the LQMM model results highlights the relevance of the non-parametric approach employed in this study. As a matter of fact, the FM-QRF offers an additional approach to gain a more comprehensive understanding of the complex dynamics affecting children's mental health, since it reveals non-linear relationships among variables that are overlooked by linear models, such as the LQMM.

In conclusion, this research contributes to the growing body of literature addressing the impact of the COVID-19 pandemic on children's mental health. The use of non-linear approaches like FM-QRF enhances the depth of the analysis, providing valuable insights for policymakers, educators, and healthcare professionals working to support and improve children's well-being.

Bibliography

- Adegboye, D., Williams, F., Collishaw, S., Shelton, K., Langley, K., Hobson, C., Burley, D., and van Goozen, S. (2021). Understanding why the COVID-19 pandemic-related lockdown increases mental health difficulties in vulnerable young children. *JCPP advances*, 1(1):e12005.
- Adrian, T., Boyarchenko, N., and Giannone, D. (2019). Vulnerable growth. *American Economic Review*, 109(4):1263–89.
- Adrian, T., Grinberg, F., Liang, N., Malik, S., and Yu, J. (2022). The term structure of Growth-at-Risk. *American Economic Journal: Macroeconomics*, 14(3):283–323.
- Akram, Q. F. (2009). Commodity prices, interest rates and the dollar. *Energy Economics*, 31(6):838–851. Energy Sector Pricing and Macroeconomic Dynamics.
- Alfö, M., Salvati, N., and Ranalli, M. G. (2017). Finite mixtures of quantile and M-quantile regression models. *Statistics and Computing*, 27(2):547–570.
- Andreani, M., Candila, V., Morelli, G., and Petrella, L. (2021). Multivariate analysis of energy commodities during the COVID-19 pandemic: Evidence from a mixed-frequency approach. *Risks*, 9(8):144.
- Athey, S., Tibshirani, J., Wager, S., et al. (2019). Generalized Random Forests. *The Annals of Statistics*, 47(2):1148–1178.
- Aydinalp, C. and Cresser, M. S. (2008). The effects of global climate change on agriculture. *American-Eurasian Journal of Agricultural & Environmental Sciences*, 3(5):672–676.
- Bangwayo-Skeete, P. F. and Skeete, R. W. (2015). Can Google data improve the forecasting performance of tourist arrivals? Mixed-data sampling approach. *Tourism Management*, 46:454–464.
- Barreca, A., Clay, K., Deschênes, O., Greenstone, M., and Shapiro, J. S. (2015). Convergence in adaptation to climate change: Evidence from high temperatures and mortality, 1900–2004. *American Economic Review*, 105(5):247–251.
- Barro, R. J. (2015). Environmental protection, rare disasters and discount rates. *Economica*, 82(325):1–23.
- Bassett, G. W. and Chen, H.-L. (2002). Portfolio style: Return-based attribution using quantile regression. In *Economic applications of quantile regression*, pages 293–305. Springer.

- Bayer, S. (2018). Combining Value-at-Risk forecasts using penalized quantile regressions. *Econometrics and statistics*, 8:56–77.
- Bayrakdar, S. and Guveli, A. (2023). Inequalities in home learning and schools' remote teaching provision during the COVID-19 school closure in the UK. *Sociology*, 57(4):767–788.
- Bernardi, M., Bottone, M., and Petrella, L. (2018). Bayesian quantile regression using the skew exponential power distribution. *Computational Statistics & Data Analysis*, 126:92–111.
- Bernardi, M., Gayraud, G., and Petrella, L. (2015). Bayesian tail risk interdependence using quantile regression. *Bayesian Analysis*, 10(3):553–603.
- Bernardi, M., Maruotti, A., and Petrella, L. (2017). Multiple risk measures for multivariate dynamic heavy-tailed models. *Journal of Empirical Finance*, 43:1–32.
- Bianchi, A., Fabrizi, E., Salvati, N., and Tzavidis, N. (2018). Estimation and testing in M-quantile regression with applications to small area estimation. *International Statistical Review*, 86(3):541–570.
- Bignardi, G., Dalmaijer, E. S., Anwyl-Irvine, A. L., Smith, T. A., Siugzdaite, R., Uh, S., and Astle, D. E. (2021). Longitudinal increases in childhood depression symptoms during the COVID-19 lockdown. *Archives of disease in childhood*, 106(8):791–797.
- Borgoni, R., Del Bianco, P., Salvati, N., Schmid, T., and Tzavidis, N. (2018). Modelling the distribution of health-related quality of life of advanced melanoma patients in a longitudinal multi-centre clinical trial using M-quantile random effects regression. *Statistical methods in medical research*, 27(2):549–563.
- Borgoni, R., Schirripa Spagnolo, F., Michelangeli, A., Salvati, N., and Carcagnì, A. (2024). Semiparametric M-quantile regression with measurement error in spatial covariates: an application to housing price modelling. *Journal of the Royal Statistical Society Series C: Applied Statistics*, 73(1):82–103.
- Bradley, R. H. and Corwyn, R. F. (2002). Socioeconomic status and child development. *Annual review of psychology*, 53(1):371–399.
- Breiman, L. (1996). Bagging predictors. *Machine learning*, 24(2):123–140.
- Breiman, L. (2001). Random Forests. *Machine learning*, 45(1):5–32.
- Breiman, L., Friedman, J., Olshen, R., and Stone, C. (1984). Classification and regression trees. wadsworth & brooks. *Cole Statistics/Probability Series*.
- Burke, M., Davis, W. M., and Diffenbaugh, N. S. (2018a). Large potential reduction in economic damages under un mitigation targets. *Nature*, 557(7706):549–553.
- Burke, M., González, F., Baylis, P., Heft-Neal, S., Baysan, C., Basu, S., and Hsiang, S. (2018b). Higher temperatures increase suicide rates in the United States and Mexico. *Nature climate change*, 8(8):723–729.

- Burke, M., Hsiang, S. M., and Miguel, E. (2015). Global non-linear effect of temperature on economic production. *Nature*, 527(7577):235–239.
- Candila, V., Gallo, G. M., and Petrella, L. (2023). Mixed-frequency quantile regressions to forecast Value-at-Risk and Expected Shortfall. *Annals of Operations Research*, pages 1–34.
- Carleton, T. A. and Hsiang, S. M. (2016). Social and economic impacts of climate. *Science*, 353(6304):aad9837.
- Cattaneo, C. and Peri, G. (2016). The migration response to increasing temperatures. *Journal of development economics*, 122:127–146.
- Christmann, A. and Steinwart, I. (2008). Consistency of kernel-based quantile regression. *Applied Stochastic Models in Business and Industry*, 24(2):171–183.
- Christoffersen, P. and Pelletier, D. (2004). Backtesting Value-at-Risk: A duration-based approach. *Journal of Financial Econometrics*, 2(1):84–108.
- Christoffersen, P. F. (1998). Evaluating interval forecasts. *International economic review*, pages 841–862.
- Cont, R. (2001). Empirical properties of asset returns: stylized facts and statistical issues. *Quantitative finance*, 1(2):223.
- Coronese, M., Lamperti, F., Chiaromonte, F., and Roventini, A. (2018). Natural disaster risk and the distributional dynamics of damages.
- Coronese, M., Lamperti, F., Keller, K., Chiaromonte, F., and Roventini, A. (2019). Evidence for sharp increase in the economic damages of extreme natural disasters. *Proceedings of the National Academy of Sciences*, 116(43):21450–21455.
- Daly, M. and Robinson, E. (2022). Psychological distress associated with the second COVID-19 wave: Prospective Evidence from the UK Household Longitudinal Study. *Journal of affective disorders*, 310:274–278.
- Damania, R., Desbureaux, S., and Zaveri, E. (2020). Does rainfall matter for economic growth? Evidence from global sub-national data (1990–2014). *Journal of Environmental Economics and Management*, 102:102335.
- Daouia, A., Girard, S., and Stupfler, G. (2018). Estimation of tail risk based on extreme expectiles. *Journal of the Royal Statistical Society Series B: Statistical Methodology*, 80(2):263–292.
- Daouia, A., Girard, S., and Stupfler, G. (2021). Expecthill estimation, extreme risk and heavy tails. *Journal of Econometrics*, 221(1):97–117.
- Davis, E., Sawyer, M. G., Lo, S. K., Priest, N., and Wake, M. (2010). Socioeconomic risk factors for mental health problems in 4–5-year-old children: Australian population study. *Academic Pediatrics*, 10(1):41–47.

- Dell, M., Jones, B. F., and Olken, B. A. (2012). Temperature shocks and economic growth: Evidence from the last half century. *American Economic Journal: Macroeconomics*, 4(3):66–95.
- Dell, M., Jones, B. F., and Olken, B. A. (2014). What do we learn from the weather? The new climate-economy literature. *Journal of Economic Literature*, 52(3):740–98.
- Deschênes, O. and Greenstone, M. (2007). The economic impacts of climate change: Evidence from agricultural output and random fluctuations in weather. *American economic review*, 97(1):354–385.
- Engle, R. F., Ghysels, E., and Sohn, B. (2013). Stock market volatility and macroeconomic fundamentals. *Review of Economics and Statistics*, 95(3):776–797.
- Engle, R. F. and Manganelli, S. (2004). CAViaR: Conditional autoregressive Value-at-Risk by regression quantiles. *Journal of Business & Economic Statistics*, 22(4):367–381.
- Fankhauser, S. and Tol, R. S. (2005). On climate change and economic growth. *Resource and Energy Economics*, 27(1):1–17.
- Farcomeni, A. (2012a). Quantile regression for longitudinal data based on latent Markov subject-specific parameters. *Statistics and Computing*, 22(1):141–152.
- Farcomeni, A. (2012b). Quantile regression for longitudinal data based on latent Markov subject-specific parameters. *Statistics and Computing*, 22:141–152.
- Flouri, E., Mavroveli, S., and Tzavidis, N. (2010). Modeling risks: effects of area deprivation, family socio-economic disadvantage and adverse life events on young children’s psychopathology. *Social psychiatry and psychiatric epidemiology*, 45:611–619.
- Flouri, E. and Tzavidis, N. (2008). Psychopathology and prosocial behavior in adolescents from socio-economically disadvantaged families: the role of proximal and distal adverse life events. *European child & adolescent psychiatry*, 17:498–506.
- Genuer, R. (2012). Variance reduction in purely Random Forests. *Journal of Nonparametric Statistics*, 24(3):543–562.
- Geraci, M. and Bottai, M. (2007). Quantile regression for longitudinal data using the asymmetric Laplace distribution. *Biostatistics*, 8(1):140–154.
- Geraci, M. and Bottai, M. (2014). Linear quantile mixed models. *Statistics and computing*, 24(3):461–479.
- Ghysels, E. and Qian, H. (2019). Estimating MIDAS regressions via ols with polynomial parameter profiling. *Econometrics and statistics*, 9:1–16.
- Ghysels, E., Sinko, A., and Valkanov, R. (2007). MIDAS regressions: Further results and new directions. *Econometric reviews*, 26(1):53–90.
- Goodman, R. (1997). The strengths and difficulties questionnaire: a research note. *Journal of child psychology and psychiatry*, 38(5):581–586.

- Goodnight, J. A., Lahey, B. B., Van Hulle, C. A., Rodgers, J. L., Rathouz, P. J., Waldman, I. D., and D'Onofrio, B. M. (2012). A quasi-experimental analysis of the influence of neighborhood disadvantage on child and adolescent conduct problems. *Journal of abnormal psychology*, 121(1):95.
- Graff Zivin, J. and Neidell, M. (2014). Temperature and the allocation of time: Implications for climate change. *Journal of Labor Economics*, 32(1):1–26.
- Hajjem, A., Bellavance, F., and Larocque, D. (2011). Mixed effects regression trees for clustered data. *Statistics & probability letters*, 81(4):451–459.
- Hajjem, A., Bellavance, F., and Larocque, D. (2014). Mixed-effects random forest for clustered data. *Journal of Statistical Computation and Simulation*, 84(6):1313–1328.
- Hastie, T., Tibshirani, R., Friedman, J., Hastie, T., Tibshirani, R., and Friedman, J. (2009). Random Forests. *The elements of statistical learning: Data mining, inference, and prediction*, pages 587–604.
- Heal, G. and Park, J. (2016). Reflections—temperature stress and the direct impact of climate change: a review of an emerging literature. *Review of Environmental Economics and Policy*.
- Hendricks, W. and Koenker, R. (1992). Hierarchical spline models for conditional quantiles and the demand for electricity. *Journal of the American statistical Association*, 87(417):58–68.
- Hsiang, S. (2016). Climate econometrics. *Annual Review of Resource Economics*, 8:43–75.
- Hwang, C. and Shim, J. (2005). A simple quantile regression via support vector machine. In *International Conference on Natural Computation*, pages 512–520. Springer.
- Jiang, W. and Yu, Q. (2023). Carbon emissions and economic growth in China: Based on mixed frequency VAR analysis. *Renewable and Sustainable Energy Reviews*, 183:113500.
- Jorion, P. (1997). *Value-at-Risk*. Irwin, Chicago.
- Kahn, M. E., Mohaddes, K., Ng, R. N., Pesaran, M. H., Raissi, M., and Yang, J.-C. (2021). Long-term macroeconomic effects of climate change: A cross-country analysis. *Energy Economics*, 104:105624.
- Kalkuhl, M. and Wenz, L. (2020). The impact of climate conditions on economic production. Evidence from a global panel of regions. *Journal of Environmental Economics and Management*, 103:102360.
- Kauhanen, L., Wan Mohd Yunus, W. M. A., Lempinen, L., Peltonen, K., Gyllenberg, D., Mishina, K., Gilbert, S., Bastola, K., Brown, J. S., and Sourander, A. (2023). A systematic review of the mental health changes of children and young people before and during the COVID-19 pandemic. *European child & adolescent psychiatry*, 32(6):995–1013.

- Kiley, M. T. (2021). Growth-at- Risk from climate change.
- King, D., Schrag, D., Dadi, Z., Ye, Q., and Ghosh, A. (2017). Climate change: A risk assessment.
- Koenker, R. (2005). Quantile regression cambridge univ.
- Koenker, R. and Bassett Jr, G. (1978). Regression quantiles. *Econometrica: journal of the Econometric Society*, pages 33–50.
- Koenker, R., Chernozhukov, V., He, X., and Peng, L. (2017). Handbook of quantile regression.
- Koenker, R. and Machado, J. A. (1999). Goodness of fit and related inference processes for quantile regression. *Journal of the american statistical association*, 94(448):1296–1310.
- Koenker, R., Ng, P., and Portnoy, S. (1994). Quantile smoothing splines. *Biometrika*, 81(4):673–680.
- Koenker, R. and Zhao, Q. (1996). Conditional quantile estimation and inference for ARCH models. *Econometric Theory*, 12(5):793–813.
- Kolstad, C. D. and Moore, F. C. (2020). Estimating the economic impacts of climate change using weather observations. *Review of Environmental Economics and Policy*.
- Kozumi, H. and Kobayashi, G. (2011). Gibbs sampling methods for bayesian quantile regression. *Journal of statistical computation and simulation*, 81(11):1565–1578.
- Kriegler, E., Bauer, N., Popp, A., Humpenöder, F., Leimbach, M., Strefler, J., Baumstark, L., Bodirsky, B. L., Hilaire, J., Klein, D., et al. (2017). Fossil-fueled development (SSP5): an energy and resource intensive scenario for the 21st century. *Global environmental change*, 42:297–315.
- Kupiec, P. (1995). Techniques for verifying the accuracy of risk measurement models. *The J. of Derivatives*, 3(2).
- Kuzin, V., Marcellino, M., and Schumacher, C. (2011). MIDAS vs. mixed-frequency VAR: Nowcasting GDP in the euro area. *International Journal of Forecasting*, 27(2):529–542.
- Laird, N. (1978). Nonparametric maximum likelihood estimation of a mixing distribution. *Journal of the American Statistical Association*, 73(364):805–811.
- Lee, S. and Noh, J. (2013). Quantile regression estimator for garch models. *Scandinavian Journal of Statistics*, 40(1):2–20.
- Li, C., Zwiers, F., Zhang, X., Li, G., Sun, Y., and Wehner, M. (2021). Changes in annual extremes of daily temperature and precipitation in CMIP6 models. *Journal of Climate*, 34(9):3441–3460.
- Lin, F.-L., Chen, Y.-F., and Yang, S.-Y. (2016). Does the value of us dollar matter with the price of oil and gold? A dynamic analysis from time–frequency space. *International Review of Economics & Finance*, 43:59–71.

- Luts, J., Molenberghs, G., Verbeke, G., Van Huffel, S., and Suykens, J. A. (2012). A mixed effects least squares support vector machine model for classification of longitudinal data. *Computational Statistics & Data Analysis*, 56(3):611–628.
- Ma, L., Mazidi, M., Li, K., Li, Y., Chen, S., Kirwan, R., Zhou, H., Yan, N., Rahman, A., Wang, W., et al. (2021). Prevalence of mental health problems among children and adolescents during the COVID-19 pandemic: A systematic review and meta-analysis. *Journal of affective disorders*, 293:78–89.
- Manganelli, S. (2004). Asset allocation by variance sensitivity analysis. *Journal of Financial Econometrics*, 2(3):370–389.
- Marino, M. F., Tzavidis, N., and Alfò, M. (2018). Mixed hidden Markov quantile regression models for longitudinal data with possibly incomplete sequences. *Statistical methods in medical research*, 27(7):2231–2246.
- Marotzke, J., Semmann, D., and Milinski, M. (2020). The economic interaction between climate change mitigation, climate migration and poverty. *Nature Climate Change*, 10(6):518–525.
- Marsh, L. C. and Cormier, D. R. (2001). *Spline regression models*. Number 137. Sage.
- Meinshausen, N. (2006). Quantile Regression Forests. *Journal of Machine Learning Research*, 7(Jun):983–999.
- Mele, M., Gurrieri, A. R., Morelli, G., and Magazzino, C. (2021). Nature and climate change effects on economic growth: an LSTM experiment on renewable energy resources. *Environmental Science and Pollution Research*, 28:41127–41134.
- Mendelsohn, R., Dinar, A., and Williams, L. (2006). The distributional impact of climate change on rich and poor countries. *Environment and development economics*, 11(2):159–178.
- Mendolia, S., Suziedelyte, A., and Zhu, A. (2022). Have girls been left behind during the COVID-19 pandemic? Gender differences in pandemic effects on children’s mental wellbeing. *Economics Letters*, 214:110458.
- Merlo, L., Maruotti, A., and Petrella, L. (2022a). Two-part quantile regression models for semi-continuous longitudinal data: A finite mixture approach. *Statistical Modelling*, 22(6):485–508.
- Merlo, L., Maruotti, A., Petrella, L., and Punzo, A. (2022b). Quantile hidden semi-Markov models for multivariate time series. *Statistics and computing*, 32(4):1–22.
- Merlo, L., Petrella, L., and Raponi, V. (2021). Forecasting VaR and ES using a joint quantile regression and its implications in portfolio allocation. *Journal of Banking & Finance*, 133:106248.

- Merlo, L., Petrella, L., and Tzavidis, N. (2022c). Quantile mixed hidden Markov models for multivariate longitudinal data: An application to children's strengths and difficulties questionnaire scores. *Journal of the Royal Statistical Society, Series C (Applied Statistics)*, 71(2):417–448.
- Metherell, T. E., Ghai, S., McCormick, E. M., Ford, T. J., and Orben, A. (2022). Digital access constraints predict worse mental health among adolescents during COVID-19. *Scientific Reports*, 12(1):19088.
- Miall, N., Pearce, A., Moore, J. C., Benzeval, M., and Green, M. J. (2023). Inequalities in children's mental health before and during the COVID-19 pandemic: findings from the UK Household Longitudinal Study. *J Epidemiol Community Health*, 77(12):762–769.
- Min, I. and Kim, I. (2004). A Monte Carlo comparison of parametric and nonparametric quantile regressions. *Applied Economics Letters*, 11(2):71–74.
- Mo, D., Gupta, R., Li, B., and Singh, T. (2018). The macroeconomic determinants of commodity futures volatility: Evidence from Chinese and Indian markets. *Economic Modelling*, 70:543–560.
- Nelder, J. A. and Mead, R. (1965). A simplex method for function minimization. *The computer journal*, 7(4):308–313.
- Nelson, G. C., Valin, H., Sands, R. D., Havlík, P., Ahammad, H., Deryng, D., Elliott, J., Fujimori, S., Hasegawa, T., Heyhoe, E., et al. (2014). Climate change effects on agriculture: Economic responses to biophysical shocks. *Proceedings of the National Academy of Sciences*, 111(9):3274–3279.
- Oloko, T. F., Adediran, I. A., and Fadiya, O. T. (2022). Climate change and asian stock markets: A GARCH-MIDAS approach. *Asian Economics Letters*, 3(Early View).
- O'Neill, B. C., Tebaldi, C., Van Vuuren, D. P., Eyring, V., Friedlingstein, P., Hurtt, G., Knutti, R., Kriegler, E., Lamarque, J.-F., Lowe, J., et al. (2016). The scenario model intercomparison project (scenariomip) for CMIP6. *Geoscientific Model Development*, 9(9):3461–3482.
- Orlov, A., Daloz, A. S., Sillmann, J., Thiery, W., Douzal, C., Lejeune, Q., and Schleussner, C. (2021). Global economic responses to heat stress impacts on worker productivity in crop production. *Economics of Disasters and Climate Change*, 5:367–390.
- Palagi, E., Coronese, M., Lamperti, F., and Roventini, A. (2022). Climate change and the nonlinear impact of precipitation anomalies on income inequality. *Proceedings of the National Academy of Sciences*, 119(43):e2203595119.
- Panagi, L., White, S. R., Pinto Pereira, S. M., Nugawela, M. D., Heyman, I., Sharma, K., Stephenson, T., Chalder, T., Rojas, N. K., Dalrymple, E., et al. (2024). Mental health in the COVID-19 pandemic: A longitudinal analysis of the clock cohort study. *PLoS Medicine*, 21(1):e1004315.

- Pandey, G. R. and Nguyen, V.-T.-V. (1999). A comparative study of regression based methods in regional flood frequency analysis. *Journal of Hydrology*, 225(1-2):92–101.
- Peng, R. D., Bobb, J. F., Tebaldi, C., McDaniel, L., Bell, M. L., and Dominici, F. (2011). Toward a quantitative estimate of future heat wave mortality under global climate change. *Environmental health perspectives*, 119(5):701–706.
- Petrella, L. and Raponi, V. (2019). Joint estimation of conditional quantiles in multivariate linear regression models with an application to financial distress. *Journal of Multivariate Analysis*, 173:70–84.
- Ravens-Sieberer, U., Kaman, A., Erhart, M., Otto, C., Devine, J., Löffler, C., Hurrelmann, K., Bullinger, M., Barkmann, C., Siegel, N. A., et al. (2021). Quality of life and mental health in children and adolescents during the first year of the COVID-19 pandemic: results of a two-wave nationwide population-based study. *European child & adolescent psychiatry*, pages 1–14.
- Reich, B. J. (2012). Spatiotemporal quantile regression for detecting distributional changes in environmental processes. *Journal of the Royal Statistical Society: Series C (Applied Statistics)*, 61(4):535–553.
- Reich, B. J., Fuentes, M., and Dunson, D. B. (2011). Bayesian spatial quantile regression. *Journal of the American Statistical Association*, 106(493):6–20.
- Reimers, F. M. (2022). *Primary and secondary education during COVID-19: Disruptions to educational opportunity during a pandemic*. Springer Nature.
- Riahi, K., Van Vuuren, D. P., Kriegler, E., Edmonds, J., O’neill, B. C., Fujimori, S., Bauer, N., Calvin, K., Dellink, R., Fricko, O., et al. (2017). The shared socioeconomic pathways and their energy, land use, and greenhouse gas emissions implications: an overview. *Global environmental change*, 42:153–168.
- Sela, R. J. and Simonoff, J. S. (2012). RE-EM trees: a data mining approach for longitudinal and clustered data. *Machine learning*, 86(2):169–207.
- Smith, L. B., Reich, B. J., Herring, A. H., Langlois, P. H., and Fuentes, M. (2015). Multilevel quantile function modeling with application to birth outcomes. *Biometrics*, 71(2):508–519.
- Somanathan, E., Somanathan, R., Sudarshan, A., and Tewari, M. (2021). The impact of temperature on productivity and labor supply: Evidence from Indian manufacturing. *Journal of Political Economy*, 129(6):1797–1827.
- Sthle, L., Wold, S., et al. (1989). Analysis of variance (ANOVA). *Chemometrics and intelligent laboratory systems*, 6(4):259–272.
- Takeuchi, I., Le, Q., Sears, T., Smola, A., et al. (2006). Nonparametric quantile estimation. *Journal of machine learning research*, 7(Jul):1231–1264.

- Taylor, J. W. (1999). A quantile regression approach to estimating the distribution of multiperiod returns. *The Journal of Derivatives*, 7(1):64–78.
- Taylor, J. W. (2019). Forecasting Value-at-Risk and Expected Shortfall using a semiparametric approach based on the asymmetric Laplace distribution. *Journal of Business & Economic Statistics*, 37(1):121–133.
- Thorn, W. and Vincent-Lancrin, S. (2022). Education in the time of COVID-19 in france, ireland, the United Kingdom and the United States: The nature and impact of remote learning. *Primary and secondary education during COVID-19: Disruptions to educational opportunity during a pandemic*, pages 383–420.
- Tian, Y., Tang, M., and Tian, M. (2016). A class of finite mixture of quantile regressions with its applications. *Journal of Applied Statistics*, 43(7):1240–1252.
- Tian, Y., Tian, M., and Zhu, Q. (2014). Linear quantile regression based on EM algorithm. *Communications in Statistics-Theory and Methods*, 43(16):3464–3484.
- Tol, R. S. (2018). The economic impacts of climate change. *Review of environmental economics and policy*.
- Tzavidis, N., Salvati, N., Schmid, T., Flouri, E., and Midouhas, E. (2016). Longitudinal analysis of the strengths and difficulties questionnaire scores of the millennium cohort study children in england using M-quantile random-effects regression. *Journal of the Royal Statistical Society Series A: Statistics in Society*, 179(2):427–452.
- Van Vuuren, D. P., Stehfest, E., Gernaat, D. E., Doelman, J. C., Van den Berg, M., Harmsen, M., de Boer, H. S., Bouwman, L. F., Daioglou, V., Edelenbosch, O. Y., et al. (2017). Energy, land-use and greenhouse gas emissions trajectories under a green growth paradigm. *Global Environmental Change*, 42:237–250.
- Vasseur, S. P. and Aznarte, J. L. (2021). Comparing quantile regression methods for probabilistic forecasting of NO₂ pollution levels. *Scientific Reports*, 11(1):11592.
- Waite, P., Pearcey, S., Shum, A., Raw, J. A., Patalay, P., and Creswell, C. (2021). How did the mental health symptoms of children and adolescents change over early lockdown during the COVID-19 pandemic in the UK? *JCPP advances*, 1(1):e12009.
- Walton, A. and Flouri, E. (2010). Contextual risk, maternal parenting and adolescent externalizing behaviour problems: The role of emotion regulation. *Child: care, health and development*, 36(2):275–284.
- Wang, Y. (1998). Mixed effects smoothing spline analysis of variance. *Journal of the royal statistical society: Series b (statistical methodology)*, 60(1):159–174.
- Wei, Y., Pere, A., Koenker, R., and He, X. (2006). Quantile regression methods for reference growth charts. *Statistics in medicine*, 25(8):1369–1382.
- Weitzman, M. L. (2014). Fat tails and the social cost of carbon. *American Economic Review*, 104(5):544–46.

- Wen, L., Liu, C., Song, H., and Liu, H. (2021). Forecasting tourism demand with an improved mixed data sampling model. *Journal of Travel Research*, 60(2):336–353.
- White, H. (1992). Nonparametric estimation of conditional quantiles using neural networks. In *Computing Science and Statistics*, pages 190–199. Springer.
- Xiao, Z. and Koenker, R. (2009). Conditional quantile estimation for generalized autoregressive conditional heteroscedasticity models. *Journal of the American Statistical Association*, 104(488):1696–1712.
- Xiong, Y., Kim, H. J., and Singh, V. (2019). Mixed effects neural networks (menets) with applications to gaze estimation. In *Proceedings of the IEEE/CVF conference on computer vision and pattern recognition*, pages 7743–7752.
- Xu, Q., Liu, S., Jiang, C., and Zhuo, X. (2021a). QRNN-MIDAS: A novel quantile regression neural network for mixed sampling frequency data. *Neurocomputing*, 457:84–105.
- Xu, Q., Zhang, J., Jiang, C., Huang, X., and He, Y. (2015). Weighted quantile regression via support vector machine. *Expert Systems with Applications*, 42(13):5441–5451.
- Xu, Q., Zhuo, X., Jiang, C., and Liu, Y. (2019). An artificial neural network for mixed frequency data. *Expert Systems with Applications*, 118:127–139.
- Xu, Y., Wang, X., and Liu, H. (2021b). Quantile-based GARCH-MIDAS: Estimating Value-at-Risk using mixed-frequency information. *Finance Research Letters*, 43:101965.
- Yao, Y. and Wang, Y. (2001). Measuring economic downside risk and severity: growth at risk. *Available at SSRN 285255*.
- Yu, K. and Moyeed, R. A. (2001). Bayesian quantile regression. *Statistics & Probability Letters*, 54(4):437–447.
- Zheng, Y., Zhu, Q., Li, G., and Xiao, Z. (2018). Hybrid quantile regression estimation for time series models with conditional heteroscedasticity. *Journal of the Royal Statistical Society. Series B (Statistical Methodology)*, 80(5):975–993.

Appendix A

Mixed-Frequency Quantile Regression Forests

This section reports additional Figures and Tables from Chapter 2.

	<i>Obs</i>	<i>Min</i>	<i>Max</i>	<i>Mean</i>	<i>SD</i>	<i>Skew.</i>	<i>Kurt.</i>
WTI	2053	-28.138	42.583	0.042	3.275	1.177	39.354
BRENT	2053	-25.639	41.202	0.036	2.922	1.107	39.192
HEAT.	2053	-22.314	14.862	0.022	2.511	-0.416	12.046
SP500	2053	-12.765	8.968	0.047	1.095	-1.039	23.955
DOLL	92	4.429	4.747	4.599	0.090	-0.439	1.638
NATGAS	31	-0.219	0.605	0.158	0.166	0.284	3.158
SAUDI_P.	31	-1.313	1.775	0.0242	0.714	0.350	2.746

Table A.1: Summary statistics of the variables included in the sample. The table reports the number of observations (*Obs*), the minimum (*Min*), maximum (*Max*) along with the mean, standard deviation (*SD*), skewness and excess kurtosis.

WTI				
	τ	0.01	0.025	0.05
<i>Static</i>	<i>0.01</i>	-	0.21	0.04
	<i>0.025</i>		-	0.12
<i>Dynamic</i>	<i>0.01</i>	-	0.12	0.01
	<i>0.025</i>		-	0.07
BRENT				
	τ	0.01	0.025	0.05
<i>Static</i>	<i>0.01</i>	-	0.08	0.007
	<i>0.025</i>		-	0.16
<i>Dynamic</i>	<i>0.01</i>	-	0.158	0.01
	<i>0.025</i>		-	0.24
HEATING OIL				
	τ	0.01	0.025	0.05
<i>Static</i>	<i>0.01</i>	-	0.08	0.01
	<i>0.025</i>		-	0.11
<i>Dynamic</i>	<i>0.01</i>	-	0.14	0.02
	<i>0.025</i>		-	0.11

Table A.2: Ratio between the number of times quantiles computed at level τ indicated in the rows are higher than those computed at level τ in the columns.

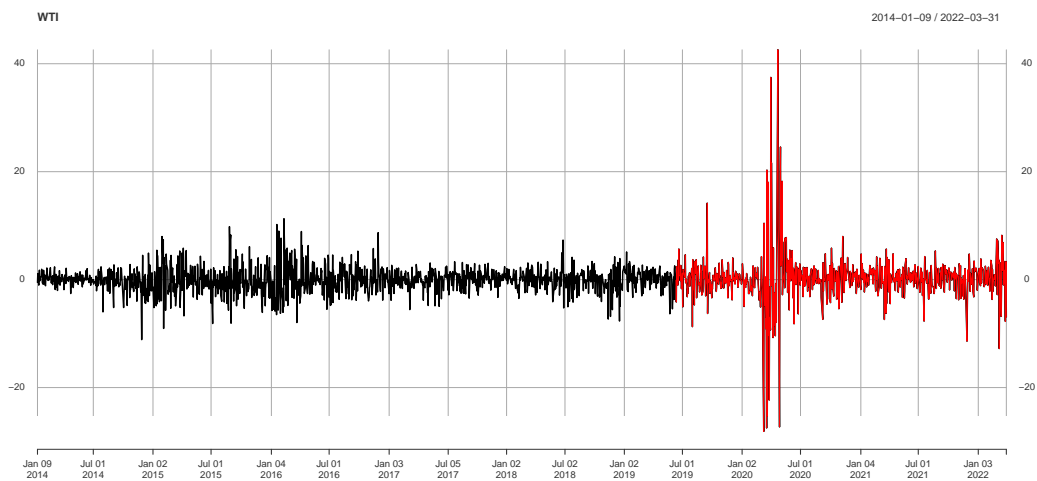


Figure A.1: WTI index time series. the black line represents the training set and the red line the out-of-sample period.

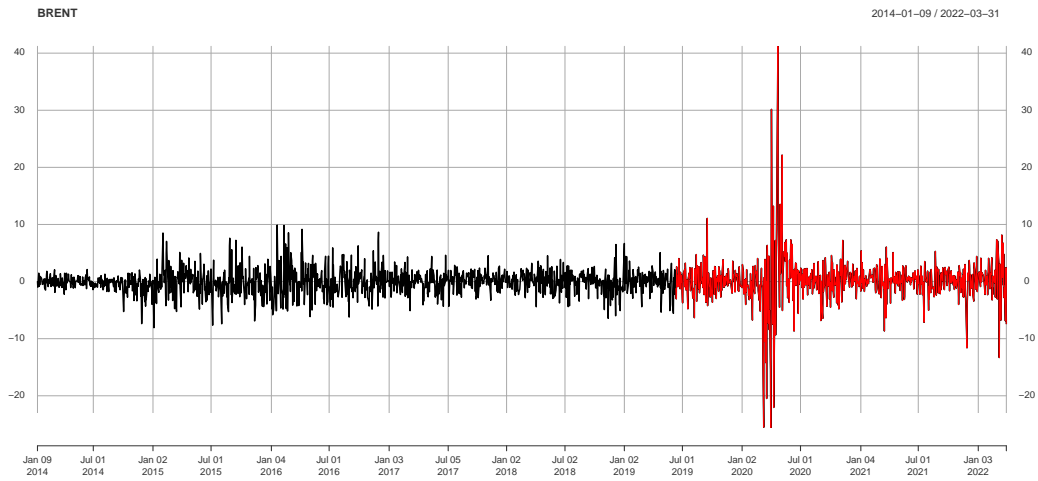


Figure A.2: Brent index time series. the black line represents the training set and the red line the out-of-sample period.

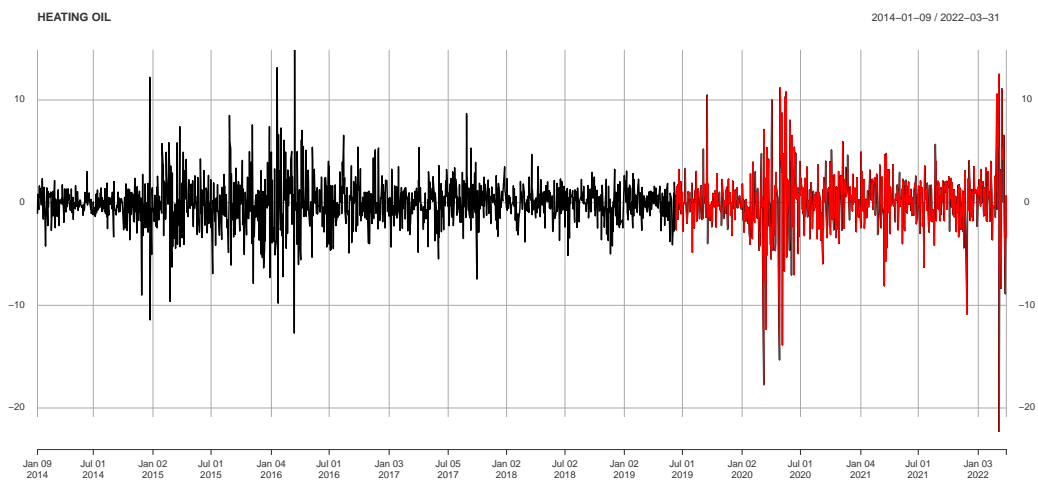


Figure A.3: Heating oil index time series. the black line represents the training set and the red line the out-of-sample period.

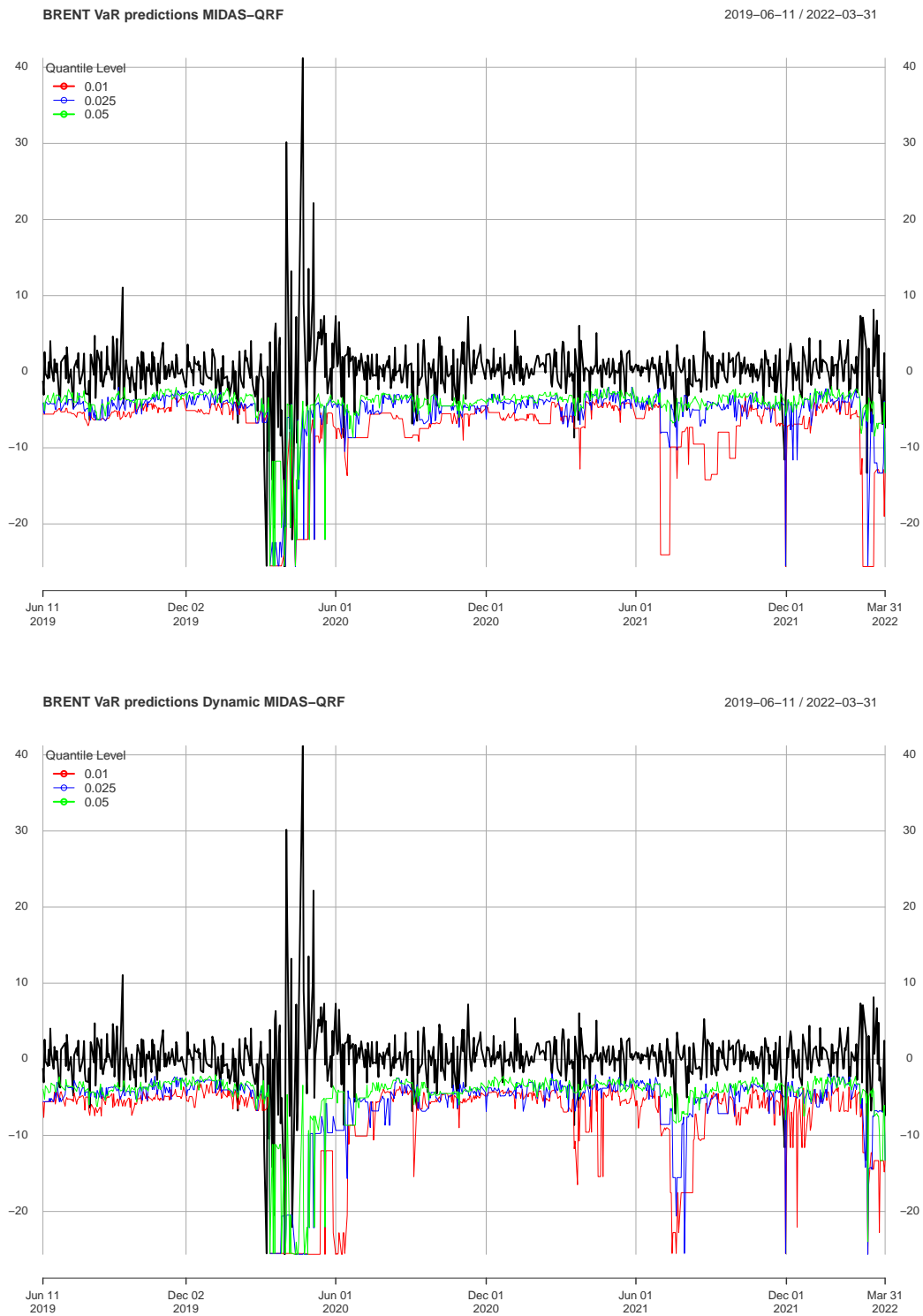


Figure A.4: Brent index (black line) out-of-sample predictions at quantile levels $\tau = 0.01, 0.025, 0.05$. The top panel and the bottom panel show the predictions obtained with the dynamic MIDAS-QRF model, respectively.

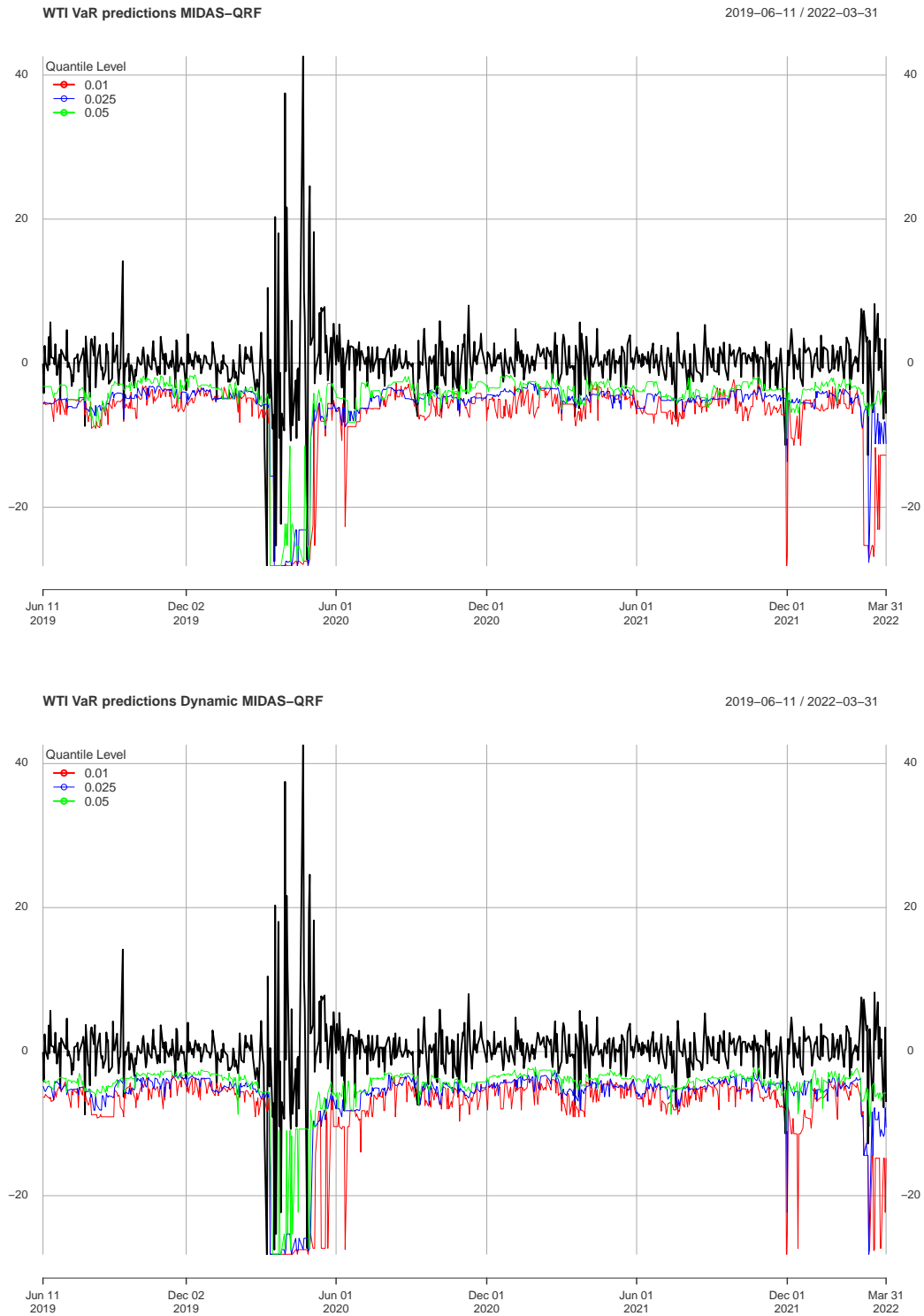


Figure A.5: WTI index (black line) out-of-sample predictions at quantile levels $\tau = 0.01, 0.025, 0.05$. The top panel and the bottom panel show the predictions obtained with the dynamic MIDAS-QRF model, respectively.

Appendix B

Finite mixtures of Quantile Regression Forests and their application to GDP growth-at-risk from climate change

This section reports the mean (in bold) and the standard error of the quantile estimates at level $\tau = 0.01, 0.5, 0.99$ for each country for the SSP1 and SSP5 scenario. The estimates are obtained via bootstrapping with 500 iterations. Each table reports the values for the years 2030, 2050, 2100.

	0.01						0.5						0.99					
	2030		2050		2100		2030		2050		2100		2030		2050		2100	
AFG	-4.56	0.39	-4.32	0.4	-4.83	0.51	6.51	0.22	6.44	0.24	6.38	0.22	21.25	0.72	20.99	0.66	21.1	0.69
ALB	-4.49	0.53	-4.51	0.53	-3.88	0.38	3.99	0.2	3.99	0.16	4.26	0.17	9.33	0.32	9.7	0.35	9.77	0.32
DZA	-4.1	0.3	-4.12	0.29	-3.85	0.24	3.53	0.08	3.35	0.08	3.56	0.08	8.75	0.25	8.96	0.36	8.71	0.23
AGO	-4	0.33	-3.82	0.31	-3.89	0.33	5.49	0.21	5.29	0.22	5.32	0.22	16.12	0.47	15.81	0.45	16.15	0.46
ATG	-16.1	0.55	-17.38	0.89	-17.17	0.91	2.65	0.48	2.35	0.48	2.49	0.5	13.03	0.41	12.65	0.41	12.97	0.43
ARG	-13.31	0.49	-13.89	0.73	-13.6	0.44	3.69	0.37	3.59	0.36	3.59	0.38	11.44	0.39	11.25	0.35	11.28	0.35
ARM	-18.12	0.55	-16.49	0.47	-17.1	0.52	4.45	0.61	6.6	0.61	6.38	0.61	16.65	0.45	17	0.44	17.08	0.45
ABW	-15.38	0.51	-15.2	0.59	-15.37	0.54	1.14	0.27	1.14	0.27	0.93	0.28	8.82	0.29	9.05	0.31	8.81	0.3
AUS	-4.35	0.64	-4.92	0.78	-3.68	0.28	3.12	0.11	3.06	0.12	3.21	0.12	8.64	0.23	8.54	0.23	8.75	0.27
AUT	-5.62	0.31	-6.57	0.36	-6.82	1.45	1.16	0.14	0.82	0.13	0.75	0.12	8.23	0.27	8.15	0.27	8.32	0.28
AZE	-6.3	0.76	-5.21	0.41	-5.02	0.35	6.86	0.22	7.12	0.2	7.08	0.2	29.95	0.9	29.86	0.91	30.71	0.89
BHS	-6.85	0.5	-6.85	0.49	-6.8	0.39	1.24	0.17	1.52	0.2	1.32	0.21	8.74	0.25	8.91	0.27	8.95	0.29
BHR	-4.05	0.26	-3.69	0.31	-4.32	0.53	3.75	0.12	4.77	0.14	4.59	0.16	8.75	0.2	8.86	0.19	9.04	0.23
BGD	-4.03	0.37	-3.88	0.36	-4.18	0.46	5.22	0.17	5.28	0.18	5.3	0.16	9.75	0.29	9.74	0.27	9.61	0.27
BRB	-6.39	0.4	-6.64	0.4	-6.4	0.29	1.22	0.18	0.99	0.2	1.38	0.18	8.45	0.27	8.59	0.28	8.8	0.27
BLR	-3.26	0.27	-4.47	0.8	-4.52	0.45	6.23	0.22	6.07	0.24	5.93	0.24	12.92	0.35	12.33	0.34	12.42	0.34
BEL	-4.47	0.65	-5.68	0.57	-5.4	0.99	1.46	0.13	0.65	0.13	1.4	0.09	8.22	0.28	8.09	0.27	8.4	0.28
BLZ	-3.91	0.3	-4.1	0.28	-4.28	0.34	3.68	0.13	3.46	0.13	3.37	0.12	12.95	0.4	12.37	0.4	12.47	0.42
BEN	-3.66	0.21	-4	0.38	-3.71	0.26	4.08	0.12	4.18	0.13	4.13	0.13	8.63	0.18	8.93	0.22	8.78	0.21
BMU	-8.68	0.34	-7.86	0.33	-8.63	0.33	1.1	0.23	1.01	0.25	0.93	0.27	10.23	0.42	10.39	0.42	10.15	0.42
BTN	-4.15	0.65	-4.29	0.46	-6.09	1.38	6.76	0.23	6.71	0.2	6.54	0.19	18.52	0.58	18.13	0.56	18.07	0.55
BOL	-3.9	0.23	-4.78	0.55	-4.51	0.34	4.07	0.11	3.7	0.11	4.01	0.1	9.83	0.33	9.58	0.29	10	0.3
BIH	-5.34	0.75	-5.5	1.04	-5.03	0.71	3.14	0.22	3.49	0.23	3.1	0.22	12.1	0.44	12.43	0.4	12.41	0.45
BWA	-9.59	0.45	-9.86	0.54	-9.5	0.52	3.96	0.42	4.05	0.33	3.99	0.36	12	0.33	11.6	0.29	11.41	0.34
BRA	-4.66	0.45	-5.5	0.83	-4.64	0.38	3.41	0.13	3.26	0.13	3.43	0.1	10.11	0.34	10.41	0.38	10.18	0.34
BRN	-4.91	0.31	-4.79	0.31	-4.98	0.29	1.14	0.14	1.14	0.19	0.89	0.17	8.74	0.29	8.85	0.3	8.75	0.3
BGR	-5.25	0.44	-5.54	0.39	-5.62	0.46	4.23	0.24	4.07	0.21	3.81	0.21	8.82	0.2	8.43	0.2	8.39	0.19
BFA	-4.03	0.33	-3.96	0.51	-3.74	0.42	5.09	0.19	5.28	0.18	5.48	0.18	9.4	0.23	9.52	0.22	9.79	0.27
BDI	-4.7	0.46	-4.72	0.45	-4.48	0.51	3.51	0.2	3.72	0.2	3.61	0.18	8.79	0.24	8.61	0.21	8.84	0.25
CPV	-4.97	0.65	-4.55	0.66	-5.08	0.55	4	0.22	3.97	0.2	3.51	0.19	16.47	0.5	16.51	0.51	16.52	0.54
KHM	-4.21	0.44	-4.33	0.45	-4.84	0.53	7.06	0.2	7.08	0.19	6.55	0.23	14.4	0.38	14.57	0.42	14.46	0.42

Table B.1 continued from previous page

	0.01				0.5				0.99									
CMR	-4.46	0.4	-4.47	0.56	-4.01	0.42	3.85	0.13	3.78	0.1	3.8	0.11	9.24	0.27	9.15	0.27	9.24	0.26
CAN	-4.52	0.28	-4.43	0.25	-4.68	0.29	3.42	0.16	3.39	0.17	3.34	0.16	9.25	0.29	9.28	0.29	9.16	0.26
CYM	-9.07	0.39	-10.12	0.98	-9.02	0.34	0.73	0.33	1.13	0.31	0.97	0.29	8.6	0.28	8.57	0.29	8.39	0.26
CAF	-51.35	2.08	-52.95	1.76	-52.08	1.85	3.2	0.64	2.97	0.66	2.84	0.67	9.23	0.25	9.17	0.27	9.17	0.25
TCD	-4.31	0.42	-4.21	0.48	-3.9	0.3	6.34	0.28	6.42	0.31	6.68	0.31	29.19	0.84	29.53	0.86	29.47	0.88
CHL	-4.19	0.31	-4.01	0.31	-3.97	0.41	4.5	0.14	4.08	0.17	4.4	0.17	9.2	0.23	8.83	0.23	9.07	0.24
CHN	-4.32	0.67	-3.98	0.29	-4.54	0.49	7.17	0.19	7.17	0.21	6.65	0.2	14.42	0.37	14.6	0.33	14.21	0.37
COL	-4.36	0.64	-4.17	0.41	-5.19	0.97	3.89	0.16	3.72	0.13	3.75	0.15	8.69	0.19	8.66	0.2	8.75	0.23
COM	-4.19	0.41	-4.23	0.64	-4.38	0.4	2.8	0.11	2.87	0.12	2.72	0.11	11.4	0.41	11.52	0.42	11.25	0.41
COD	-8.79	0.77	-8.26	0.39	-8.18	0.46	5.44	0.4	5.5	0.36	5.32	0.41	11.18	0.33	10.99	0.32	11.12	0.34
COG	-8.9	0.43	-8.41	0.37	-8.43	0.44	5.54	0.42	5.65	0.43	5.61	0.39	13.37	0.43	13.26	0.4	13.38	0.44
CRI	-5.52	0.62	-5.31	0.45	-5.14	0.46	3.71	0.13	3.56	0.09	3.62	0.11	9.41	0.35	9.42	0.34	9.52	0.34
CIV	-7.13	0.28	-6.96	0.34	-6.68	0.35	1.71	0.24	1.84	0.25	1.69	0.22	10.82	0.39	11.21	0.41	10.89	0.38
HRV	-9.14	0.5	-10.55	1.06	-10.29	1.52	1.92	0.25	2.17	0.26	1.22	0.25	8.45	0.26	8.73	0.27	8.36	0.27
CUW	-5.3	0.44	-4.99	0.49	-5.32	0.44	1.24	0.12	1.28	0.14	1.13	0.12	8.4	0.26	8.73	0.28	8.55	0.29
CYP	-8.65	0.48	-7.96	0.29	-8.59	0.57	2.74	0.31	2.99	0.31	2.93	0.32	8.75	0.25	8.44	0.21	8.22	0.21
CZE	-6.64	0.43	-7.2	0.36	-7.57	0.91	2.54	0.2	2.25	0.21	2.56	0.18	7.92	0.22	7.88	0.21	8.33	0.23
DNK	-6.17	0.42	-5.76	0.37	-7.87	1.33	1.19	0.17	1.16	0.16	1.32	0.19	8.55	0.28	8.13	0.26	8.43	0.27
DJI	-4.38	0.64	-4	0.42	-4.39	0.54	6.86	0.25	6.71	0.25	6.63	0.22	9.04	0.17	9.07	0.19	8.86	0.15
DMA	-5.92	0.67	-5.67	0.8	-5.31	0.35	1.5	0.15	1.25	0.14	1.46	0.15	8.64	0.28	8.57	0.28	8.69	0.26
DOM	-4.31	0.28	-4.9	0.46	-4.86	0.35	4.03	0.11	3.95	0.12	3.83	0.11	10.91	0.37	10.9	0.36	10.5	0.34
ECU	-4.14	0.28	-3.94	0.36	-4.14	0.34	3.84	0.12	3.74	0.13	3.79	0.15	9.98	0.32	9.75	0.34	9.73	0.31
EGY	-4.61	0.71	-4.73	0.81	-3.66	0.32	3.72	0.09	3.56	0.1	4.06	0.11	9.67	0.34	9.59	0.39	9.53	0.29
SLV	-4.26	0.3	-4.61	0.5	-3.92	0.31	1.26	0.17	1.14	0.14	1.39	0.14	8.74	0.27	8.53	0.27	8.71	0.27
GNQ	-11.01	0.46	-10.89	0.43	-10.65	0.38	6.4	0.51	6.58	0.48	6.5	0.46	56.33	1.93	54.96	1.9	56.32	1.9
EST	-17.89	0.56	-17.56	0.73	-18.25	0.79	5.3	0.72	5.23	0.75	5.38	0.77	11.49	0.3	10.96	0.34	11.29	0.32
SWZ	-4.15	0.36	-4.28	0.36	-4.84	1.02	3.4	0.14	3.27	0.14	3.63	0.12	8.54	0.22	8.79	0.25	9.12	0.28
ETH	-4.32	0.38	-4.12	0.39	-4.14	0.42	7	0.21	7.23	0.23	6.96	0.22	14.7	0.37	15.07	0.39	14.53	0.39
FJI	-4.42	0.41	-4.49	0.4	-4.42	0.41	1.33	0.15	1.18	0.15	1.45	0.15	8.57	0.25	8.72	0.27	8.68	0.26
FIN	-10.84	0.57	-12.73	1.03	-12.46	1	1.85	0.28	1.52	0.29	1.53	0.28	8.78	0.28	8.18	0.25	8.11	0.25
FRA	-4.65	0.4	-5.35	0.55	-5.43	1.06	1.23	0.13	1.24	0.12	1.21	0.14	8.23	0.27	8.24	0.28	8.39	0.27
GAB	-6.81	0.43	-6.53	0.43	-6.73	0.42	1.36	0.24	1.54	0.2	1.32	0.24	8.59	0.25	8.67	0.26	8.44	0.26

Table B.1 continued from previous page

	0.01				0.5				0.99									
GMB	-10.84	0.51	-11.47	0.67	-11.52	0.97	3.55	0.35	3.55	0.42	3.59	0.36	9.69	0.28	9.95	0.32	9.85	0.32
GEO	-6.18	0.49	-5.42	0.35	-5.4	0.41	3.67	0.27	5.02	0.26	4.95	0.26	12.56	0.37	12.93	0.39	12.88	0.38
DEU	-7.15	0.36	-8.01	0.57	-7.52	0.42	1.09	0.19	0.82	0.18	1.3	0.18	8.41	0.27	8.06	0.26	8.39	0.27
GHA	-4.02	0.3	-3.86	0.48	-3.63	0.47	5.06	0.15	5.21	0.16	5.24	0.16	15.37	0.54	15.7	0.54	15.59	0.53
GRL	-12.98	0.49	-12.68	0.46	-14.1	0.99	1.06	0.28	1.19	0.23	0.93	0.3	8.71	0.27	8.95	0.27	9.12	0.31
GUM	-9.19	0.37	-9.04	0.42	-8.64	0.44	0.79	0.19	1.01	0.21	1	0.22	12.71	0.54	13.03	0.56	12.91	0.51
GIN	-4.06	0.33	-4.22	0.41	-3.8	0.47	3.39	0.11	3.28	0.14	3.44	0.1	8.87	0.28	8.98	0.28	8.95	0.29
GNB	-3.78	0.42	-4.94	0.57	-4.54	0.58	3.82	0.15	3.16	0.17	3.35	0.14	8.64	0.21	8.64	0.2	8.7	0.19
GUY	-4.66	0.41	-4.75	0.4	-5.27	0.55	2.77	0.18	2.58	0.2	2.65	0.17	8.99	0.27	9.3	0.32	8.76	0.25
HTI	-4.56	0.32	-4.8	0.35	-4.87	0.32	2.11	0.21	2.06	0.22	1.98	0.21	8.77	0.26	8.66	0.27	8.62	0.26
HND	-8.39	0.48	-8.72	0.59	-8.84	0.56	1.34	0.22	1.26	0.19	1.22	0.22	8.67	0.26	8.32	0.25	8.49	0.25
HKG	-5.75	0.44	-5.56	0.45	-7.7	1.55	3.43	0.24	3.47	0.27	3.41	0.2	9.93	0.36	10.18	0.41	10.04	0.39
HUN	-3.99	0.41	-5.17	0.45	-4.88	0.97	3.49	0.19	1.17	0.47	3.36	0.21	10.18	0.37	10.07	0.33	10.08	0.35
ISL	-8.35	0.34	-9.01	0.49	-8.72	0.33	3.13	0.28	3.04	0.28	3.17	0.25	8.96	0.3	8.63	0.25	8.95	0.29
IND	-9.4	0.37	-9.19	0.41	-10.39	0.89	2.32	0.34	2.6	0.34	2.28	0.38	8.92	0.25	9.04	0.26	8.86	0.25
IDN	-4.26	0.65	-4.03	0.4	-4.21	0.47	6.84	0.2	6.89	0.21	6.79	0.23	9.94	0.27	10.14	0.26	10.13	0.27
IRN	-4.22	0.65	-3.64	0.32	-3.92	0.28	4.63	0.12	5.03	0.15	5.09	0.13	8.9	0.24	8.71	0.22	8.66	0.2
IRL	-50.85	2.02	-55.14	1.75	-53.94	1.58	3.93	0.7	3.64	0.75	2.47	0.69	53.34	2	54.85	2.05	54.6	2.04
IMN	-7.91	0.44	-8.56	0.75	-7.61	0.25	3.74	0.29	3.61	0.3	3.98	0.27	10.1	0.34	10.01	0.34	10.28	0.34
ITA	-4.39	0.59	-3.81	0.41	-4.1	0.42	3.84	0.12	4.13	0.13	3.8	0.12	10.03	0.3	10.33	0.34	10.13	0.32
JAM	-6.94	0.26	-7.41	0.58	-7.18	0.29	1.07	0.23	1.1	0.23	0.87	0.24	8.61	0.27	8.74	0.27	8.7	0.28
JPN	-8.06	0.47	-7.57	0.39	-8.02	0.44	1.22	0.16	1.3	0.17	1.03	0.16	8.76	0.28	8.53	0.26	8.81	0.32
JOR	-7.75	0.93	-6.64	0.36	-7.01	0.36	0.71	0.11	1.48	0.11	1.35	0.12	8.38	0.29	8.49	0.29	8.63	0.29
KAZ	-4.13	0.33	-4.11	0.31	-3.97	0.3	4.42	0.14	4.17	0.11	4.37	0.14	10.5	0.39	10.21	0.38	10.5	0.36
KEN	-3.67	0.39	-3.58	0.39	-4.18	0.39	7.07	0.21	7.2	0.23	6.74	0.19	14.16	0.35	14.29	0.36	13.71	0.33
KIR	-4.58	0.57	-4.52	0.53	-3.84	0.36	3.73	0.11	3.54	0.14	3.78	0.13	8.79	0.22	8.64	0.21	9.06	0.24
PRK	-5.4	1.07	-5.84	1.14	-6.89	1.82	1.37	0.1	1.04	0.12	0.85	0.14	8.61	0.27	8.34	0.26	8.47	0.3
KWT	-4	0.32	-3.68	0.37	-4.76	0.68	4.32	0.13	4.53	0.13	3.98	0.11	9.03	0.29	9.32	0.26	9.09	0.3
KGZ	-9.69	0.7	-9.7	1.02	-9.71	0.71	3.91	0.33	3.99	0.29	3.75	0.29	16.97	0.57	16.25	0.54	16.19	0.51
LAO	-4.1	0.45	-4.17	0.45	-5.13	0.76	4.22	0.21	4.4	0.24	4.01	0.25	11.46	0.37	11.5	0.34	11.56	0.37
LVA	-3.39	0.35	-4.45	0.69	-4.56	0.54	6.99	0.21	6.84	0.22	7.04	0.2	11.18	0.31	10.65	0.29	10.41	0.28
LBN	-17.7	0.41	-17.67	0.83	-17.21	0.39	5.3	0.6	5.64	0.57	5.64	0.58	12.5	0.39	12.5	0.32	12.6	0.35

Table B.1 continued from previous page

	0.01			0.5			0.99											
LSO	-5.57	0.44	-5.33	0.78	-4.73	0.5	3.17	0.11	3.22	0.13	3.66	0.14	11.85	0.44	11.97	0.45	12.57	0.47
LBR	-4.4	0.64	-4.14	0.25	-4.27	0.64	3.58	0.11	3.53	0.1	3.59	0.1	8.91	0.26	9.1	0.27	8.89	0.24
LBY	-44.41	1.66	-44.71	1.56	-44.38	1.62	4.88	0.73	4.64	0.72	4.96	0.73	11.79	0.38	12.2	0.43	12.18	0.39
LIE	-69.49	1.67	-68.92	2.11	-69.93	1.44	2.25	0.63	2.31	0.6	1.88	0.66	62.14	2.01	60.75	2.36	62.64	2
LUX	-16.44	0.54	-17.61	0.46	-19	1.45	4.05	0.67	3.97	0.7	3.94	0.69	11.74	0.28	12.33	0.33	12.02	0.3
MAC	-6.41	0.45	-6.22	0.47	-8.79	1.68	2.63	0.32	2.73	0.24	2.69	0.17	9.31	0.38	9.82	0.4	9.47	0.4
MDG	-4.59	0.41	-4.43	0.3	-4.99	0.54	6.73	0.32	6.86	0.34	6.7	0.28	27.49	0.88	27.7	0.9	27.56	0.91
MWI	-15.65	0.38	-15.93	0.36	-16.98	0.48	3.01	0.53	3.12	0.51	3	0.52	10.42	0.31	10.36	0.32	10.53	0.35
MYS	-7.28	0.38	-7.09	0.42	-7.28	0.42	4.44	0.22	4.43	0.21	4.27	0.23	10.16	0.33	10.32	0.33	10.58	0.31
MDV	-4.44	0.31	-4.17	0.44	-4.23	0.35	4.93	0.2	15.73	1.25	4.71	0.16	10.09	0.31	10.91	0.45	9.72	0.31
MLI	-18.33	0.76	-17.17	0.75	-17.46	0.74	5.94	0.67	6.19	0.63	6.03	0.61	27.08	0.9	27.67	0.87	27.15	0.83
MLT	-4.56	0.66	-4.39	0.34	-5.18	0.91	4.18	0.13	4.25	0.13	4.09	0.14	17.19	0.53	17.05	0.56	16.63	0.56
MHL	-5.08	0.51	-4.72	0.52	-4.33	0.49	3.1	0.23	3.24	0.21	3.61	0.18	18.88	0.67	18.91	0.72	18.68	0.63
MRT	-8.32	0.55	-7.58	0.3	-8.44	0.54	0.73	0.23	1.04	0.23	0.64	0.21	8.63	0.28	8.53	0.26	8.67	0.27
MUS	-6.88	0.39	-6.93	0.42	-6.75	0.44	3.19	0.25	3.1	0.26	3.2	0.27	18.83	0.77	18.97	0.76	19.18	0.77
MEX	-4.15	0.41	-4.2	0.43	-4.1	0.42	3.81	0.1	3.67	0.13	3.89	0.09	8.84	0.22	8.55	0.23	8.87	0.21
FSM	-7.09	0.39	-6.44	0.28	-6.35	0.34	1.97	0.26	2.02	0.26	2.09	0.23	8.59	0.28	8.88	0.3	8.58	0.26
MDA	-6.82	0.58	-6.26	0.3	-7.73	1.49	1.1	0.14	1.24	0.17	0.97	0.15	8.19	0.27	8.39	0.27	8.02	0.27
MCO	-8.61	0.97	-7.93	0.87	-7.7	0.46	5.51	0.33	5.83	0.3	5.51	0.3	9.71	0.24	10.05	0.26	9.61	0.28
MNE	-4.34	0.4	-5.12	0.94	-3.98	0.39	6.74	0.27	6.89	0.3	6.9	0.25	16.97	0.46	17.34	0.47	17.19	0.46
MAR	-8.77	0.44	-8.23	0.44	-9.83	1.54	3	0.3	3.19	0.26	2.84	0.31	9.47	0.31	9.67	0.31	9.39	0.35
MOZ	-4.96	0.95	-4.42	0.38	-5.13	0.96	3.96	0.1	3.9	0.1	3.87	0.11	10.35	0.34	10.06	0.33	10.22	0.35
MMR	-3.98	0.44	-4.33	0.65	-4.02	0.67	6.98	0.22	7.11	0.22	7.01	0.2	13.32	0.36	13.2	0.38	13.31	0.4
NAM	-3.88	0.27	-4.77	0.8	-3.92	0.32	6.96	0.19	6.94	0.17	6.9	0.2	16.8	0.38	17.09	0.4	17.14	0.4
NRU	-3.88	0.25	-4.18	0.38	-4.7	0.49	4.25	0.14	4.14	0.21	4.19	0.12	12.22	0.39	12.44	0.42	12.5	0.39
NPL	-33.64	1.98	-33.09	1.86	-35.07	2	6.06	0.76	6.32	0.77	5.59	1.16	29.78	0.87	28.97	0.9	29.36	0.89
NLD	-3.7	0.3	-4.96	0.52	-4.89	1.04	3.98	0.11	3.16	0.09	3.83	0.11	9.45	0.3	8.7	0.31	9.34	0.28
NCL	-6.14	0.46	-6.2	0.45	-6.05	0.43	1.18	0.16	1.21	0.13	1.16	0.15	8.57	0.3	8.57	0.25	8.56	0.23
NIC	-4.61	0.38	-4.51	0.39	-4.37	0.4	2.54	0.21	2.55	0.19	2.69	0.16	8.77	0.29	8.4	0.22	8.45	0.24
NER	-5.32	0.35	-4.59	0.47	-4.43	0.34	3.68	0.16	3.77	0.18	3.82	0.19	8.43	0.2	8.71	0.21	8.87	0.22
NGA	-4.46	0.27	-4.28	0.43	-4.29	0.41	4.43	0.25	4.54	0.23	4.59	0.23	10.84	0.33	11.14	0.34	11.15	0.33
MKD	-4.06	0.37	-4.07	0.39	-4.23	0.64	6.53	0.19	6.34	0.19	6.6	0.2	17.18	0.56	17.77	0.57	17.71	0.59

Table B.1 continued from previous page

	0.01			0.5						0.99								
MNP	-6.08	0.54	-5.89	0.43	-5.85	0.45	3.31	0.18	3.21	0.23	3.22	0.24	9.62	0.3	10.28	0.39	9.55	0.32
OMN	-3.87	0.48	-3.67	0.45	-3.86	0.43	1.34	0.13	1.51	0.12	1.27	0.13	8.28	0.25	8.52	0.26	8.14	0.25
PAK	-4.83	0.46	-4.42	0.44	-6.33	1.61	3.56	0.2	3.71	0.2	3.37	0.2	9.95	0.32	9.92	0.32	9.81	0.32
PLW	-4.94	0.53	-4.52	0.45	-5.09	0.79	3.82	0.11	3.92	0.11	3.64	0.12	9.47	0.29	9.1	0.27	9.39	0.31
PAN	-8.94	0.37	-9.52	0.73	-9.88	0.54	1.14	0.32	0.78	0.29	0.95	0.31	8.44	0.25	8.89	0.3	8.47	0.25
PNG	-4.5	0.79	-4.11	0.41	-3.89	0.29	6.45	0.21	6.42	0.2	6.26	0.22	12.89	0.37	12.89	0.36	12.81	0.32
PRY	-5.48	0.6	-5.74	0.48	-4.95	0.4	3.53	0.23	3.34	0.24	3.51	0.2	13.5	0.39	13.26	0.42	13.71	0.43
PER	-4.47	0.4	-4.81	0.53	-4.8	0.44	3.75	0.2	3.51	0.21	3.56	0.27	11.11	0.34	11.19	0.34	11.29	0.35
PHL	-4.54	0.46	-4.71	0.63	-4.56	0.42	5.02	0.15	5.06	0.2	4.75	0.22	9.64	0.26	9.53	0.28	9.64	0.29
POL	-4.11	0.37	-5.54	0.6	-5.31	0.69	4.75	0.17	4.17	0.14	4.67	0.16	8.66	0.22	7.96	0.19	8.69	0.2
PRT	-3.89	0.36	-3.99	0.28	-5.27	0.97	3.66	0.1	3.49	0.09	3.44	0.09	9.61	0.32	9.53	0.32	9.28	0.31
PRI	-5.64	0.41	-5.97	0.37	-5.49	0.29	1.19	0.2	1.29	0.15	1.22	0.14	8.81	0.29	8.69	0.29	8.58	0.28
QAT	-5.78	0.31	-5.6	0.42	-5.81	0.39	0.84	0.17	1.43	0.14	1.28	0.15	10.01	0.36	10.11	0.37	10.01	0.36
ROU	-3.61	0.31	-5.07	0.95	-3.77	0.48	7.18	0.2	6.77	0.21	6.86	0.19	26.96	0.76	27.09	0.76	26.71	0.76
RUS	-6.81	0.34	-6.62	0.24	-6.77	0.28	3.47	0.3	3.66	0.29	3.66	0.29	11.3	0.35	11.08	0.35	11.08	0.35
RWA	-10.42	0.47	-11	0.99	-11.16	0.97	4.28	0.39	4.29	0.35	4.37	0.36	11.47	0.39	11.16	0.36	10.99	0.35
WSM	-4.2	0.46	-5.01	0.99	-4.21	0.37	6.81	0.26	6.9	0.24	7.06	0.23	14.07	0.45	13.83	0.36	14.15	0.41
SMR	-6.71	0.52	-6.1	0.45	-5.77	0.46	2.8	0.22	2.76	0.19	2.89	0.25	7.94	0.18	8.35	0.18	8.54	0.22
STP	-15.08	0.48	-14.81	0.54	-15.58	0.89	0.75	0.52	0.69	0.43	0.47	0.46	8.93	0.3	8.93	0.35	9.03	0.31
SAU	-4.04	0.38	-3.95	0.36	-4.04	0.36	4.14	0.11	4.23	0.14	4.24	0.12	9.85	0.32	10	0.34	9.91	0.33
SEN	-5.4	0.36	-5.62	0.36	-6.15	0.78	3.92	0.22	3.68	0.21	3.38	0.23	14.25	0.48	14.33	0.49	14.49	0.54
SRB	-3.97	0.44	-3.91	0.4	-3.97	0.42	3.63	0.12	3.66	0.12	3.44	0.12	9.12	0.28	9.12	0.32	9.05	0.28
SYC	-5.83	0.97	-5.95	0.85	-5.53	0.53	4.1	0.25	3.95	0.25	3.95	0.22	9.15	0.22	9.34	0.23	9.17	0.24
SLE	-8.45	0.38	-8.11	0.37	-8.01	0.44	1.32	0.2	1.28	0.18	1.53	0.19	11.21	0.42	11.62	0.49	11.6	0.43
SGP	-8.27	0.5	-7.81	0.63	-8.3	0.95	5.73	0.26	5.71	0.25	5.64	0.28	27.13	0.9	27.78	0.88	26.81	0.89
SXM	-4.71	0.65	-5.32	1.04	-4.23	0.32	4.79	0.28	4.65	0.22	4.8	0.22	14.83	0.44	14.53	0.42	14.48	0.42
SVK	-3.9	0.34	-4.94	0.44	-4.59	0.53	1.46	0.06	1.01	0.07	1.4	0.07	8.26	0.26	8.27	0.26	8.55	0.27
SVN	-8.16	1.51	-7.44	0.54	-8.46	1.53	3.68	0.26	3.88	0.25	3.14	0.26	11.19	0.35	11.27	0.33	11.14	0.38
SLB	-9.58	0.25	-9.72	0.28	-9.31	0.35	2.51	0.33	2.62	0.31	3.02	0.32	8.76	0.27	8.48	0.22	8.76	0.23
SOM	-17.67	0.48	-17.82	0.46	-18.08	0.54	3.45	0.67	3.71	0.66	3.14	0.64	11.14	0.35	11.49	0.37	10.96	0.37
ZAF	-3.96	0.28	-4.64	0.67	-4.32	0.45	6.93	0.26	6.93	0.24	6.87	0.21	9.17	0.2	9.08	0.18	9.21	0.2
SSD	-4.38	0.43	-4.33	0.66	-4.32	0.43	3.25	0.18	3.43	0.14	3.32	0.14	8.59	0.23	8.83	0.25	8.3	0.22

Table B.1 continued from previous page

	0.01			0.5			0.99											
LKA	-6.37	0.42	-6.47	0.28	-6.8	0.51	1.79	0.16	1.51	0.22	1.69	0.16	8.59	0.25	8.56	0.26	8.6	0.24
KNA	-4.07	0.42	-5.09	1.61	-4.09	0.38	5.55	0.23	5.24	0.22	5.44	0.22	11.87	0.37	11.54	0.32	11.59	0.3
LCA	-6.27	0.39	-6.33	0.55	-5.86	0.36	2.84	0.21	2.83	0.22	2.85	0.24	12.53	0.43	12.33	0.41	12.63	0.44
MAF	-5.89	0.64	-6.62	1.02	-5.53	0.33	1.16	0.26	1.01	0.18	1.22	0.18	8.73	0.3	8.47	0.27	8.61	0.28
SDN	-7.08	0.39	-6.62	0.38	-6.74	0.25	1.17	0.16	1.28	0.16	1.31	0.17	8.48	0.24	8.6	0.26	8.65	0.25
SUR	-18.87	0.68	-19.52	0.93	-19.23	0.78	3.67	0.73	3.68	0.69	3.66	0.72	9.75	0.32	9.7	0.3	9.41	0.31
SWE	-3.62	0.28	-3.79	0.35	-4.59	0.53	4.1	0.16	3.92	0.13	3.98	0.14	10.1	0.31	9.35	0.29	9.67	0.32
CHE	-8.35	0.56	-8.42	0.5	-9.55	1.57	2.17	0.19	2.26	0.22	1.57	0.21	8.61	0.24	8.53	0.23	8.41	0.23
SYR	-5.03	0.46	-3.95	0.31	-3.92	0.24	0.9	0.19	2.09	0.16	2.22	0.18	8.32	0.25	8.54	0.26	8.75	0.26
TZA	-3.83	0.34	-3.96	0.64	-4.18	0.41	7.2	0.2	7.05	0.2	6.93	0.2	13.14	0.33	12.91	0.29	12.91	0.35
THA	-4.14	0.45	-4.45	0.65	-5.04	0.76	6.45	0.2	6.4	0.22	6.3	0.21	10.99	0.31	11.08	0.37	11	0.3
TLS	-4.21	0.52	-4.3	0.37	-4.26	0.48	3.93	0.12	3.94	0.14	3.44	0.12	10.81	0.41	10.59	0.36	10.33	0.36
TGO	-8.08	0.42	-8.08	0.39	-8.1	0.5	3.91	0.33	3.92	0.35	3.96	0.36	16.66	0.48	16.32	0.48	16.51	0.5
TON	-6.33	0.4	-6.21	0.36	-7.7	1.54	3.92	0.27	3.87	0.27	3.64	0.25	9.12	0.24	8.75	0.23	8.92	0.22
TTO	-7.68	0.35	-7.16	0.36	-7.68	0.37	1.12	0.21	1.15	0.17	0.97	0.18	8.79	0.29	8.82	0.28	8.53	0.3
TUN	-6.37	0.62	-6.01	0.43	-6.3	0.29	3.85	0.24	3.83	0.25	3.7	0.24	15.02	0.48	15.01	0.48	15.11	0.49
TUR	-4.86	0.59	-4.23	0.41	-4.28	0.46	3.49	0.18	3.67	0.17	3.57	0.16	8.58	0.32	9.11	0.28	8.99	0.28
TKM	-8.35	0.47	-8.1	0.43	-8.28	0.43	3.93	0.44	5.91	0.39	5.94	0.39	12.36	0.33	12.29	0.35	12.33	0.37
TCA	-4.42	0.64	-3.65	0.32	-3.88	0.31	7.06	0.22	7.16	0.21	7.19	0.26	16.21	0.41	15.86	0.42	16.07	0.43
TUV	-5.01	0.37	-4.83	0.35	-4.79	0.4	1.15	0.19	1.07	0.16	1.25	0.18	9.39	0.39	9.48	0.4	9.05	0.33
UGA	-9.37	0.9	-9.76	0.91	-9.62	0.88	1.19	0.23	1.16	0.27	1.23	0.19	11.85	0.49	11.61	0.46	11.29	0.45
UKR	-4.06	0.43	-4.18	0.4	-3.53	0.42	6.26	0.21	6.51	0.23	6.47	0.21	12	0.34	12.02	0.32	11.75	0.31
ARE	-17.82	0.32	-17.79	0.34	-17.53	0.35	3.65	0.68	3.4	0.66	3.59	0.68	12.28	0.36	12.21	0.35	12.21	0.34
GBR	-6.25	0.29	-6.77	0.37	-7.48	0.98	3.87	0.26	3.92	0.23	4.02	0.27	12.92	0.39	12.44	0.38	13.01	0.4
USA	-6	0.27	-5.57	0.3	-5.64	0.26	1.33	0.21	1.68	0.22	1.56	0.19	8.41	0.25	8.82	0.26	8.67	0.25
URY	-4.65	0.41	-6.6	1.57	-4.54	0.35	1.76	0.13	1.56	0.12	1.64	0.11	8.52	0.25	8.38	0.26	8.59	0.24
UZB	-10.04	0.98	-9.13	0.49	-10.33	0.97	3.62	0.28	3.66	0.28	3.63	0.27	10.69	0.35	10.23	0.34	10.59	0.34
VUT	-4.26	0.41	-4.42	0.42	-4	0.41	6.85	0.22	6.9	0.2	6.86	0.2	11.23	0.32	11.3	0.34	11.12	0.29
VEN	-6.84	0.38	-6.94	0.4	-7.85	1.02	2.99	0.29	2.82	0.32	2.74	0.3	9.09	0.26	9.1	0.26	8.95	0.28
VIR	-4.11	0.42	-4.24	0.39	-4.08	0.44	6.31	0.25	6.31	0.22	6.44	0.19	9.27	0.2	8.9	0.2	9.22	0.2
YEM	-17.35	0.94	-15.73	0.39	-16.24	0.5	4.31	0.68	4.34	0.69	4.02	0.68	21.59	0.75	21.45	0.73	21.71	0.74

Table B.1 continued from previous page

	0.01				0.5				0.99									
ZWE	-4.14	0.39	-4.54	0.52	-4.64	0.57	6.7	0.2	6.7	0.21	6.66	0.2	11.25	0.3	11.11	0.3	11.1	0.3

Table B.1: Mean (in bold) and standard error of the quantile estimates at level $\tau = 0.01, 0.5, 0.99$ for the SSP1 scenario.

	0.01						0.5						0.99					
	2030		2050		2100		2030		2050		2100		2030		2050		2100	
AFG	-4.54	0.46	-4.73	0.35	-4.28	0.36	6.49	0.23	6.26	0.24	6.27	0.24	21.11	0.7	21.76	0.77	21.21	0.76
ALB	-3.96	0.4	-4.42	0.47	-5.01	1	4.41	0.15	4.2	0.17	4.4	0.16	9.68	0.33	9.57	0.32	9.49	0.33
DZA	-4.17	0.26	-3.71	0.26	-3.7	0.27	3.45	0.09	3.65	0.11	3.37	0.08	8.65	0.22	8.88	0.24	8.73	0.25
AGO	-3.58	0.25	-4.07	0.29	-3.8	0.3	5.43	0.21	5.2	0.24	5.31	0.21	15.96	0.44	15.94	0.48	16.07	0.48
ATG	-16.87	0.9	-17.21	0.86	-17.16	0.89	2.51	0.49	2.4	0.52	2.26	0.47	12.82	0.42	12.82	0.41	12.39	0.39
ARG	-13.77	0.55	-13.44	0.45	-13.79	0.49	3.62	0.39	3.61	0.36	3.79	0.36	11.18	0.35	11.61	0.35	11.48	0.36
ARM	-17.66	0.44	-16.55	0.46	-16.48	0.46	6.26	0.61	6.38	0.6	5.94	0.58	16.72	0.46	17.05	0.47	16.6	0.45
ABW	-15.21	0.56	-15.61	0.62	-15.94	0.67	1.16	0.27	0.89	0.27	0.68	0.28	8.71	0.27	8.7	0.29	8.71	0.29
AUS	-4.14	0.51	-4.05	0.3	-3.86	0.29	3.26	0.11	3.08	0.11	3.15	0.11	8.57	0.23	8.65	0.22	8.71	0.24
AUT	-5.42	0.28	-6.2	0.5	-5.63	0.26	1.2	0.15	1.06	0.15	1.39	0.15	8.63	0.27	8.34	0.26	8.45	0.27
AZE	-5.19	0.38	-4.94	0.39	-5.06	0.38	6.93	0.21	7.08	0.2	6.7	0.18	30.1	0.88	30.28	0.88	30.6	0.87
BHS	-6.97	0.7	-7.39	0.67	-7.82	0.97	1.31	0.17	1.05	0.18	1.19	0.17	8.55	0.25	8.59	0.26	8.73	0.26
BHR	-3.78	0.64	-4.4	0.52	-4.11	0.54	4.46	0.12	4.23	0.13	4.27	0.12	8.83	0.21	9.08	0.21	8.78	0.22
BGD	-3.89	0.38	-4.11	0.42	-3.98	0.36	5.15	0.13	5.26	0.15	5.05	0.15	9.77	0.29	9.9	0.31	9.72	0.27
BRB	-6.21	0.27	-6.73	0.3	-7.4	0.7	1.16	0.22	1.07	0.18	1.2	0.18	8.49	0.27	8.63	0.28	8.77	0.27
BLR	-4.64	0.78	-4.12	0.28	-4.37	0.38	5.98	0.23	6.02	0.26	6.16	0.22	12.97	0.37	12.63	0.36	12.69	0.33
BEL	-4.54	0.33	-4.75	0.31	-4.74	0.64	1.41	0.12	1.33	0.14	1.45	0.1	8.36	0.25	8.5	0.27	8.44	0.25
BLZ	-3.66	0.29	-3.93	0.3	-3.98	0.52	3.71	0.14	3.51	0.12	3.43	0.15	13.01	0.44	13.07	0.42	12.98	0.43
BEN	-3.69	0.26	-4.05	0.26	-4	0.25	4.33	0.11	4.11	0.1	4.18	0.1	8.78	0.19	8.6	0.19	8.73	0.2
BMU	-8.79	0.36	-8.45	0.33	-8.6	0.38	0.97	0.24	0.82	0.28	1.06	0.25	10.26	0.4	10.17	0.4	10.25	0.42
BTN	-4.72	0.64	-4.17	0.42	-4.18	0.39	6.65	0.2	6.66	0.21	6.68	0.22	18.07	0.55	18.28	0.54	18.04	0.53
BOL	-3.71	0.24	-3.92	0.38	-3.68	0.25	4.06	0.09	4.03	0.1	4.05	0.1	9.92	0.3	9.83	0.31	10.06	0.32
BIH	-4.71	0.44	-6.12	1.09	-5.08	0.8	3.41	0.21	3.19	0.19	3.36	0.24	12.55	0.45	12.64	0.43	12.24	0.41
BWA	-8.52	0.41	-8.9	0.43	-9.64	1.01	4.16	0.36	3.98	0.35	4.23	0.39	11.62	0.33	11.37	0.32	11.57	0.34
BRA	-4.3	0.31	-4.39	0.33	-4.17	0.35	3.62	0.14	3.32	0.13	3.65	0.13	10.34	0.36	10.38	0.33	10.12	0.31
BRN	-4.52	0.31	-5.04	0.29	-4.46	0.26	1.21	0.16	1.11	0.12	1.21	0.17	8.78	0.28	8.57	0.25	8.58	0.26
BGR	-5.84	0.48	-5.95	0.49	-5.42	0.42	4.09	0.21	3.91	0.2	4.18	0.24	8.9	0.21	8.62	0.19	8.85	0.25
BFA	-3.89	0.33	-3.68	0.26	-3.8	0.32	5.28	0.18	5.12	0.16	5.25	0.17	9.38	0.22	9.5	0.24	9.56	0.21
BDI	-3.87	0.24	-4.48	0.36	-4.09	0.3	3.82	0.19	3.67	0.18	3.85	0.17	8.67	0.2	8.86	0.21	8.64	0.2
CPV	-4.18	0.31	-4.75	0.65	-4.15	0.32	4.01	0.23	4.14	0.2	4.03	0.22	16.7	0.53	16.36	0.51	16.73	0.52
KHM	-4.12	0.65	-5.49	1.6	-3.82	0.31	7.11	0.19	7.08	0.19	6.96	0.2	14.6	0.41	14.85	0.42	14.38	0.38

Table B.2 continued from previous page

	0.01			0.5			0.99											
CMR	-4	0.41	-4.23	0.42	-4.01	0.34	3.87	0.1	3.8	0.1	4.01	0.08	9.09	0.25	9.13	0.25	9.33	0.25
CAN	-4.61	0.25	-4.58	0.27	-4.55	0.32	3.34	0.16	3.36	0.15	3.23	0.16	9.23	0.27	9.16	0.3	9.11	0.29
CYM	-8.55	0.34	-9.32	0.42	-8.98	0.35	0.91	0.28	1	0.37	0.88	0.29	8.68	0.28	8.91	0.34	8.6	0.27
CAF	-52.03	1.78	-51.7	1.76	-52.08	1.82	3.16	0.66	3.01	0.71	3.24	0.62	9.39	0.27	9.26	0.25	9.34	0.26
TCD	-4.04	0.21	-3.94	0.34	-3.45	0.25	6.48	0.27	6.44	0.29	6.86	0.29	28.94	0.83	29.11	0.83	29.32	0.84
CHL	-4.13	0.3	-4.28	0.63	-3.91	0.42	4.39	0.14	4.43	0.15	4.52	0.18	9	0.23	9.06	0.24	9.04	0.23
CHN	-3.97	0.28	-4.13	0.32	-3.93	0.33	7.14	0.2	7.11	0.2	7.18	0.19	14.61	0.37	14.88	0.38	14.71	0.35
COL	-3.8	0.27	-4.2	0.39	-4.05	0.41	3.93	0.11	3.78	0.12	3.81	0.15	8.8	0.19	8.61	0.19	8.78	0.21
COM	-3.82	0.28	-4.14	0.44	-3.83	0.29	2.96	0.12	2.83	0.14	2.82	0.1	11.22	0.39	11.52	0.41	11.51	0.42
COD	-8.04	0.37	-8.25	0.54	-8.14	0.42	5.48	0.41	5.29	0.36	5.57	0.36	10.89	0.33	10.8	0.3	10.8	0.31
COG	-8.58	0.42	-8.76	0.32	-8.73	0.33	5.48	0.42	5.57	0.4	5.74	0.38	12.93	0.4	12.98	0.4	13.19	0.42
CRI	-4.65	0.45	-5.52	0.84	-5.59	0.74	3.95	0.09	3.68	0.11	3.84	0.11	9.34	0.31	9.37	0.34	9.32	0.32
CIV	-6.95	0.25	-7.23	0.3	-7.07	0.29	1.81	0.26	1.68	0.24	1.95	0.22	10.91	0.37	10.77	0.4	11.07	0.39
HRV	-8.75	0.44	-9.51	0.64	-8.6	0.4	2.14	0.28	1.83	0.25	2.1	0.27	8.74	0.29	8.47	0.26	8.8	0.28
CUW	-5.18	0.44	-5.28	0.45	-5.34	0.41	1.42	0.11	1.06	0.11	1.01	0.1	8.62	0.27	8.56	0.27	8.55	0.29
CYP	-8.51	0.72	-7.82	0.25	-8.11	0.74	2.7	0.34	3.07	0.31	3.03	0.38	8.44	0.22	8.57	0.24	8.78	0.23
CZE	-6.48	0.36	-7.38	0.62	-8.14	1.12	2.69	0.2	2.2	0.2	2.67	0.21	8.61	0.24	8.28	0.19	8.49	0.23
DNK	-6.47	0.62	-6.55	0.41	-6.36	0.36	1.26	0.18	1.11	0.2	1.24	0.14	8.56	0.26	8.4	0.27	8.38	0.26
DJI	-4.27	0.63	-4.08	0.4	-4.03	0.34	6.72	0.24	6.77	0.25	6.77	0.26	8.94	0.16	9.01	0.19	9.11	0.16
DMA	-5.57	0.44	-5.81	0.66	-6.49	0.86	1.28	0.17	1.41	0.12	1.4	0.13	8.51	0.27	8.81	0.29	8.65	0.27
DOM	-4.88	0.63	-4.83	0.65	-4.82	0.64	3.97	0.1	3.83	0.11	3.91	0.09	10.69	0.34	10.75	0.33	10.56	0.33
ECU	-4.11	0.3	-4.17	0.44	-3.92	0.4	3.93	0.11	3.83	0.11	3.98	0.14	9.69	0.31	9.76	0.29	9.75	0.31
EGY	-4.24	0.28	-3.85	0.28	-4.11	0.65	3.69	0.12	3.75	0.1	3.97	0.11	9.45	0.31	9.62	0.28	9.71	0.32
SLV	-4.28	0.31	-3.87	0.27	-3.89	0.25	1.29	0.1	1.36	0.12	1.26	0.14	8.7	0.26	8.52	0.27	8.47	0.26
GNQ	-11.22	0.42	-11.28	0.42	-10.97	0.4	6.71	0.47	6.47	0.45	6.8	0.49	56.36	1.92	56.03	1.9	54.94	1.89
EST	-19.32	1.07	-18.92	0.91	-17.15	0.52	5.13	0.76	5.59	0.74	5.5	0.75	11.31	0.33	11.58	0.32	11.53	0.31
SWZ	-3.97	0.25	-4.05	0.36	-3.6	0.35	3.51	0.12	3.54	0.11	3.48	0.14	8.52	0.22	8.86	0.25	8.59	0.23
ETH	-3.77	0.28	-4.47	0.41	-4.41	0.4	7.07	0.25	6.82	0.24	7.27	0.23	14.68	0.42	14.74	0.35	14.63	0.35
FJI	-4.41	0.42	-4.6	0.42	-4.52	0.42	1.38	0.13	1.18	0.14	1.39	0.13	8.61	0.26	8.57	0.25	8.51	0.26
FIN	-12.64	1.01	-12.6	0.99	-12.36	1	1.26	0.29	1.77	0.3	1.6	0.28	8.47	0.26	8.28	0.24	8.56	0.28
FRA	-5.73	1.05	-4.77	0.38	-5.61	1.06	1.16	0.13	1.39	0.14	1.39	0.12	8.34	0.26	8.5	0.26	8.41	0.26
GAB	-6.26	0.38	-6.55	0.41	-6.81	0.42	1.6	0.18	1.43	0.19	1.74	0.19	8.51	0.24	8.56	0.24	8.72	0.27

Table B.2 continued from previous page

	0.01		0.5		0.99													
GMB	-10.73	0.47	-11.48	0.97	-11.14	0.99	4.13	0.38	3.68	0.35	3.8	0.34	9.87	0.3	9.88	0.3	9.98	0.29
GEO	-5.76	0.4	-5.9	0.65	-5.39	0.36	5.1	0.26	5.03	0.28	4.56	0.26	12.93	0.36	13.02	0.4	12.78	0.34
DEU	-7.55	0.38	-7.74	0.41	-7.62	0.41	1.09	0.2	1.32	0.18	1.39	0.17	8.48	0.26	8.58	0.27	8.45	0.26
GHA	-3.75	0.33	-4.59	0.79	-4.11	0.41	5.36	0.18	5.24	0.16	5.24	0.16	15.45	0.54	15.43	0.53	15.39	0.56
GRL	-13.1	0.41	-12.9	0.46	-13.83	0.95	1.03	0.27	1.25	0.3	0.87	0.29	8.7	0.28	8.76	0.28	8.58	0.26
GUM	-8.63	0.5	-8.67	0.5	-9.09	0.44	1.21	0.2	1.38	0.24	1.04	0.22	12.92	0.52	12.97	0.51	12.7	0.52
GIN	-3.77	0.42	-4.45	0.61	-3.99	0.63	3.52	0.1	3.22	0.1	3.63	0.12	8.94	0.28	8.7	0.27	9.15	0.28
GNB	-3.87	0.41	-4.17	0.47	-3.95	0.41	3.81	0.17	3.37	0.17	3.6	0.16	9.03	0.21	8.55	0.19	8.77	0.2
GUY	-4.69	0.4	-4.3	0.41	-4.71	0.43	2.78	0.2	2.73	0.17	2.57	0.17	9	0.28	8.92	0.27	9.01	0.27
HTI	-5.01	0.64	-5.06	0.81	-5.21	0.8	2.05	0.2	1.9	0.22	1.87	0.21	8.66	0.25	8.51	0.26	8.75	0.25
HND	-8.26	0.54	-8.29	0.51	-9.11	1	1.37	0.19	1.25	0.18	1.12	0.22	8.62	0.26	8.66	0.28	8.68	0.26
HKG	-5.54	0.34	-5.22	0.35	-5.39	0.42	3.62	0.2	3.71	0.21	3.7	0.25	10.04	0.39	10.15	0.4	10.16	0.41
HUN	-4.89	0.78	-5.17	0.81	-4.88	0.63	3.54	0.19	3.3	0.19	3.16	0.19	10.37	0.33	10.33	0.32	10.1	0.34
ISL	-8.61	0.36	-8.68	0.44	-8.2	0.31	3.07	0.26	3.15	0.28	3.09	0.25	8.69	0.23	8.86	0.27	8.73	0.27
IND	-9.76	0.87	-10.13	0.85	-10.47	0.88	2.43	0.35	2.4	0.36	2.34	0.36	9.13	0.26	9.07	0.26	9.12	0.25
IDN	-3.8	0.33	-4.3	0.44	-3.89	0.34	7.06	0.19	6.61	0.19	6.8	0.21	10.12	0.27	9.9	0.26	10.03	0.26
IRN	-3.78	0.25	-4.55	0.64	-4.09	0.35	4.84	0.13	4.77	0.11	4.83	0.14	8.55	0.2	8.77	0.23	8.86	0.26
IRL	-51.25	2.02	-52.08	2.01	-50.94	2.08	3.92	0.66	4.01	0.68	4.11	0.67	53	2.03	53.93	2.09	54.07	2.04
IMN	-7.45	0.45	-7.69	0.26	-8.34	0.52	3.68	0.28	3.91	0.29	3.96	0.31	9.98	0.35	10.03	0.34	10.31	0.35
ITA	-4.26	0.37	-4.4	0.49	-4.35	0.4	3.7	0.14	3.88	0.11	3.97	0.13	10.08	0.3	10.21	0.33	10.17	0.33
JAM	-6.52	0.31	-7.45	0.44	-7.13	0.61	1.22	0.22	0.94	0.23	1.09	0.2	8.71	0.27	8.65	0.27	8.55	0.27
JPN	-8.12	0.62	-7.46	0.42	-7.4	0.49	1	0.19	1.01	0.16	1.26	0.18	8.46	0.26	8.33	0.25	8.72	0.27
JOR	-8.27	0.98	-7.52	0.92	-7.68	0.89	0.9	0.1	1.18	0.11	1.32	0.12	8.49	0.29	8.56	0.29	8.5	0.3
KAZ	-4.13	0.26	-3.87	0.29	-3.99	0.31	4.32	0.12	4.58	0.13	4.4	0.12	10.37	0.38	10.7	0.39	10.58	0.36
KEN	-3.66	0.28	-3.86	0.28	-4.07	0.33	7.01	0.21	6.88	0.18	7.08	0.22	14.02	0.37	13.73	0.34	13.95	0.35
KIR	-4.16	0.64	-4.42	0.99	-4.5	0.99	4.03	0.15	3.97	0.15	3.78	0.15	9.08	0.21	9.12	0.23	8.78	0.2
PRK	-4.08	0.3	-6	1.16	-4.93	0.61	1.4	0.12	1.27	0.15	1.37	0.11	8.61	0.27	8.47	0.26	8.54	0.27
KWT	-4.11	0.3	-3.72	0.41	-4.08	0.36	4.16	0.13	4.52	0.14	4.33	0.13	8.85	0.25	9.09	0.25	9.03	0.27
KGZ	-9.31	0.47	-9.79	0.56	-9.68	0.63	3.76	0.29	3.86	0.3	3.79	0.29	16.48	0.55	16.48	0.52	16.39	0.55
LAO	-3.87	0.33	-4.3	0.4	-4.03	0.3	4.23	0.26	4.07	0.23	4.29	0.26	10.98	0.32	11.56	0.35	11.3	0.33
LVA	-4.08	0.32	-3.82	0.31	-4.56	0.48	6.95	0.21	7.28	0.21	6.99	0.2	11.3	0.31	11.27	0.32	11.05	0.31
LBN	-17.18	0.44	-17.12	0.51	-16.76	0.47	5.34	0.56	5.69	0.6	5.56	0.55	12.31	0.34	12.87	0.39	12.58	0.32

Table B.2 continued from previous page

	0.01				0.5				0.99									
LSO	-4.24	0.31	-5	0.82	-4.28	0.5	3.44	0.12	3.24	0.13	3.29	0.13	12.38	0.44	12.36	0.47	12.04	0.44
LBR	-3.93	0.36	-4.38	0.43	-4.68	0.64	3.77	0.13	3.52	0.09	3.63	0.1	8.93	0.23	8.84	0.22	8.91	0.24
LBY	-43.72	1.73	-43.55	1.59	-44.53	1.8	4.92	0.71	5	0.73	4.98	0.73	11.95	0.41	12	0.39	11.89	0.36
LIE	-68.16	1.99	-71.83	1	-68.19	1.99	2.34	0.67	2.08	0.62	2.42	0.65	59.93	2.39	61.83	1.97	62.2	2.01
LUX	-17.41	0.59	-17.61	0.7	-16.99	0.57	3.88	0.66	3.88	0.67	4.01	0.7	12	0.34	12.19	0.31	12.11	0.29
MAC	-6.21	0.42	-6.3	0.42	-6.09	0.42	2.87	0.18	2.95	0.17	3.02	0.2	9.49	0.38	9.6	0.39	9.49	0.38
MDG	-4.28	0.33	-4.5	0.32	-4.87	0.86	6.92	0.31	6.88	0.29	6.84	0.29	27.24	0.86	27.45	0.85	27.95	0.91
MWI	-15.89	0.44	-16.76	0.37	-15.3	0.4	3.21	0.55	3	0.51	3.15	0.51	10.53	0.33	10.72	0.32	10.63	0.33
MYS	-7.12	0.41	-7.13	0.39	-6.79	0.39	4.66	0.21	4.32	0.21	4.56	0.25	10.42	0.33	10.3	0.32	10.41	0.33
MDV	-4.07	0.28	-4.04	0.25	-4.58	0.45	4.96	0.16	4.93	0.16	4.85	0.19	9.96	0.29	9.89	0.3	10	0.3
MLI	-17.01	0.37	-16.32	0.42	-17.25	0.76	6.01	0.71	6.17	0.6	6.17	0.65	26.93	0.88	26.94	0.92	27.08	0.83
MLT	-4.4	0.34	-4.37	0.45	-5.03	0.73	4.02	0.15	3.84	0.14	4.1	0.13	16.54	0.56	16.65	0.56	16.89	0.57
MHL	-4.63	0.48	-4.16	0.38	-3.87	0.4	2.99	0.36	3.25	0.22	3.71	0.19	18.79	0.7	18.87	0.74	18.48	0.65
MRT	-7.64	0.31	-7.8	0.59	-8.06	0.43	1.01	0.25	0.61	0.69	0.99	0.23	8.54	0.25	8.68	0.28	8.71	0.27
MUS	-6.83	0.41	-6.81	0.41	-6.54	0.41	3.26	0.25	3.13	0.25	3.27	0.29	19.01	0.75	19.04	0.74	19.35	0.73
MEX	-3.71	0.26	-3.93	0.39	-3.77	0.31	4	0.1	3.99	0.11	3.97	0.1	8.98	0.24	8.89	0.23	8.9	0.22
FSM	-6.52	0.31	-6.42	0.28	-6.49	0.33	2.11	0.25	2.34	0.24	2.03	0.23	9.11	0.38	8.44	0.24	8.78	0.27
MDA	-6.57	0.45	-6.54	0.45	-5.85	0.31	1.32	0.15	1.13	0.14	1.2	0.17	8.49	0.27	8.25	0.26	8.75	0.32
MCO	-8.3	0.69	-8.01	0.9	-7.62	0.43	5.51	0.34	5.51	0.32	5.52	0.31	9.66	0.26	9.52	0.25	9.52	0.27
MNE	-4.53	0.46	-6.17	1.31	-5.7	1.03	6.76	0.23	6.54	0.25	6.96	0.23	17.13	0.46	16.97	0.45	17.34	0.45
MAR	-8.24	0.42	-8.34	0.45	-8.74	0.43	2.94	0.28	2.94	0.27	2.81	0.28	9.44	0.31	9.33	0.32	9.4	0.3
MOZ	-4.11	0.38	-4.5	0.45	-3.8	0.39	4.1	0.1	3.79	0.12	3.92	0.11	10.27	0.32	10.26	0.32	10.19	0.31
MMR	-3.96	0.65	-4.1	0.41	-4.54	0.44	6.9	0.21	6.94	0.2	6.73	0.22	13.33	0.33	13.52	0.39	13.39	0.36
NAM	-4.14	0.8	-4.02	0.52	-3.93	0.64	7.12	0.2	6.96	0.19	7.13	0.23	16.97	0.42	16.75	0.42	17.23	0.44
NRU	-4.41	0.45	-3.59	0.3	-4.2	0.55	4.31	0.16	4.51	0.15	4.52	0.16	12.33	0.38	12.85	0.46	12.63	0.37
NPL	-31.32	1.94	-31.2	1.84	-32.04	1.79	6.19	0.74	6.4	0.75	6.18	0.78	28.54	0.82	29.45	0.87	28.81	0.9
NLD	-4.13	0.24	-3.9	0.23	-3.83	0.25	3.88	0.09	3.93	0.09	3.99	0.11	9.26	0.29	9.33	0.29	9.26	0.3
NCL	-6.25	0.46	-6.1	0.46	-5.94	0.35	1.14	0.14	1.3	0.12	1.31	0.16	8.48	0.26	8.74	0.26	8.54	0.24
NIC	-4.16	0.39	-4.29	0.41	-5.8	1.47	2.86	0.17	2.57	0.17	2.52	0.16	8.74	0.22	8.57	0.23	8.53	0.24
NER	-4.76	0.29	-4.47	0.26	-4.23	0.33	3.85	0.18	3.68	0.18	4.15	0.18	8.63	0.2	8.68	0.2	8.96	0.2
NGA	-4.68	0.63	-4.71	0.63	-4.73	0.64	4.76	0.22	4.5	0.23	4.59	0.22	10.98	0.32	10.94	0.33	11.02	0.32
MKD	-3.88	0.31	-5.51	1.17	-5.39	1.18	6.75	0.21	6.23	0.19	6.5	0.19	17.99	0.6	17.54	0.56	17.31	0.58

Table B.2 continued from previous page

	0.01			0.5			0.99											
MNP	-5.58	0.42	-5.3	0.44	-5.66	0.43	3.38	0.18	3.5	0.25	3.14	0.19	9.65	0.31	10.03	0.33	9.46	0.32
OMN	-3.97	0.19	-3.78	0.26	-3.49	0.19	1.35	0.13	1.43	0.13	1.57	0.13	8.31	0.23	8.6	0.28	8.66	0.26
PAK	-4.39	0.33	-4.64	0.35	-4.55	0.36	3.7	0.18	3.65	0.19	3.79	0.2	9.92	0.32	10.01	0.35	10	0.33
PLW	-4.91	0.99	-4.16	0.26	-4.43	0.54	3.98	0.12	3.77	0.12	3.78	0.11	9.31	0.29	9.27	0.28	9.35	0.31
PAN	-9.65	0.71	-9.7	0.56	-9.84	0.9	1.16	0.27	0.96	0.26	1.24	0.34	8.52	0.27	8.81	0.3	8.65	0.27
PNG	-4.41	0.63	-4.91	0.98	-3.89	0.4	6.27	0.2	6.28	0.22	6.51	0.23	12.97	0.37	12.74	0.32	12.95	0.37
PRY	-4.83	0.41	-5.42	0.46	-5.18	0.39	3.76	0.23	3.46	0.2	3.61	0.23	13.78	0.44	13.72	0.41	13.99	0.46
PER	-4.37	0.41	-4.59	0.5	-4.38	0.41	3.75	0.21	3.58	0.23	3.87	0.22	11.09	0.35	11.24	0.37	11.14	0.32
PHL	-4.95	0.79	-4.36	0.43	-4.25	0.4	5.2	0.19	4.97	0.18	5.12	0.18	9.78	0.28	9.48	0.27	9.54	0.26
POL	-4.87	0.81	-4.48	0.29	-4.69	0.65	4.75	0.16	4.79	0.17	4.82	0.16	8.78	0.24	8.94	0.22	8.98	0.23
PRT	-4.64	0.64	-4.42	0.43	-4.45	0.8	3.42	0.1	3.48	0.12	3.56	0.14	9.47	0.31	9.38	0.3	9.59	0.32
PRI	-5.55	0.4	-5.66	0.38	-6	0.4	1.36	0.13	1.26	0.13	1.24	0.16	8.64	0.27	8.78	0.27	8.63	0.27
QAT	-5.69	0.45	-6.7	0.62	-5.89	0.59	1.21	0.13	0.73	0.11	1.12	0.11	10.15	0.39	10.17	0.37	9.97	0.38
ROU	-3.95	0.25	-4.19	0.35	-3.8	0.21	6.92	0.2	6.88	0.18	6.6	0.22	27.26	0.78	26.93	0.75	26.46	0.79
RUS	-7.1	0.26	-6.66	0.31	-6.77	0.27	3.52	0.3	3.62	0.28	3.68	0.3	11.01	0.35	10.91	0.33	10.92	0.33
RWA	-10.12	0.48	-9.96	0.42	-10.3	0.48	4.29	0.37	4.36	0.39	4.48	0.33	11.46	0.38	11.37	0.35	11.23	0.33
WSM	-4.31	0.5	-4.23	0.35	-4.32	0.32	7.08	0.25	6.94	0.24	6.96	0.24	13.86	0.37	13.56	0.35	14.38	0.47
SMR	-6.93	1	-7.05	1.06	-6.33	0.61	2.89	0.2	2.67	0.2	3	0.2	8.64	0.2	8.59	0.23	8.35	0.2
STP	-15.44	0.93	-15.51	0.9	-14.62	0.46	0.96	0.45	0.65	0.48	0.8	0.48	8.66	0.31	8.73	0.33	8.76	0.3
SAU	-3.7	0.35	-4.54	0.94	-3.98	0.94	4.48	0.11	4.4	0.14	4.6	0.12	9.97	0.33	10.11	0.33	10.28	0.33
SEN	-5.13	0.37	-5.38	0.65	-5.55	0.64	4.16	0.23	3.75	0.25	3.89	0.23	14.31	0.48	14.32	0.48	14.22	0.49
SRB	-4.11	0.33	-4.9	0.81	-4.09	0.43	3.53	0.11	3.3	0.11	3.67	0.11	9.03	0.29	8.85	0.3	8.79	0.31
SYC	-5.13	0.51	-4.86	0.28	-4.66	0.3	4.21	0.26	4.11	0.25	4.12	0.23	9.31	0.25	9.24	0.24	9.27	0.24
SLE	-8.07	0.4	-8.14	0.3	-8.14	0.37	1.45	0.21	1.31	0.15	1.47	0.19	11.85	0.43	11.38	0.43	11.57	0.44
SGP	-8.34	0.41	-7.81	0.41	-7.84	0.76	5.55	0.31	17.01	1.23	5.85	0.28	26.95	0.91	27.26	0.86	27.9	0.87
SXM	-3.93	0.25	-4.39	0.4	-4.58	0.49	4.89	0.24	4.72	0.24	4.62	0.25	15.07	0.45	14.81	0.43	14.65	0.43
SVK	-4.31	0.46	-5.65	0.97	-5.28	0.82	1.62	0.06	1.18	0.06	1.4	0.08	8.79	0.26	8.42	0.24	8.43	0.26
SVN	-6.74	0.48	-7.8	0.64	-7.27	0.34	3.91	0.26	3.57	0.3	3.84	0.3	11.62	0.37	11.26	0.36	11.56	0.37
SLB	-9.67	0.31	-9.71	0.27	-9.5	0.29	2.66	0.36	2.68	0.32	2.69	0.3	8.6	0.22	8.61	0.23	8.5	0.22
SOM	-18.12	0.48	-18.25	0.5	-17.41	0.51	3.22	0.68	3.37	0.65	3.64	0.7	11.14	0.39	11.12	0.35	11.34	0.38
ZAF	-3.84	0.32	-3.83	0.27	-3.89	0.44	6.91	0.22	6.92	0.22	6.92	0.24	8.98	0.18	8.97	0.17	8.89	0.17
SSD	-4.48	0.64	-4.34	0.37	-4.45	0.67	3.28	0.16	3.27	0.15	3.34	0.16	8.45	0.23	8.85	0.25	8.66	0.22

Table B.2 continued from previous page

	0.01				0.5				0.99									
LKA	-6.32	0.29	-6.44	0.41	-6.21	0.63	1.77	0.18	1.55	0.21	1.61	0.14	8.59	0.27	8.45	0.26	8.56	0.26
KNA	-3.61	0.35	-4.15	0.4	-3.97	0.28	5.48	0.2	5.32	0.23	5.23	0.2	11.62	0.32	11.66	0.3	11.29	0.28
LCA	-6.34	0.41	-6.04	0.41	-6.87	0.58	2.84	0.21	2.85	0.21	2.89	0.23	12.49	0.45	12.68	0.43	12.73	0.49
MAF	-5.07	0.29	-5.59	0.42	-5.67	0.5	1.27	0.2	1.13	0.2	1.09	0.19	8.62	0.27	8.69	0.28	8.59	0.26
SDN	-6.42	0.37	-6.53	0.39	-6.4	0.3	1.43	0.15	1.24	0.14	1.45	0.17	8.45	0.25	8.83	0.26	8.6	0.25
SUR	-18.98	0.65	-19.56	0.9	-19.02	0.71	3.8	0.67	3.73	0.66	3.44	0.68	9.82	0.32	9.9	0.31	9.7	0.31
SWE	-4.33	0.36	-3.85	0.23	-4.89	0.62	3.76	0.12	4	0.13	3.75	0.12	9.68	0.33	9.97	0.3	9.91	0.3
CHE	-7.84	0.41	-8.03	0.41	-7.9	0.45	2.06	0.24	2.25	0.2	2.22	0.22	8.41	0.24	8.41	0.21	8.61	0.25
SYR	-4.26	0.24	-3.88	0.26	-4.04	0.25	1.82	0.17	1.99	0.17	1.92	0.17	8.44	0.26	8.58	0.26	8.57	0.27
TZA	-3.7	0.24	-3.67	0.28	-4.06	0.27	7.06	0.2	7.01	0.21	6.99	0.22	13.28	0.32	13.54	0.39	12.81	0.32
THA	-3.98	0.64	-4.24	0.42	-3.85	0.31	6.46	0.22	6.23	0.2	6.49	0.23	11.27	0.31	11.25	0.34	11.18	0.33
TLS	-4.85	0.6	-4.48	0.64	-4.25	0.45	3.91	0.2	4.13	0.13	3.76	0.14	10.44	0.39	10.53	0.38	10.46	0.38
TGO	-7.98	0.4	-8.25	0.37	-8.25	0.38	3.91	0.36	3.76	0.35	3.88	0.35	16.68	0.51	16.4	0.46	16.44	0.51
TON	-6.11	0.38	-6.53	0.41	-6.24	0.39	3.8	0.25	3.87	0.26	3.89	0.26	8.88	0.21	8.95	0.22	9.01	0.24
TTO	-7.21	0.38	-7.65	0.6	-7.23	0.35	1.13	0.18	1.17	0.17	1.35	0.19	8.71	0.29	8.88	0.3	8.85	0.32
TUN	-6.26	0.41	-5.98	0.29	-6.31	0.42	3.77	0.24	3.69	0.27	3.8	0.24	14.99	0.45	15.25	0.51	14.95	0.49
TUR	-4.72	0.46	-4.42	0.42	-4.11	0.41	3.42	0.15	3.73	0.17	3.62	0.18	8.88	0.28	9.07	0.32	8.99	0.36
TKM	-8.32	0.39	-8.39	0.41	-7.57	0.42	5.77	0.41	5.81	0.38	6.08	0.41	12.16	0.36	12.21	0.33	12.49	0.36
TCA	-3.83	0.25	-3.78	0.26	-4.88	0.99	7.07	0.18	6.84	0.25	6.84	0.23	16.08	0.38	15.99	0.39	15.75	0.38
TUV	-5.21	0.53	-5.23	0.44	-4.82	0.46	1.29	0.16	1.01	0.17	1.25	0.15	9.37	0.32	9.72	0.38	9.92	0.43
UGA	-8.88	0.4	-8.84	0.36	-9.68	0.86	1.08	0.24	0.99	0.23	1.21	0.22	11.34	0.48	11.34	0.44	11.44	0.47
UKR	-4.24	0.32	-4	0.42	-3.96	0.38	6.29	0.19	6.52	0.2	6.37	0.2	12	0.3	11.87	0.31	11.98	0.34
ARE	-17.46	0.35	-17.65	0.3	-17.71	0.34	3.6	0.69	3.67	0.65	3.94	0.66	12.27	0.36	12.48	0.34	12.37	0.35
GBR	-6.73	0.39	-6.59	0.27	-6.37	0.3	4.01	0.25	3.95	0.24	4.09	0.23	12.98	0.38	13.07	0.42	12.99	0.39
USA	-5.48	0.26	-5.48	0.28	-6.07	0.37	1.64	0.22	1.52	0.23	1.42	0.21	8.65	0.25	8.71	0.25	8.57	0.25
URY	-5.36	0.76	-4.51	0.31	-4.57	0.5	1.8	0.12	1.76	0.11	1.6	0.11	8.32	0.24	8.68	0.24	8.39	0.25
UZB	-9.6	0.4	-9.35	0.39	-9.42	0.98	3.51	0.28	3.58	0.25	3.77	0.29	10.49	0.37	10.54	0.32	10.81	0.35
VUT	-3.92	0.4	-4.4	0.42	-3.93	0.41	7	0.25	6.97	0.2	6.91	0.2	11.14	0.27	11.21	0.29	11.17	0.28
VEN	-6.77	0.39	-6.77	0.42	-7.1	0.39	3	0.29	2.8	0.24	2.91	0.31	8.96	0.26	8.96	0.26	9.22	0.27
VIR	-3.97	0.39	-4.2	0.42	-4.17	0.42	6.29	0.18	6.19	0.2	6.43	0.19	8.75	0.15	8.92	0.18	8.83	0.18
YEM	-16.61	0.37	-16.91	0.44	-16.37	0.48	4.19	0.7	3.94	0.67	4.22	0.68	21.35	0.75	21.74	0.75	21.82	0.77

Table B.2 continued from previous page

	0.01				0.5				0.99									
ZWE	-4.14	0.44	-4.44	0.46	-4	0.43	6.87	0.2	6.52	0.23	6.73	0.23	11.33	0.32	11.21	0.3	11.21	0.33

Table B.2: Mean (in bold) and standard error of the quantile estimates at level $\tau = 0.01, 0.5, 0.99$ for the SSP5 scenario.

Appendix C

The Impact of the COVID-19 Pandemic on Risk Factors for Children's Mental Health

This section reports additional Figures from Chapter 4.

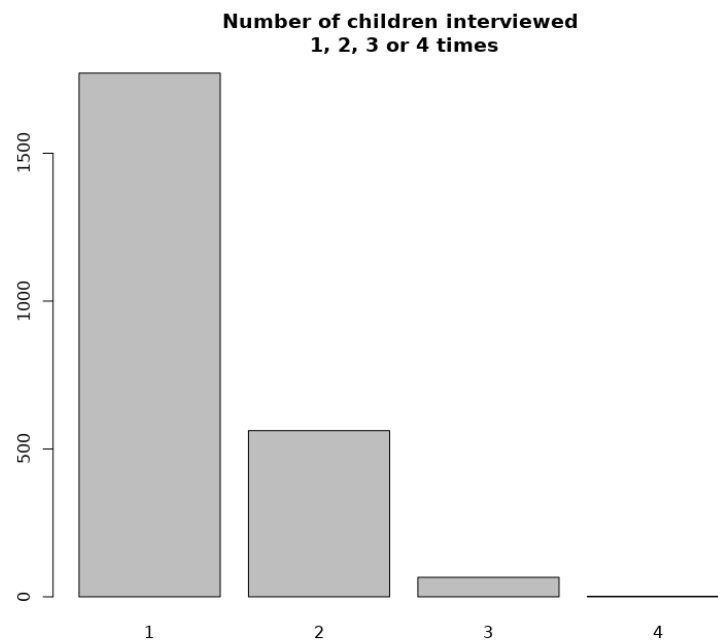


Figure C.1: Bar plot showing the number of children interviewed 1, 2, 3 or 4 times during the sample period.

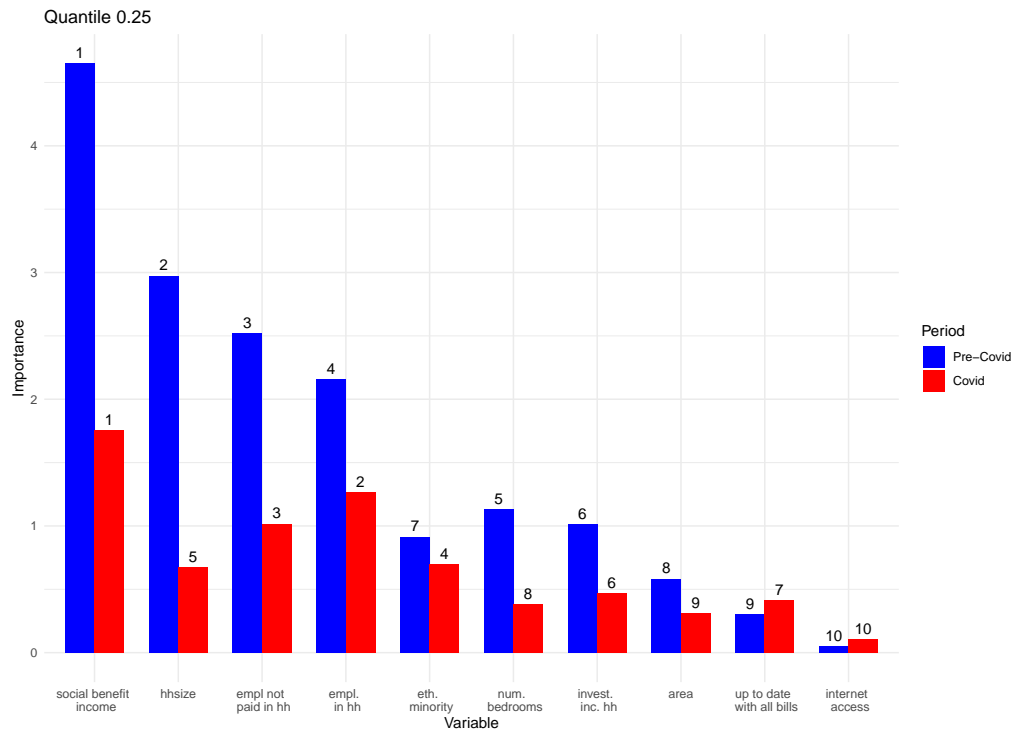


Figure C.2: Bar plot showing the Variable Importance extracted from the FM-QRF for each covariate at quantile level $\tau = 0.25$.

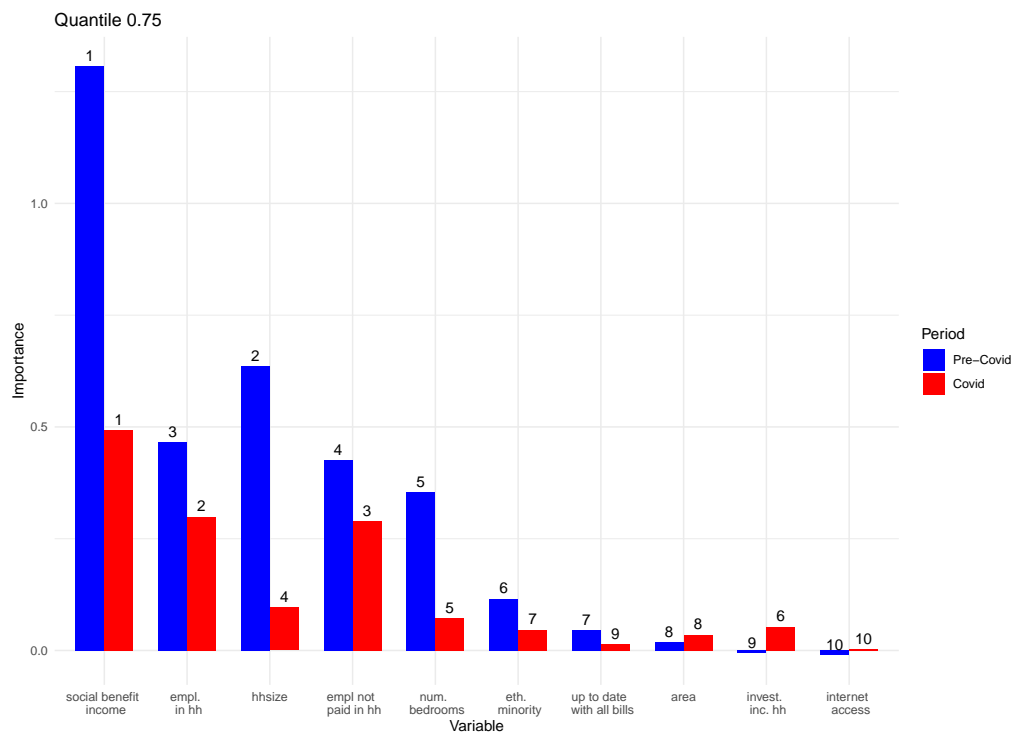


Figure C.3: Bar plot showing the Variable Importance extracted from the FM-QRF for each covariate at quantile level $\tau = 0.75$.